AALBORG UNIVERSITY

Department of Civil Engineering

Evaluation of the power production performance of the WavePiston wave energy converter

Supervisor:

Jens Peter Kofoed

Student reference:

Elisa Angelelli

12023

9th Semester

2009/2010

PREFACE

My name is Elisa Angelelli, I'm a student of the master degree and I come from Italy.

This document represents the conclusion of the last five years of university in Civil Engineering with the Specialization in Hydraulic spent in Alma Mater Studiorum of Bologna.

The experimental studied included in this document were made possible thanks to the work in the laboratory of Aalborg University, in Denmark.

During the ending of my university period I felt the need to spend a period abroad, the main reasons belonged to two types: the first was that I regret the idea to finish the university study without carry out any practical stuff, but only theoretical topics; and the second was about the disappointment that I felt to go in the world of work with a limited knowledge of English and use of it even less.

Both the issues were approached and almost resolved during this period abroad as an Erasmus student.

And last but not least, the topic of my study: since in the last three years of university I chose a specialization regarding the water, it was really likely that I found myself working in something related to the water, but usually when you thought to the water you usually mean the fresh water: as aqueduct, hydroelectric, etc...but the curiosity for new research and the willingness to find new prospects for green energy led me to a new scenario: the energy of the sea!

Hence with the Erasmus period in Denmark, I could work in the laboratory on a new wave energy converter, called the WavePiston, with the collaboration of two of its inventors (Kristian Glebøl and Martin von Bülow) and Arthur Pecher, under the supervision of Jens Peter Kofoed.

To conclude, I would only add that I've never done before a kind of document as this, I mean for the English language either for the scientific typology, thus I apologize for any inaccuracies of form or language.

May 2010, Aalborg

INDEX

FIGURE INDEX

TABLE INDEX

ABSTRACT

In the early 1970 the community has started to realize that have as a main principle the industry one, with the oblivion of the people and health conditions and of the world in general, it could not be a guideline principle.

Undoubtedly, the subsequent oil's crisis, with a sudden price increase has accelerated the need for new cleaner energy sources, more durable and more politically stable.

There are different typologies of renewable energy sources, from the solar energy, the wind energy, the hydropower energy, to get the recent marine energy.
The sea, as an energy source, has the characteristic of offering different types of exploitation: from one based on temperature difference between surface and depth, to one based on osmotic principles related to different salinity, to the one likelier linked to tide drops, to finally the one a bit more discontinuous, but perhaps best known: the wave energy.

Over the last 15 years the Countries interested in the renewable energies grew. Therefore many devices have came out, first in the world of research, then in the commercial one; these converters are able to achieve an energy transformation into electrical energy. There are different classifications of the wave energy converters, for example, according to their placement, or by their operation.

The purpose of this work is to analyze the efficiency of a new wave energy converter, with the aim of determine the feasibility of its actual application in different wave conditions: from the energy sea state of the North Sea, to the more quiet of the Mediterranean Sea.

The following document is divided into several phases: in the first phase there is a description of the actual energy situation and the past and present reasons for which is necessary to use different energy sources by those currently mainly used, such as coal, oil and fuel oil. Conclusion of this phase is the rapid presentation of the main renewable sources, with a particular attention to the marine energy and to those devices able to exploit it.

The second phase of the project is the experimental investigation conducted at the University of Aalborg, in Denmark, on a wave energy converter of recent invention called WavePiston. This study has the aim to obtain a average annual value of the efficiency, an installed power generated value, and consequently a relative value of annual energy extractable. To increase the reliability of this work, there are analyzed the main characteristics that may affect the model efficiency, such as changes in wave height, wave period and angle of wave incidence; friction problems (PTO loading), variations in efficiency due to the presence of several energy absorption elements in the same device, or different shape of them.

Finally the last step proposes a numerical modelling of the device in question, to ascertain its efficiency regardless the laboratory results. This phase is concluded with some comments and suggestions concerning the system under consideration.

May 2010, Aalborg

ABSTRACT

È dai primi anni del 1970 che si è iniziato a capire che il solo principio dell'industria con l'incuranza delle condizioni salutari delle persone e del mondo in generale non poteva essere un principio guida.

La successiva crisi del petrolio con un improvviso aumento del prezzo, ha sicuramente accelerato la necessità di nuove fonti energetiche più pulite, più durature e più politicamente stabili.

Di fonti energetiche rinnovabili ne esistono di diverse tipologie dalla solare, all'eolica, all'idroelettrica per arrivare alla più recente energia marina.
Il mare, come fonte energetica, ha la caratteristica di offrire diverse tipologie di sfruttamento: da quella basata sulla differenza termica tra superficie e profondità, a quella basata sui principi osmotici legati a differenti salinità, a quella più prevedibile legata ai dislivelli di marea, ad infine quella un po' più discontinua ma forse più conosciuta: l'energia da onda.

Negli ultimi 15 anni sono stati sempre più in aumento i Paesi interessati in questo ambito e di conseguenza, si sono affacciati, prima nel mondo della ricerca, poi in quello commerciale, sempre più dispositivi atti a realizzare questa trasformazione energetica. Di tali convertitori di energia ondosa ne esistono diverse classificazioni, in base al loro collocamento, o in base al loro funzionamento.

Scopo di tale lavoro è quello di analizzare l'efficienza di un nuovo convertitore di energia ondosa al fine si stabilire la fattibilità di una sua reale applicazione in diverse condizioni ondose: dalle più energetiche del Mare del Nord, alle più quiete del Mar Mediterraneo.

Il seguente documento è articolato in più fasi: vi è una prima fase descrittiva della situazione energetica odierna e dei motivi passati e presenti per i quali è necessario ricorrere a fonti energetiche differenti dalle prevalenti attualmente in uso, quali carbone, petrolio e oli combustibili. Conclusione di tale fase è la veloce presentazione delle principali fonti rinnovabili, mostrando particolare attenzione per quella marina e per i dispositivi in grado di sfruttare quest'ultima.

La seconda fase del progetto rappresenta lo studio sperimentale condotto nell'Università di Aalborg, in Danimarca, riguardo un convertitore di energia ondosa di recente invenzione chiamato WavePiston. Tale studio ha l'intento di ottenere un valore di efficienza medio annuale, un valore di potenza nominale generata e quindi un relativo valore di energia annua estraibile. Per rendere più attendibile tale lavoro si sono analizzate le principali caratteristiche che possono influenzare l'efficienza del dispositivo come variazioni delle caratteristiche ondose quali: altezza, periodo e angolo di incidenza dell'onda; problemi di frizione (PTO loading), variazioni di efficienza legata alla presenza di più elementi di assorbimento energetico nello stesso dispositivo, o ad elementi di diversa forma.

Infine l'ultima fase propone una modellazione numerica del dispositivo in esame, al fine di conoscere l'efficienza dello stesso a prescindere dalla possibilità di avere risultati di laboratorio. Tale fase è conclusa con alcune osservazioni e suggerimenti riguardanti il sistema in esame.

Maggio 2010, Aalborg

1- Introduction

1.1- Preface

One of the most important principles of physics is called entropy, and it is related to the continuous and perpetual transformation from one situation to another.

In physics, entropy is a quantity that is interpreted as a measure of the chaos of a physical system or the universe in general. The concept of entropy was introduced in the early nineteenth century, as part of thermodynamics, to describe the observation that all the transformations occurred invariably in one direction only, namely towards greater disorder. Hence in classical thermodynamics the entropy is a state function, which quantifies the unavailability of a system to generate work. The entropy of an isolated system always increases; and the processes, which entropy increases, can occur spontaneously.

In particular, the term entropy was first introduced by Rudolf Clausius in his "*Abhandlungen über die mechanische Wärmetheorie*" (Treaty on the mechanical theory of heat), published in 1864. In German, the word entropy derives from the Greek εν, "inside", and τροπή, "change", "turning point", "revolution". The concept of entropy gained great popularity between the '800 and the '900, and it was extended to areas not strictly physical, such as social sciences, the signal theory, the information theory.

Not surprisingly, during the same period there is a huge transformation process that generally takes the name of the Industrial Revolution.

The term "Industrial Revolution" means a process of economic evolution that leads from an agriculture and craft-trade system to a modern industrial system characterized by the general use of machines fed by power and by the use of new inanimate energy sources, such as fossil fuels. As with many historical processes, even for the industrial revolution there is no certain start date, although the key invention is the steam engine. It started in the United Kingdom, then subsequently it spread throughout Europe, North America, and eventually the whole world.

The feature of the Industrial Revolution is the leap in the ability to produce goods; in human history the greatest constraint on increasing the production of goods is the energy problem. For many centuries, humanity had only mechanical energy provided by the work of men and animals, which did not give any possibility to raise production. Industrial development required greater amounts of energy, much higher than that provided by man, and the abundant coal deposits in England facilitated that kind of development, and the steam engine gave a way to the production of a tremendous amount of energy, as never experienced before.

The industrial revolution led to a profound and irreversible transformation of the productive, economic and technological system as well as the whole social system. The consequences were an increased consumption of goods, the share of income, different class relations, a change in culture, politics, general living conditions, with expansionary effects on the level populations.

In spite of several negative effects on the urban proletariat, due to initial conditions of economic exploitation and uncontrolled urbanization, in the long run the Industrial Revolution raised the welfare conditions of an increasingly larger percentage of the population, leading by the end of the nineteenth century to a general improvement in the health conditions.

In the last two centuries, from the beginning of the industrial revolution, the European population grew almost fourfold, life expectancy rose from values between 25 and 35 years to values exceeding 75 years. The population raise became a factor in the development of the economy, pushing more and more people towards various forms of consumerism, but also led to new social and political problems, such as the related disorderly urbanization of large cities and the distribution of resources.

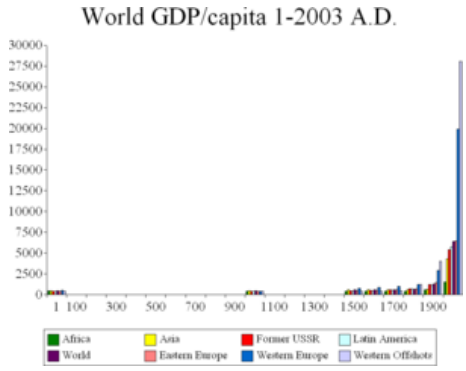

Figure 1.1: The regional GDP (Gross Domestic Production) per capita changed very little for the most of the human history before the Industrial Revolution. The empty areas mean no data, and not very low levels.

The epoch of the development in the technology and comfort might be traced back to the beginning of the industrial revolution. This era is characterized by an increasing world population and consequentially its needs, such as different comfort: appliances and electricity, vehicles and petroleum.

The petroleum and the coal are called fossil fuels. Fossil fuels are non-renewable resources, because they take millions of years to form, and the reserves are being depleted much faster than new ones are being formed.

The use of these resources was not rational, and therefore as the demand increased as much as the huge exploitation of the energy resources increased, mainly those called fossil fuels. The production and use of fossil fuels raised environmental concerns, however a first downsizing came only after a the oil crisis in 1970.

The 1970s oil crisis really began in 1973. The major cause lay on the fact that oil prices were quadrupled by OPEC, in fact the prices raised from only 25 cents to over a dollar in few months, and that was accompanied with stock market crash. Along with the increased government spending which came with the Vietnam War, the oil crisis led to severe inflations in the United States.

In October of 1973 Middles-eastern OPEC nations stopped exports to the U.S.A. and other western nations. They meant to punish the western nations for supporting Israel, their foe, but they also realized their

strong influence on the world through the oil control.
The embargo forced America to reconsider its policy about energy, its cost and supply, about which no one had worried until 1973. There was an immediate drop in the building of houses with gas heating, because other forms of energy were more affordable at this time. Tax credits were offered to those who developed and used alternative sources for energy. These included solar and wind power. Nixon, who was president at that time, ordered the department of defence to create a stockpile of oil in case the country needed the military to carry it through a time of chaos. There was a large cutback in oil consumption. Nixon formed the Department and it became a cabinet office. It developed the national energy policy. It made plans to make the U.S.A. an energy independent company.

Figure 1.2: The voluntary gas stations decision to fix a limit.

Gas stations would voluntarily close on Sundays and also would not sell more than ten gallons of gasoline to a customer at a time. They felt that these efforts would help the public to become more fuel-efficient. The community helped to retain energy as well. Families turned their thermostats down and became more fuel-efficient. Companies and industries switched their energy source to coal. People searched for alternative energy sources. The embargo ended was in March 1975, when the Arabs began to ship oil to Western nations again, but this time at inflated prices. Never had the price of an essential commodity risen so quickly and dramatically. The vulnerability of the Western world had truly been revealed.

1.2- Current energy situation

A global movement toward the generation of renewable energy is under way to help to solve the increased energy needs. Awareness of the need of a more liveable world, combined with economical requirements related to the exhaustibility of the major resources in use, is one of the main reasons for the current research in the renewable energy.

As stated by the entropy principle, the natural climatic variations are always present, but in recent years anthropological changes lead to a worse situation, with the consequent of a greater need to find efficient and sustainable solutions.

The anthropological consequent are found in a variation of the mean of climate parameters, and moreover in the change of the pattern of these values over the years. From this point of view, the main changes caused by man are:

- woods deforestation in order to convert zone in arable grounds and grazes;
- great greenhouse effect: CO_2 gasses emission from factories and vehicles;
- great greenhouse effect: methane from extensive breeding and rice fields.

Today the presence of many sources of energy enables a considerable development of infrastructure and an acceleration of the industrialization process. Nevertheless, the main source remains the fossil fuel, which cover, at present, about 80% of energy needs worldwide, in particular 34.3% oil, 20.9% gas, 25.1% coal; and this implies three actual problems, which could affect irreparably natural resources availability for future generations.

The first problem is intrinsic to the nature of the source itself, i.e. its exhaustibility. In the last 150 years, around the half of the available resources was consumed, with a peak of the demand for energy in the last 30 years.

Reserves, i.e. quantities available	Detected [Gtoe]	Estimated [Gtoe]
Coal: 36% Europe, 30% Asia, 30% North America	700	3400
Oil: 60% Middle East, 11% Europe, 10% Central and South America, 6% North America, 10% Africa, 3% Asia	150	300
Natural gas: 40% Europe, 35% Middle East, 8% Asia, 5% North America	150	400
Uranio (^{235}U): 25% Asia, 20% Ausralia, 20% North America (Canada), 18% Africa (Niger)	60	250
Uranio (^{238}U)	3500	15000

Table 1.1: Quantities of energy resources available in 2006, source IEA.
The values are expressed in Gtoe. A toe is a ton of oil equivalent and it is a unit of energy: it represents the amount of energy released by burning one ton of crude oil, approximately 42 GJ. Multiples of the toe are used, in particular the megatoe (Mtoe, one million toe) and the gigatoe (Gtoe, one billion toe).

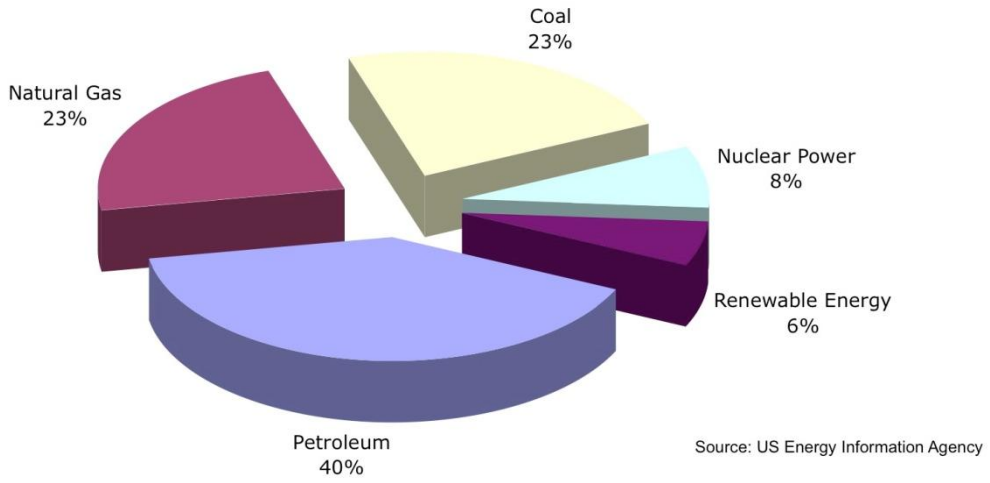

Figure 1.3: Total energy consumption in the 2006, the 86% of human consumption is fossil fuel (natural gas, coal, petroleum), source International Energy Agency (IEA).

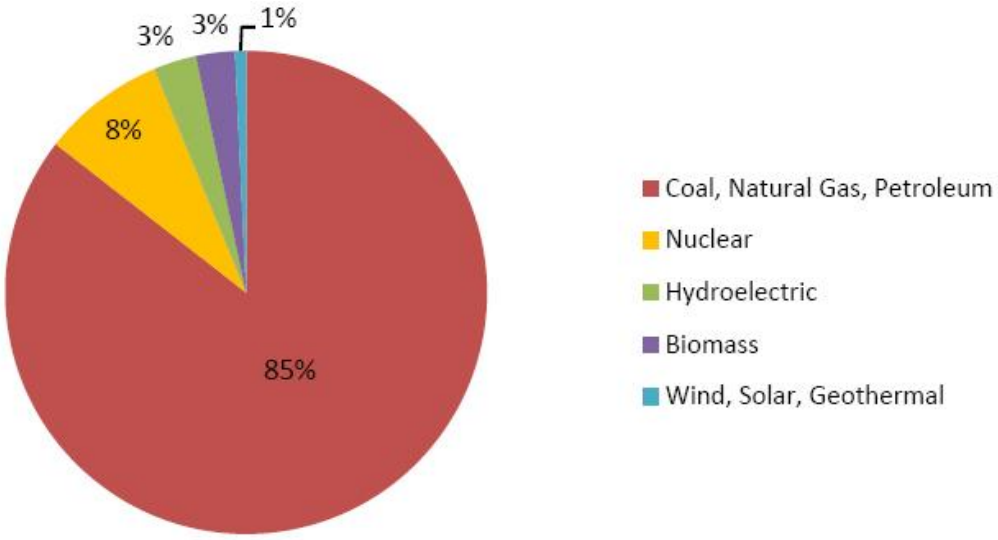

Figure 1.4: Analogue energy consumption in the 2006, source Fuel Group.

The pictures above explain how the total consumption of 11Gtoe was allocated in 2006, in particular: 2.7 Gtoe for coal, 3.8 for oil, 2.3 for natural gas, 0.7 for nuclear, 0.2 for hydropower, and only 0.04 Gtoe for geothermal, solar and wind.

Considering the reserves combined with the utilization, it is possible to estimate the duration for each not-renewable energy resource. For example, the oil can be used for 150/3.8 = 39.4, about 40 years, while for the coal, its duration is approximately 700/2.7 = 260 years.

Nevertheless, these estimates are optimistic because they do not consider the rate of consumption growth, approximately 2% per year.

The second problem is related to the particular distribution of fossil fuels on the planet. Although the countries, defined as "developed", have limited resources, they consume over 50% of the world energy. Nearly 70% of oil reserves is located in the Middle East and more than 75% of natural gas reserves is divided between the Middle East and the Countries of the former Soviet Union, which are far away from areas of consumption, and certainly have a precarious political situation.

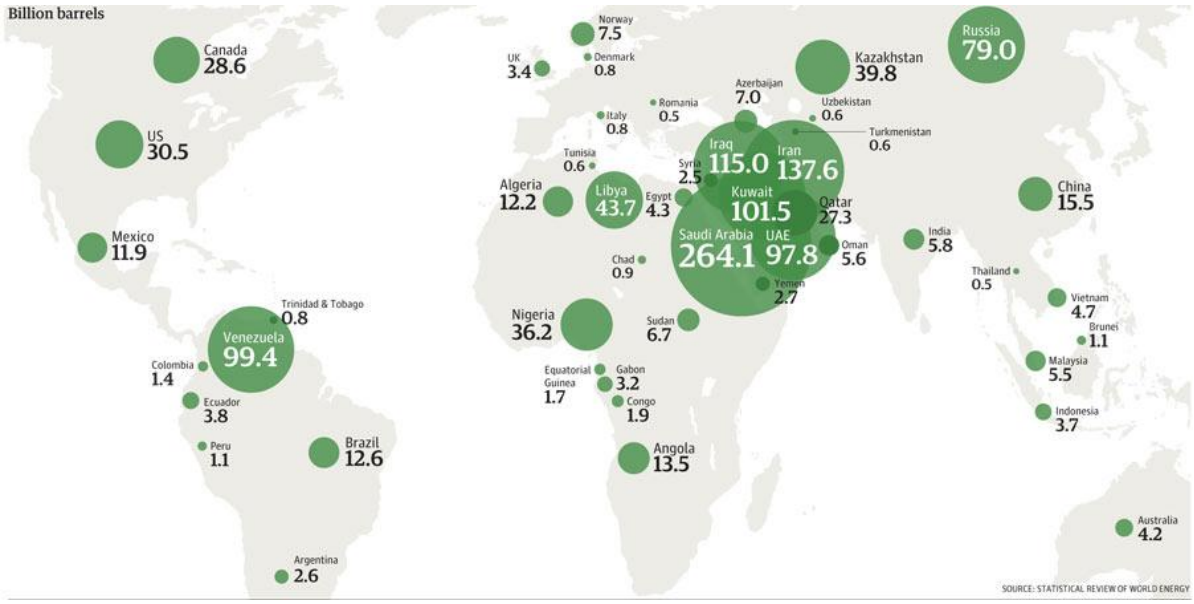

Figure 1.5:The world's proven oil reserves, source Statistical Review of World Energy

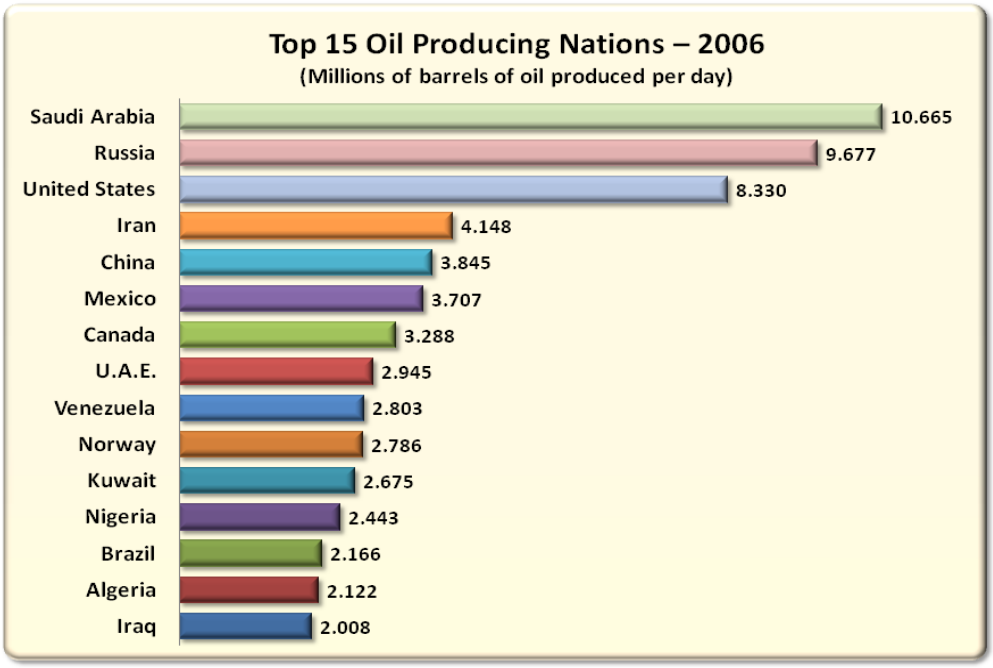

Figure 1.6: Major oil producer Nation in 2006, source Energy Information Administration, U.S. Department of energy http://tonto.eia.doe.gov/country/index.cfm

A final aspect is related to environmental issues involved in the exploitation of fossil fuel. A huge amount of carbon dioxide (CO_2) emissions is caused by the combustion of these substances, which are responsible for the greenhouse effect, and consequently the overheating of the lower atmosphere and earth crust. According to several scientists, the climate change started many decades ago was due to the burning of fossil resources.

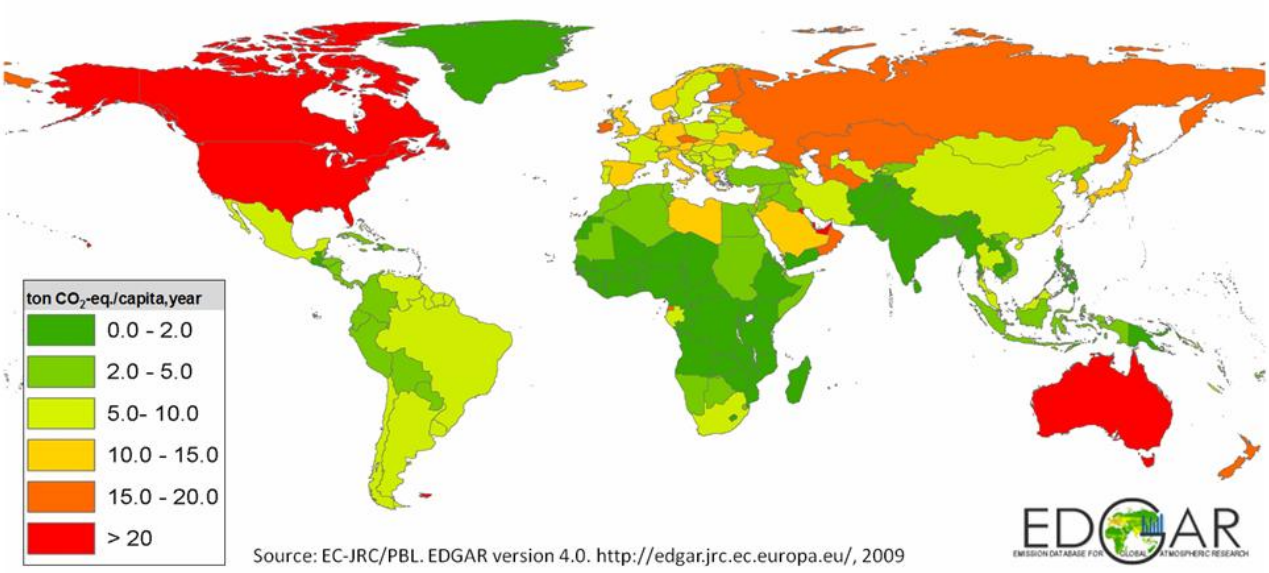

Figure 1.7: World map on the Carbon dioxide emission in 2009, source Emission Database for Global Atmospheric Research (EDGAR) http://egar.jrc.ec.europa.eu

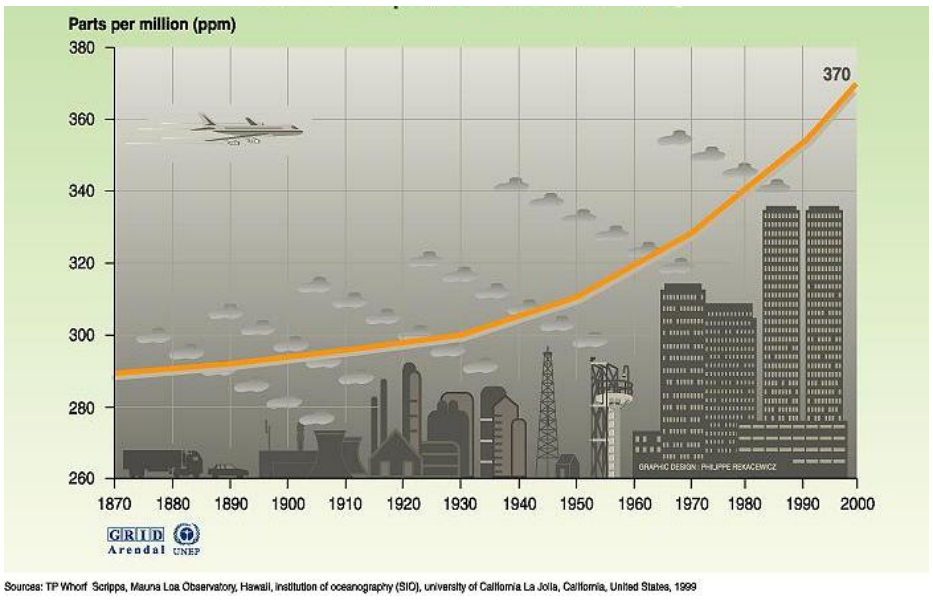

Figure 1.8: Trend of the global atmospheric concentration of CO_2, source Mauna Loa Observatory (UNEP)

The table below lists some of the main greenhouse gases and their concentrations in pre-industrial times and in 1994. GWP is an attempt to provide a simple measure of the relative effects of different greenhouse

gases. The future global warming commitment of a greenhouse gas can be calculated over a chosen time horizon (such as 100 years) by multiplying the appropriate GWP by the amount of gas emitted, however GWPs values have a typical uncertainty of $\pm$ 35%, and GWPs need to take into account any indirect effects of the emitted gases for a correct future warming.

Greenhouse gases	Chemical formula	Pre-industrial concentration	Concentration in 1994	Atmospheric lifetime (years)***	Anthropogenic sources	Global warming potential (GWP)*
Carbon-dioxide	CO_2	278 000 ppbv	358 000 ppbv	Variable	Fossil fuel combustion Land use conversion Cement production	1
Methane	CH_4	700 ppbv	1721 ppbv	12,2 +/- 3	Fossil fuels Rice paddies Waste dumps Livestock	21 **
Nitrous oxide	N_2O	275 ppbv	311 ppbv	120	Fertilizer industrial processes combustion	310
CFC-12	CCl_2F_2	0	0,503 ppbv	102	Liquid coolants. Foams	6200-7100 ****
HCFC-22	$CHClF_2$	0	0,105 ppbv	12,1	Liquid coolants	1300-1400 ****
Perfluoromethane	CF_4	0	0,070 ppbv	50 000	Production of aluminium	6 500
Sulphur hexa-fluoride	SF_6	0	0,032 ppbv	3 200	Dielectric fluid	23 900

Note : pptv= 1 part per trillion by volume; ppbv= 1 part per billion by volume, ppmv= 1 part per million by volume

* GWP for 100 year time horizon. ** Includes indirect effects of tropospheric ozone production and stratospheric water vapour production. *** On page 15 of the IPCC SAR. No single lifetime for CO_2 can be defined because of the different rates of uptake by different sink processes.**** Net global warming potential (i.e., including the indirect effect due to ozone depletion).

GRID Arendal UNEP

Figure 1.9: The main greenhouse gases, source Intergovernmental Panel on Climate Change (IPCC)

In a short time, industrialized countries will need to reduce emissions of greenhouse gases against air pollution, diversify the energy market and provide an adequate energy supply. On the other hand, renewable energies are a real opportunity for developing countries, in order to start a sustainable progress.

The renewable (solar, wind, geothermal and ocean) energies might provide power at competitive prices from inexhaustible sources and in a sustainable manner. In the wake of the 1970s energy crisis, a number of wave energy Research & Development (R&D) programmes were established, but, in contrast with wind energy, these efforts were not sustained, consequently there was very limited innovation in the ocean energy sector from the mid-1980s to late 1990s.

Renewed policy interest (and public and private funding) over the last decade has motivated a resurgence in innovation activity, and the emergence of multiple device designs.
An energy resource can only be successfully exploited if the resource itself is well understood and defined. For this reason the next chapter deals with the study of a wave data analysis, such as wave theory and wave power calculation procedure. The literature study is concluded with a discussion of the current wave energy conversion technology. The environmental impact varies according to the type of device and location, but usually tidal barrage has a most significant impact.

1.3- Research of a green solution

This is a time of unprecedented attention on energy systems, certainly since the energy crisis of the 1970s.

The broad acceptance that carbon dioxide (CO_2) and other greenhouse gas (GHG) emissions are responsible for climate change has made of the decarbonisation an international policy priority (Intergovernmental Panel on Climate Change, IPCC, 2007). Ambitious targets for economy-wide decarbonisation and low carbon technology deployment are being established across international policy, industry and research communities.

Although a replacement for the Kyoto Protocol was not successfully negotiated in Copenhagen, the issues of greenhouse gas emissions reductions and energy efficiency are clearly introduced on the international agenda.

The renewable energy, currently known and exploitable, are:

bio-energy	geothermal	hydropower
	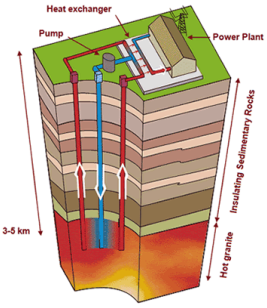	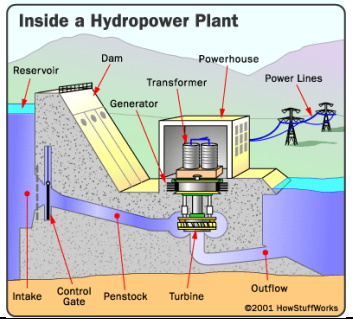

wind energy systems
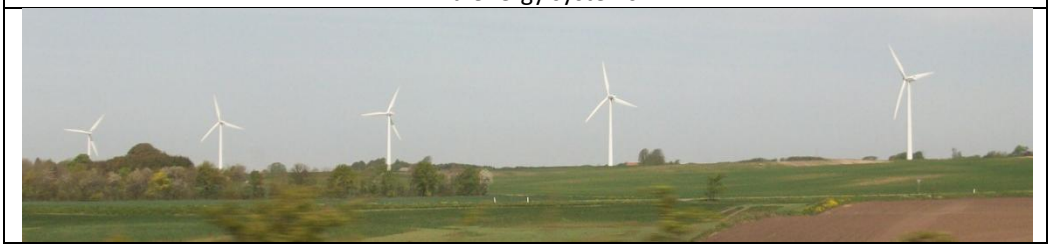

hydrogen	photovoltaic power systems	solar heating and cooling	ocean energy systems
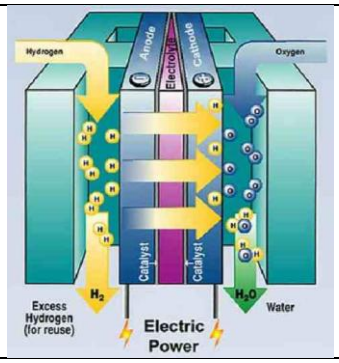	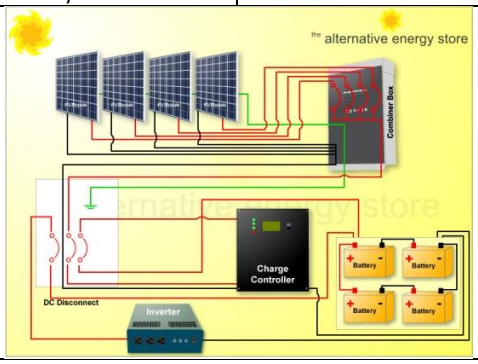		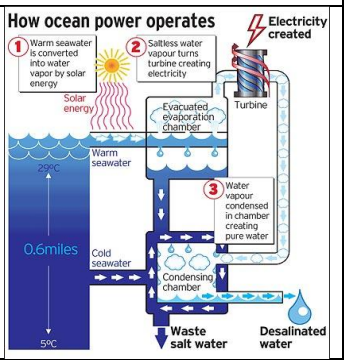

As salt water covers about two-third of the world it seems to be a good candidate to study. Wave and tidal energies are included in the ocean energy, and they are an emerging technology field with considerable promise. Ocean energy innovation and industrial systems are at a relatively early stage of development as compared, for example, to wind power. There is still a wide range of engineering concepts for capturing wave energy, including oscillating water columns, overtopping devices, point absorbers, terminators, attenuators and flexible structures. Tidal current energy exhibits less variety, with most prototype designs based on horizontal axis turbines, but vertical-axis rotors, reciprocating hydrofoils and Venturi-effect devices are also being developed. As related above, all this kind of devices are presented in the next chapter.
Unfortunately, at the moment, none of the technologies associated with these renewable energy source are developed sufficiently to provide a real and fast solution to the world's energy needs, and this means that the research and the funding in this area are recommended to go on.

1.3.1- United Kingdom

In 1956 coal supplied 85% of the UK's energy needs. Then the growth in the use of petroleum for the transport sector, gas and nuclear to generate electricity and gas for heating have seen coal share of energy supplied fall below 50% in 1970 and below 20% in 1996. In 2007 gas supplied 41% of UK energy, petroleum 33% and coal 17% of UK Energy.

Renewable generation made up 5.9% of UK electricity supply in 2008. Provisional results show that UK emissions of greenhouse gases stood at 624 million tonnes of carbon dioxide equivalent in 2008. This was 19% less than 1990, but the rate of decline has slowed in recent years. The British's target is to collect 15% of its energy requirements from renewable sources by 2020.

The UK has the largest wave and tidal resources in Europe, so marine renewable energy is a candidate for contributing to this target. It is estimated that Britain has access to a third of Europe's wave and half of Europe's tidal power resources. As the figure below shows, UK tidal resources are concentrated in 7 main locations while wave resources are more extensive, both in the UK and worldwide.

The UK Government made a number of announcements about marine energy in the UK Renewable Energy Strategy in July 2009, allocating up to an additional £60 million for a suite of measures which will accelerate the development and deployment of wave and tidal energy in the UK, as investment in the New and Renewable Energy Centre in Northumbria, expansion of the European Marine Energy Centre in Orkney, alongside the planned fund in Wave Hub in Cornwall. This will provide the UK with an unparalleled marine energy testing, development and demonstration infrastructure.

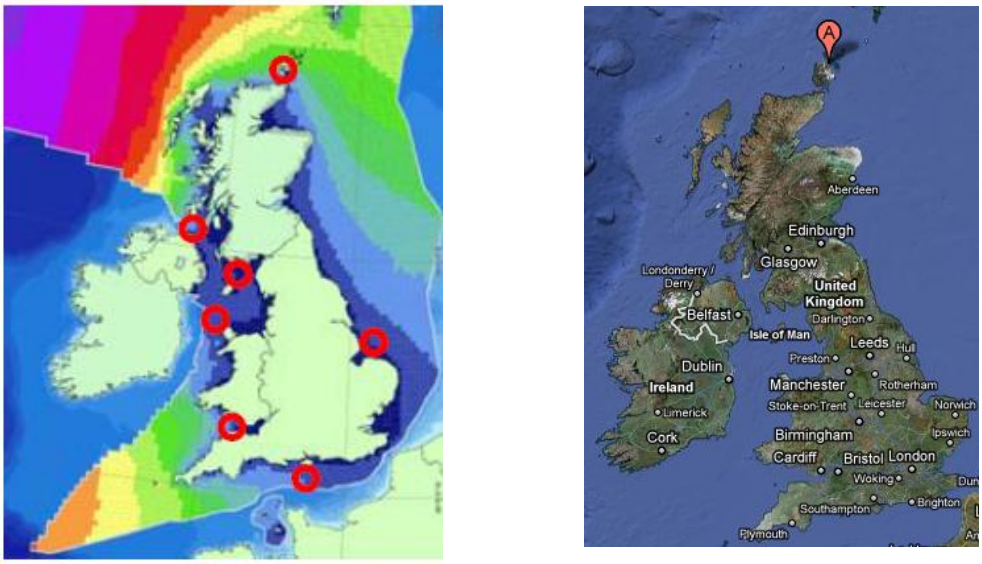

Figure 1.10: On the left: Wave and Tidal Resources in the UK.
Red circles show some of the most significant tidal power sites.
Coloured bands show wave resource, with purple denoting the greatest resource.
Source Parliamentary Office of Science and Technology (postnote January 2009 Number 324 Marine Renewable)
On the right: Position of the Orkney Islands in the UK. Source http://maps.google.com

1.3.1.1- The Orkney Islands

The Orkney Islands cover an area of nearly 975 km^2, comprising about 70 islands of which 17 are inhabited by a population of approximately 20000. With 50 years experience in the renewable sector, Orkney is now recognised internationally as having some of the best resources in Europe for the research, development and testing of wind, wave and tidal technologies. It is estimated that the Orkney Islands could generate 18000 GWh of renewable energy annually and this is reflected in the location of the European Marine Energy Centre (EMEC) wave and tidal test facilities: at a site, tidal steams run at up 4m/s and are among the fastest in Europe; while the wave test site receives uninterrupted waves from across the Atlantic with a maximum wave height of around 15m in the last 50 year.

The small island community of Westray has aims to supply its needs only with renewable energy, with a combination of technologies including a run biogas facility. The number of local businesses and organisations actively engaged in commercial scale on renewable energies continues to grow. To support this project, it has been recently created a master's degree in Renewable Energy at the International Centre for Island Technology. Due to the success of local renewable initiatives, plans are now in place to increase the grid capacity such that Orkney can become a net energy producer to the UK in the near future.

1.3.2- Portugal

In Portugal, the main research and development activities focus on:

- oscillating water column (OWC) plants, in particular concerning the improvement of the operating conditions about the Pico OWC plant that first entered into service in 1999, and also development of equipment as turbines, for this technology;
- one and two bodies floating devices.

In the field of tidal energy, theoretical and numerical work has been carried out on the hydrodynamic modelling of horizontal axis marine current turbines.

Wave Energy Centre (WavEC) is a private non-profit association created in 2003. WavEC's objective is to promote and support the cooperation among companies, research and financing institutions and other entities, aiming at the development, promotion, support for commercialisation and transfer to the industry of wave energy technologies. In the 2009 the main projects were connected to 3 European funded plans:

1. EquiMar – *Equitable Testing and Evaluation of Marine Energy Extraction Devices in Terms of Performance, Cost and Environmental Impact* (FP7-RTD); WavEC leads the environmental research component;
2. Wavetrain2 – *People Initial Training Network Programme of the European Union*; project coordinated by WavEC;
3. CORES – *Components for Ocean Renewable Energy Systems* (FP7-RTD) – WavEC is responsible for developing the numerical wave-to-wire model of a floating OWC system.

1.3.3- Denmark

Plans are being made to create a Danish Wave Energy Centre (DanWEC) for testing wave energy systems in Hanstholm as a next step, following small-scale experiments in the sheltered sea in Nissum Bredning (NB). During 2009, Wave Star Energy A/S installed a 50 kW section prototype in the North Sea in Hanstholm. At the moment three different Danish concepts are installed in NB. Finally, the Lindø Offshore Renewables Centre (LORC) has been founded with the vision to establish a world-class Research & Development centre concernig future offshore renewable energy systems.

Funding for wave energy projects in Denmark can be applied in competition with other renewable energy projects, through different national support programmes, to help companies involved in the project to overcome the difficult phases leading to a full commercial exploitation.

Research & Development activities are carried on via the Public Service Obligation (PSO) on the basis of tariffs charged for the transmission of electricity and natural gas in Denmark.

Energinet.dk administrates the funds and wave energy R&D can be supported within two support strings:

- ForskEL – Supports R&D within environmentally friendly technologies for electricity generation.
- ForskVE – Supports projects with the purpose of spreading small renewable-technologies as photovoltage, wave-energy and biogas.

The programmes cover all renewable energies. Typically wave energy receives less than 5 % of these funds. The Danish Council for Strategic Research and the Danish National Advanced Technology also cover non-energy projects.

The main Danish Universities and institutions active in ocean energy Research & Development projects are Aalborg University and the Danish Hydraulic Institute (DH I) in Copenhagen.
The main wave energy technology projects being developed in Denmark are:

1. Wave Star Energy: A prototype section of the Wave Star converter was installed facing the North Sea in 7 m deep water connected to shore in Hanstholm, in September 2009. The section consists of two floats of diameter 5 m. The project has received funding from EUDP, PSO and private investment. The local electricity company Thy-MorsEnergi is involved regarding the grid connection.
2. Floating Power Plant: Floating Power plant finished the first test at sea in 2009 at the sheltered sea outside Vindeb. This will be followed by a second test starting in spring 2010. In parallel with open sea testing, Research & Development work in wave flumes is being carried out.
3. Wave Dragon: Wave Dragon has been reinstalled in the scale test site Nissum Bredning (NB), the structure has an installed power of 20 kW. The purpose of the extended test is to gain as much data from the device as possible.
4. Dexa: Dexa wave energy converter has been built in scale 1:10 and being tested in Nissum Bredning in 5 meter water depth. The device was installed in March 2009, the Power Take-Off (PTO) has been improved and presently it has been operating successfully for the last two months.
5. Leacon: A 1:10 scale model of the Leacon device has been built and installed with one electrical generator and one pneumatic damper for power dissipation. The device will be installed in the spring of 2010 in Nissum Bredning and join the Wave Dragon and the 1:10 scale Wave Star.
6. Crestwing: this floating WEC has been tested at Aalborg University with positive results in 2009. In 2010 a design study will be carried out including survival and performance testing to evaluate the costs of energy. Depending on the results the next phase could be the building of a prototype.

1.3.4- Italy

Some government initiatives, for example the high incentive concerning the renewable energy, imply an increasing Italian interest in harnessing wave and tidal technologies to produce clean energy.
Many universities and companies specialized in research and innovative design are involved in Research and Development in this field. Italy's major policy to support the deployment of renewable energies is based on a quota system combined with a green certificate trading scheme that became operational in 2001 (introduced by Legislative decree 79/99). During 2009, Law 244/07 has been enacted, which revises the Green Certificates System (GC) and introduces a feed-in tariff mechanism, in particular an increase in the incentive duration, that will be for 15 years, rather than 12 years. The total amount of GCs is differentiated by energy source, according to their technology maturity, so wave and tidal energy receives the higher support. The renewable obligation, set for 2009 at 5.3 %, increases annually by 0.75% up to 2012.
Universities are the key players involved in researches concerning the exploitation of marine tidal and river current to produce energy. Among these, the Alma Mater Studiorum of Bologna, in particular the

Department of Structural, Transport, Water and Survey Engineering (DISTART) is developing a project called “Environmental Design of Low-Crested Structures”. This project is included in the “Theseus Project” which is an European plan born after the consideration that most of the European coasts are highly populated and economically essential, and they are already threatened by coastal erosion and flooding. The aim is to develop an integration approach for the assessment and the management of erosion and flood risk.

Furthermore, the University of Naples “Federico II”, in particular the ADAG research group of Department of Aerospace Engineering (DIAS), in collaboration with *Parco Scientifico e Tecnologico del Molise* (Scientific and Technological Park of Molise), has developed a very attractive project of the last period in the field of renewable energy production using marine source, named GEM.

GEM project consists of a submerged floating body, linked to the seabed by a tether. In this hull there are even electrical generators and auxiliary systems. Two turbines are installed outside the floating body. A special diffuser has been designed to increase the output power for very low speed currents. Due to a relatively safe and easy self-orienting behaviour, GEM is a good candidate to solve some problems involved with oscillating and reversing streams, typical of tidal currents. An additional advantage is the possibility of avoiding the use of expensive submarine foundations on the seabed. After several numerical investigations, a series of experimental tests has been carried out in the towing tank of the Department of Naval Engineering at the University of Naples. Now the full-scale prototype system (100 kW to operate in 2.5 knots water current) is ready to be built and it will be probably installed before the end of 2010 near Venice in a very slow speed current.
At the moment there are other two different projects, which involve the ADAG Research Group of the Department of Aerospace Engineering of the “Federico II” University. They are:

- The FRI-EL SEA POWER System: it consists of a vessel or pontoon, moored to seabed, to which several lines of horizontal-axis hydro turbines are attached. After several numerical simulations, first validation of the studies has been made by testing a prototype of the system in the water towing tank of the Naval Engineering Department of the University of Naples “Federico II”.
- The KOBOLT Turbine is conducted in collaboration with “Ponte di Archimede international SPA”, a company that works in the field of research and development into alternative and renewable energy sources, specialising in the environmental aspects of this work. The Kobold Turbine is a submerged vertical-axis turbine for exploitation of marine currents installed in the Strait of Messina, 150 m off the coast of Ganzirri, since 2002.

2- Marine Energy

As mentioned above, the marine energy is one of the renewable energies, and in the recent years it is in developing, and it could potentially represent a very practical solution. Indeed in accord to what is claimed by the Marine Foresight Panel (UK) it is declarable that "if was possible to turn less than 0,1% of all renewable available ocean energy into electric energy, it would be able to satisfy more than 5 times the present global demand energy". (UK Office of Science and Technology, 1999).

The list of Countries seriously committed in turning marine energy in electricity is growing. It can be asserted that all this Countries are looking for find the greatest way to take profit by the sea respecting the variety of ocean space uses present in this moment. The actual scenario is the need of knowing the right priorities among navigation, fishery, military purposes, renewable energy, oil and gas, aquacultures, etc.

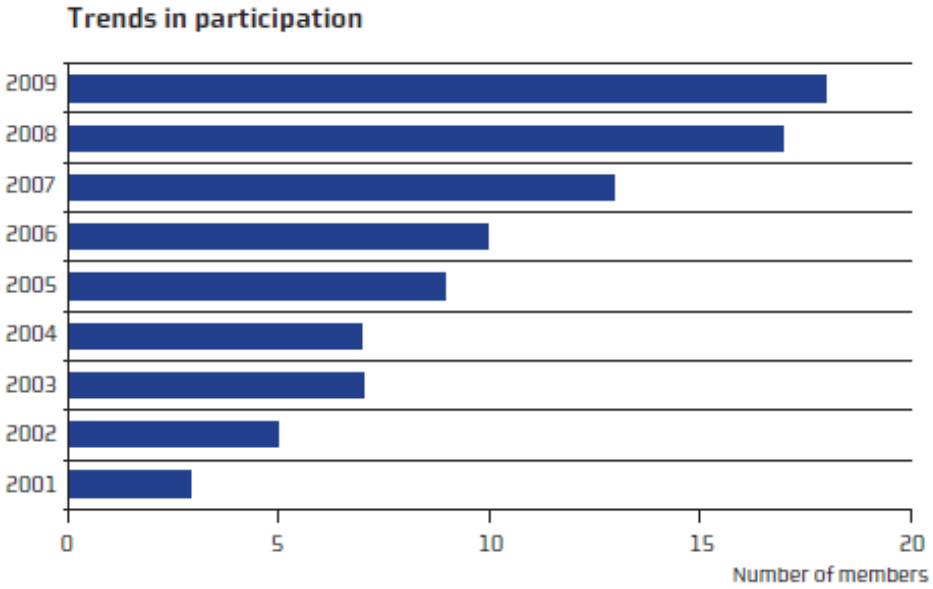

Figure 1.3: OES-IA Membership Growth

Figure2.1: List of the Countries concerned in marine energy, Ocean Energy System source "Annual Report 2009"

The most interesting areas for marine renewable energy conversion, namely shallow to intermediate water depths (30-200m) relatively close to the coast, are intrinsically subject to the highest competition.

It can be affirmed that the main benefits of the ocean energy are:

- the unlimited aspect, i.e. Oceans and Sea cover 2/3 of the World;
- the predictable aspect;
- the renewable aspect, considering the water cycle, it is claimed that a source is renewable when the consummation time is really slower than the production ones;
- zero carbon emission, this last is a truly positive aspect whereas the actual research regard the limitation of the green house effect and fall within the standard set from European Union (EU).

The renewable energy comes from the oceans appears in numerous forms, amongst salinity gradient by osmotic energy, tidal energy, wave energy, different temperature by thermal energy (OTEC) , however the most popular are the wave energy and the tidal energy.

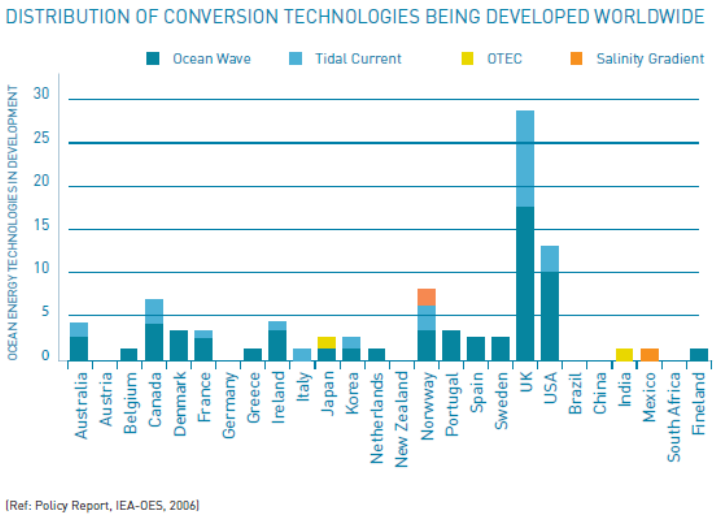

*Figure2.2: Ocean Energy Source "**OCEAN ENERGY** OPPORTUNITY, PRESENT STATUS AND CHALLENGES"*

Figure2.3: Real example of wave energy converter: Wave Dragon, Nissum Brendning, Denmark
picture's source Ocean Energy System "OCEAN ENERGY OPPORTUNITY, PRESENT STATUS AND CHALLENGES"

Figure2.4: Real example of wave energy converter: Pelamis, Northern Portugal
picture's source Ocean Energy System "OCEAN ENERGY OPPORTUNITY, PRESENT STATUS AND CHALLENGES"

Figure2.5: Real example of wave energy converter: PowerBuoy free-floating point absorber, Hawaii
picture's source Ocean Energy System "OCEAN ENERGY OPPORTUNITY, PRESENT STATUS AND CHALLENGES"

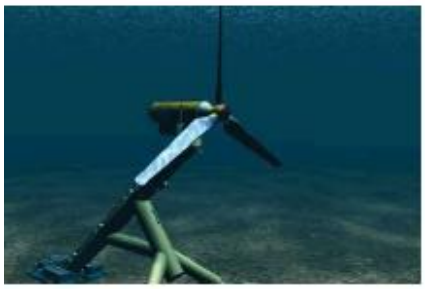

Figure2.6: Real example of tidal current energy converter: The Blue Concept, Norway
picture's source Ocean Energy System "OCEAN ENERGY OPPORTUNITY, PRESENT STATUS AND CHALLENGES"

Figure2.7: Real example of tidal current energy converter: Kinetic Hydro Power System, U.S.A.
picture's source Ocean Energy System "OCEAN ENERGY OPPORTUNITY, PRESENT STATUS AND CHALLENGES"

Figure2.8: Real example of tidal current energy converter: Seaflow, Devon, U.K.
picture's source Ocean Energy System "OCEAN ENERGY OPPORTUNITY, PRESENT STATUS AND CHALLENGES"

Figure2.9: Real example of tidal current energy converter: Enermar System, Messina, Italy
picture's source Ocean Energy System "OCEAN ENERGY OPPORTUNITY, PRESENT STATUS AND CHALLENGES"

Figure2.10: Real example of tidal current energy converter: Open-Centre Turbine, Scotland
picture's source Ocean Energy System "OCEAN ENERGY OPPORTUNITY, PRESENT STATUS AND CHALLENGES"

Figure2.11: Real example of osmotic energy converter, salinity gradient: Osmotic Power, Norway
picture's source Ocean Energy System "OCEAN ENERGY OPPORTUNITY, PRESENT STATUS AND CHALLENGES"

Figure2.12: Real example of thermal gradient OTEC Device Thermo-dynamic Rankine cycle, Japan
picture's source Ocean Energy System "OCEAN ENERGY OPPORTUNITY, PRESENT STATUS AND CHALLENGES"

2.1- Main typology of ocean energy

Even if there are different typology of ocean energy the most popular and widespread are the tidal and the wave energy.

The tide is a natural motion of water masses caused essentially by Moon attraction on the water masses combined with Earth rotation around the Sun. The dissipate energy by tidal movements causes on an infinitesimal level a reduction of the distance between Earth and Moon and a slowing down of Earth. The tidal energy consists in take advantage of the natural potential energy variations associated to the tidal ebb and flow water elevation turns near to shore.

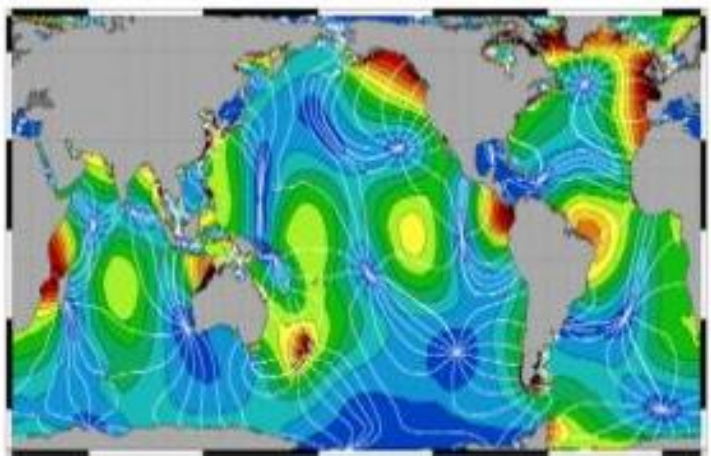

Figure2.13: Tidal Energy Patterns

The colours in the map indicate where tides are strongest, with blues being weaker areas and reds being stronger. In almost a dozen places on this map the lines appear to converge. Notice how at each of these places the surrounding colour is blue. These convergent areas are called amphidromes, places where there is little or no apparent tide. This is not to say that the surface of the ocean in these places doesn't move, or doesn't rise and fall with wind, momentum, inertia, and other forces acting on it. But for the purposes of studying the tides from space in an effort to understand how energy is conserved and distributed, these areas a mathematically still.

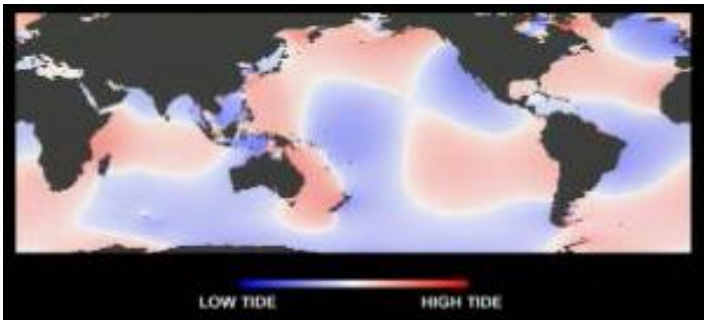

Figure2.14: Tidal Energy Patterns

Even in the last map there is the tidal energy tidal; blue signifies places where the ocean level is lower than the average reference height, and red shows areas where it's higher. Between the darkest blue and the brightest red is a range of more than 15m, displaced by lunar tidal forces. White areas separating the blues and reds approximate the "zero" point, a reference sea level against which other areas are compared. This is called an amphidrome, a place with little or no tide at all.

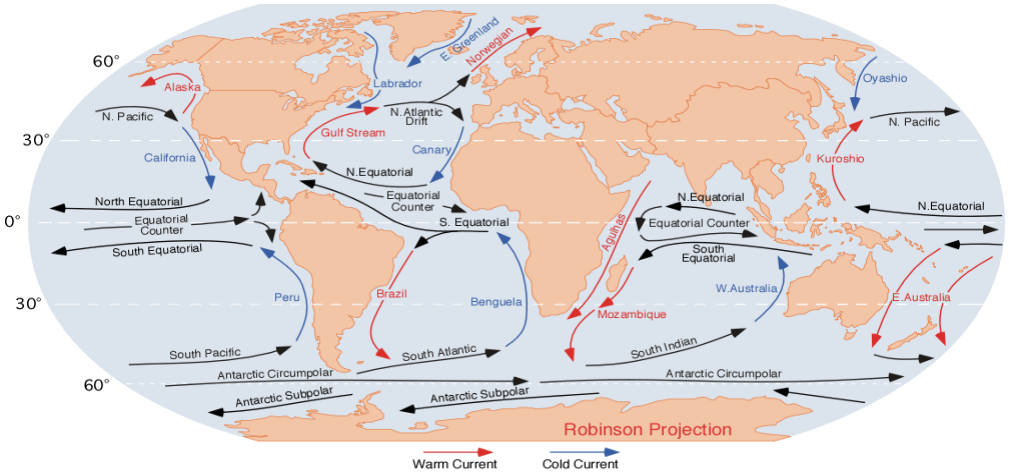

Figure2.15: Map of Surface Ocean Currents.
On this illustration red arrows indicate warm currents, while cold currents are displayed in blue.

Instead, the wave energy is due to the water movement on the sea surface. The wind action on the water surface causes the wave origination and development; since wind is due to the sun action on the atmosphere, the wave are actually a solar energy stock. Under water surface, the individual water particles carry out some circular movements, while the energy transmission is in the same direction of the wave propagation. In the absence of streams no net water movement happens during energy transport; this one is totally different from tidal energy, where water and energy move together. The wave power is expressed in kW per meter of wave crest [kW/m], and its maximum value is around 70 kW/m, usually in the zone between 30° and 60° of latitude, on both hemispheres cause of the wind blowing predominantly from western direction.

Furthermore the wave energy has the vantage to be a concentrated source of energy with lower hourly and daily variations than other renewable resources such as wind, sun or ocean currents.

In addiction the wave energy has the favorable seasonal variations that follows the trend of electricity consumption in Western Europe. Finally, a further advantage of the energy produced by waves is the low environmental impact and visual.

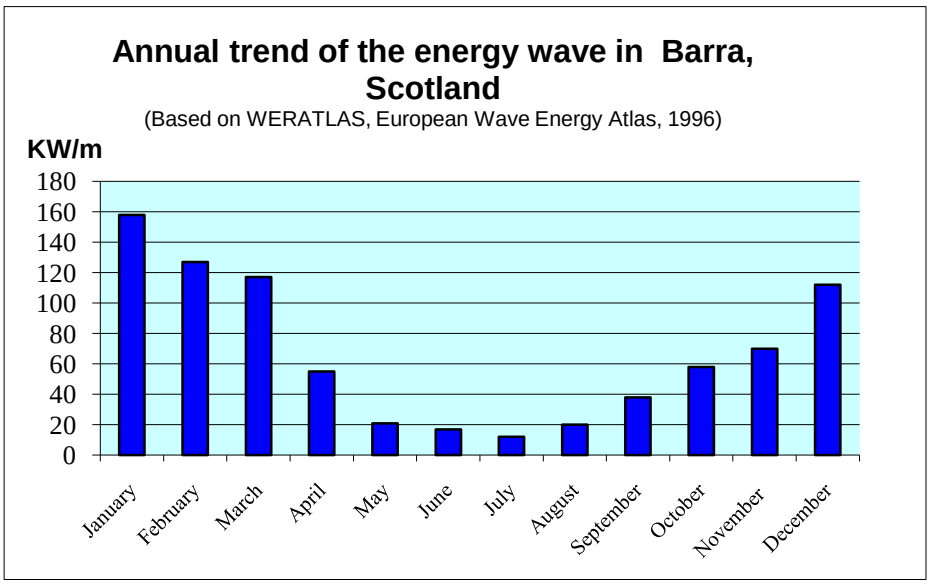

Figure2.16: Annual trend of energy wave in Scotland, source WERATLAS, European Wave Energy Atlas,1996

Fugro OCEANOR is a global provider of integrated real-time environmental monitoring and information systems for oceans, rivers and lakes, groundwater and soil. The systems are often used by institutes to collect data for scientific studies, and are also often used in connection with offshore oil and gas production, harbour monitoring, sea- and fresh-water quality monitoring and weather forecasting.

Based on their global wave data base, OCEANOR have carried out a number of wave energy pre-feasibility and resource studies around the World over the last 15 years. For example a wave energy resource assessment program was carried out during 1987 to 1995 for the South Pacific Applied Geoscience Commission (SOPAC) based in Suva, Fiji with funding from the Norwegian Agency for International Development (NORAD). The aim was to map the ocean wave climate off the shores of several South Pacific island nations with the main objective to evaluate the wave energy resource of the islands needed to study the feasibility of developing wave power as a future clean energy source. The data collection was primarily carried out by moored data buoys off the shores of the following islands in the South Pacific: Rarotonga in the Cook Islands, Kadavu in the Fiji group, Tongatapu in the Kingdom of Tonga, Funafuti in the Tuvalu group, Efate in Vanuatu and Upolu in Western Samoa. Towards the end of the project this information was supplemented by satellite data from OCEANOR's World Wave Atlas data base.

2.2- Wave Energy

Since the primary document's purpose is to study successful the conversion of wave energy to electricity, it is essential to have an adequate knowledge of energy wave.

In all the paper the linear wave theory was used to define the parameters relevant to wave power, due to the reason that in deep sea and intermediate water depth the linear wave theory describes wave parameters sufficiently accurate and in the easiest way.

The linear (or Airy) wave theory describes ocean waves as sum of simple sinusoidal waves. The part of the wave profile with the maximum elevation above the still water level (SWL) is called the wave crest and the part of the wave profile with the lowest depression is the wave trough.

The distance from the SWL to the crest or the trough is the amplitude (a) of the wave and the wave height (H) is defined as the total distance from the trough to the crest, so it is the double of the amplitude. The wavelength (L) of a regular wave at any depth is the horizontal distance between successive points of equal amplitude and phase for example from crest to crest or trough to trough and is defined according to the linear theory by:

$$L = \frac{gT^2}{2\pi}\tanh\left(\frac{2\pi}{L}h\right)$$

Where:

- g = gravitation constant;
- T = wave period (the time required for one wavelength to pass a fixed point);
- h = water depth (distance from ocean floor to SWL);

In deep water where h is large (h/L> ½), the hyperbolic *tanh* function tends to unity and the equation becomes:

$$L_0 = \frac{gT^2}{2\pi}$$

The elevation of the water surface relative to the still water level is indicates with the symbol η, and the equation describing this free surface as a function of time *t* and horizontal distance *x* for a simple sinusoidal wave is shown in the next equation:

$$\eta = \frac{H}{2}\cos\left(\frac{2\pi}{L}x - \frac{2\pi}{T}t\right)$$

The figure below illustrates all the relevant parameters for an oceanic wave, since now described.

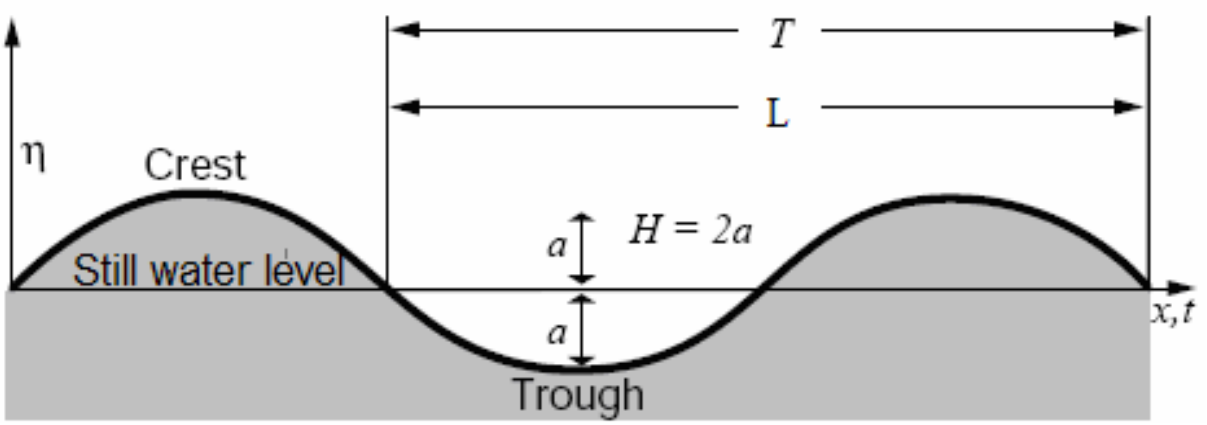

Figure2.17: Main parameters of a wave.

Off shore in a typical wave the molecules of water moving describe circular orbits. This behavior depends on ratio between the wave height and the water depth through the waves move. When the waves approach the coast the orbits change from circular to elliptical. For each wave the major lost of energy happened when it start to warn the seabed and change the shape orbit. The dissipation gets relevant when the water depth is lesser the half of length wave. Many natural factors as refraction and reflection, generate points where the concentration of energy is high, called hot spot.

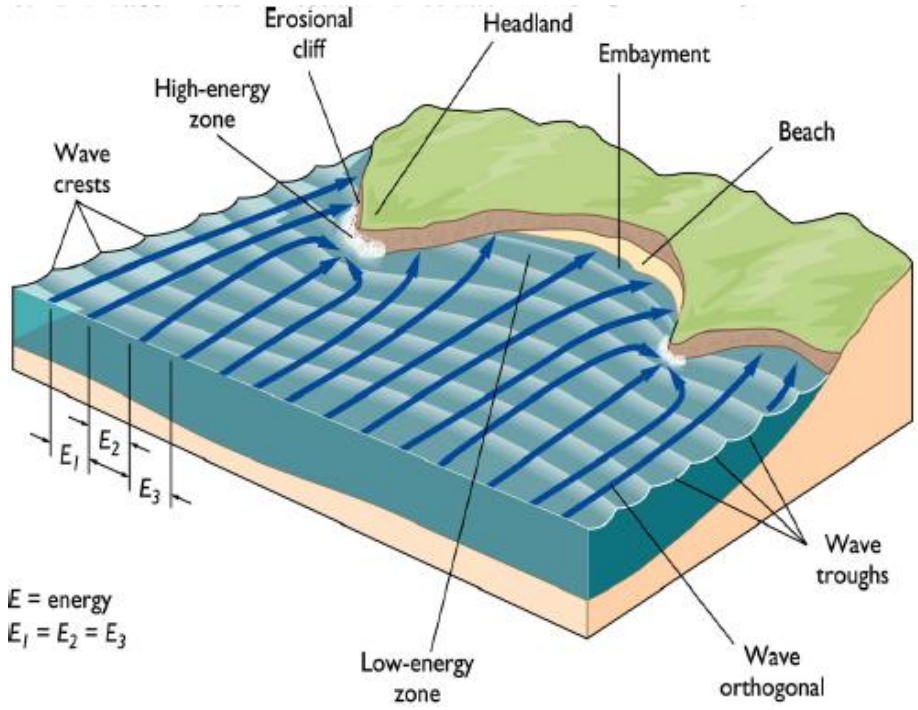

Figure2.18: High-energy zone: Hot spots

The propagation speed or celerity of a regular wave is given by:

$$c = \frac{L}{T} = \frac{gT}{2\pi}\tanh\left(\frac{2\pi}{L}h\right)$$

The rate at which wave energy propagates is directly dependant on the group velocity of the wave. The group velocity (C_g) is given as a function of the velocity of a single wave as:

$$c_g = c * n = c * \left[\frac{1}{2}\left(1 + \frac{4\pi\, h/_L}{senh(\frac{4\pi}{L}h)}\right)\right]$$

In deep water the constant n simplifies to n = 0.5, so the group velocity becomes the half of the velocity of a single wave.

In reality the waves are mostly generated by wind, which exerts a shear stress on the surface of the sea. This effect of friction, combined with air pressure differences between the upwind and the lee side of a wave crest, contributes to transfer energy to the waves, causing their growth. The wave height is determined by wind speed, the duration of time which the wind is blowing, the distance over wind blows (the "fetch"), the depth and the shape of the seafloor. Larger waves are generally more powerful, but wave power is also determined by wave speed, wave length and water density.

However in theory in agreement with the linear assumption there are precise hypothesis stating that the wave power is dependent on energy density and equations to determine energy density is therefore derived in the following section.

The total energy of a wave system is the sum of its kinetic energy and its potential energy. The kinetic energy is that part of the total energy due to water particle velocities associated with wave motion. Whereas the potential energy is that part of the energy resulting from part of the fluid mass being above and below the medium water level.

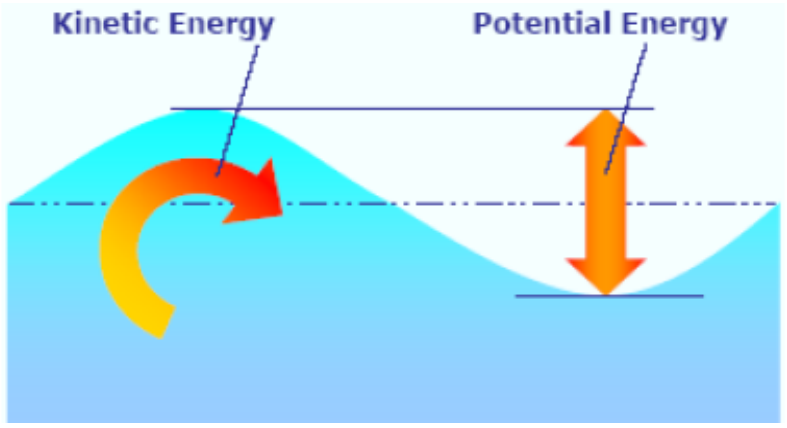

Figure2.19: The two component of the wave energy: the kinetic and the potential energy

The total energy of an oceanic wave is given by:

$$E = E_K + E_P = \int_x^{x+L} \int_{-h}^{\eta} \rho \frac{u^2 + w^2}{2} \cdot dz \cdot dx + \int_x^{x+L} \rho g \left[\frac{(\eta + d)^2}{2} - \frac{d^2}{2} \right] \cdot dx$$

Where:

- E_K = kinetic energy [J];
- E_P = potential energy [J];
- ρ = density of sea water [kg/m^3];
- u = fluid velocity in x-direction [m/s];
- w = fluid velocity in z-direction [m/s].

According to the linearity theory, if all waves are propagated in the same direction, potential and kinetic energy components are equal, and the total wave energy in one wavelength per unit crest width (w_c) is given by:

$$E = E_K + E_P = \frac{\rho g H^2 L}{16} + \frac{\rho g H^2 L}{16} = \frac{\rho g H^2 L}{8}$$

The total average wave energy per unit surface area is called *Specific energy* or *energy density* ($\bar{E}$) and it is given by:

$$\bar{E} = \frac{E}{L} = \frac{\rho g H^2}{8}$$

Wave energy flux is the rate at which energy is transmitted in the direction of wave propagation across a vertical plane perpendicular to the direction of the wave that advances and extends down the entire depth. Assuming the linear theory, the average energy flux per unit wave crest width ($\bar{P}$) transmitted across a vertical plane perpendicular to the direction of wave advance is:

$$\bar{P} = \frac{1}{T} \int_t^{t+r} \int_{-h}^{\eta} p \cdot u \cdot dz \cdot dt$$

Where:

- p = gauge pressure;
- t = start time;
- r = end time.

Integration of the equation that was shown above is simplified to: $\bar{P} = \bar{E} n C = \bar{E} C_g$

The wave energy flux (*P*) is also called *wave power*. The wave theory indicates that wave power is dependent on three basic wave parameters: wave height, wave period and water depth.

Nevertheless the real sea is composed by an irregular wave situations, in first approximation the following formula can be used to estimate the energy flux of an irregular wave in deep water conditions:

$$P = \frac{\rho g^2 T_e H^2}{\beta \pi}$$

Where:

- P= wave energy flux per unit wave crest length [kW/m];
- ρ = mass density of the sea water 1030 [kg/m^3];
- g = acceleration by gravity 9.81 [m/s^2];
- T_e= energy period [s];
- β = is a coefficient may be 64 for irregular waves or 32 for regular waves.

The real sea is random and irregular as it is possible to note in the next two figures.

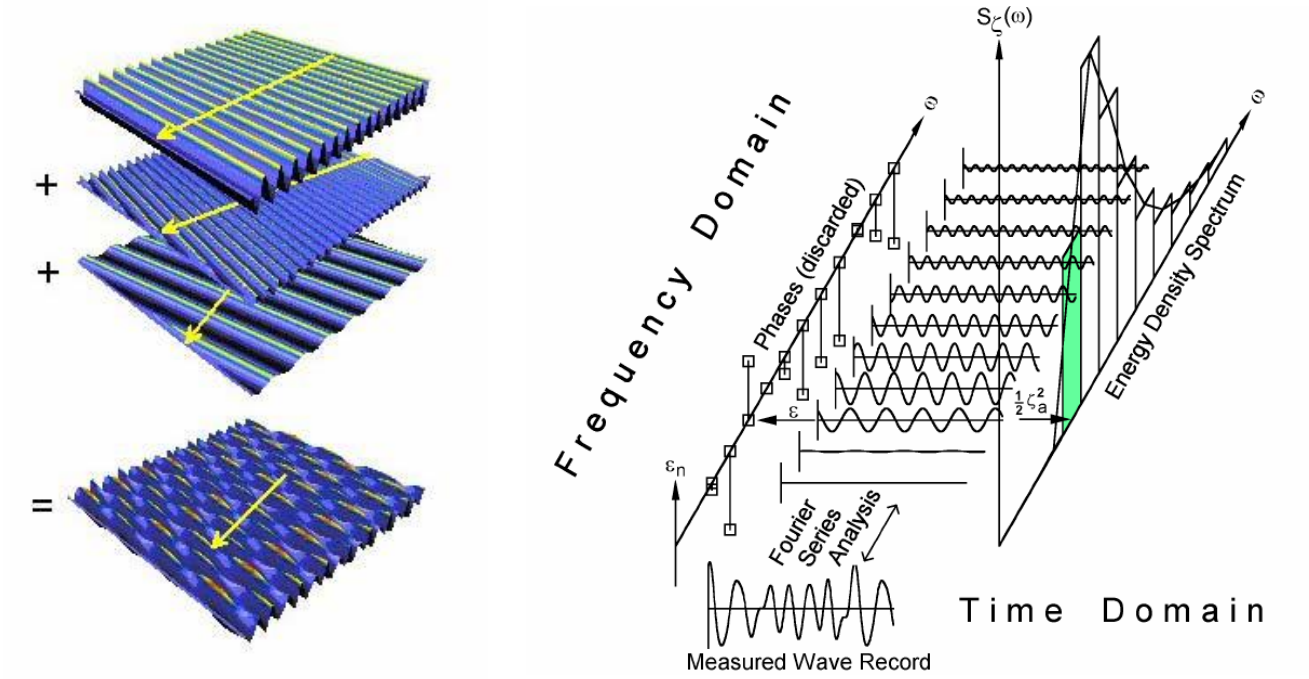

Figure2.20: On the left: Decomposition of a 2D irregular wave state.

On the right: Decomposition of a single irregular wave, it is analyzed as a sum of many single regular waves.

These figures show how random surface elevation records can be deconstructed into a series of sinusoidal components using a Fourier series analysis. Each sinusoidal component has unique basic parameters. Its

amplitude and frequency is used to produce a distribution of wave energy density as a function of frequency. This distribution indicates the variation of the surface elevation of the record from the mean and is called the one dimensional- or frequency spectrum (E(f)).

The inverse of the frequency ($1/\omega_p$) in the recorded wave energy density spectrum at which maximum energy density occurs is known as the peak period (T_p) of the record. This is a very important parameter frequently used in coastal engineering applications.

Another important wave parameter that can be derived from the E(f) is the significant wave height (H_s or $H_{1/3}$), and it is defined as the average height of the highest third wave heights recorded over the sampling period. H_s can also be derived from the variance of the record or the integral of the variance in the spectrum and is then denoted H_{m0}. It is generally assumed that $H_s \approx H_{m0}$ and therefore H_s can determined by:

$$H_s \cong 4\sqrt{M_0}$$

Where: $M_0 = \int_0^\infty E(f)df = \sigma_\eta^2$

$(\sigma_\eta)^2$ is the variance of surface elevation over the recording period.
Where σ_η is the standard deviation of surface elevation over the recording period.

In order to determine wave power for a measured wave record a regular wave height parameter is required containing the same wave energy density as the measured irregular $T_p = 1/\varpi_p$ wave record. This equivalent wave height is known as the root-mean-square wave height (H_{RMS}) and can be determined as $H_{RMS} = H_s/\sqrt{2}$. Similarly to the equivalent wave height parameter, H_{RMS}, a regular wave period parameter is required with equivalent energy density to that of the irregular wave record. The wave period parameter that will be used in the wave power analysis of this study is called the energy period (T_e). T_e effectively divides the energy density spectrum in two halves of equal area, and for this reason T_e is determined by integrating the wave energy density spectrum.

The previous figure illustrates how each sinusoidal component of an irregular sea state has a propagation direction. Wave energy density is thus also a function of direction. Energy density as a function of direction and frequency is called a directional energy or 2D spectrum. An example of a 2D spectrum is shown in the first figure below.

To conclude it is presented the main popular standard spectral. Indeed the wave energy density spectra can be represented by standard spectral shapes, the two most common are the Pierson-Moskowitz (PM) and JONSWAP spectrum. The shape of a wave energy density function is defined in terms of its peak-enhancement factor (γ), and it is the ratio of the maximum energy density of a JONSWAP; a PM spectrum is therefore a JONSWAP spectrum with $\gamma = 1$. The JONSWAP distribution is fetch limited and its peak energy density is spread over a narrower range of frequencies.

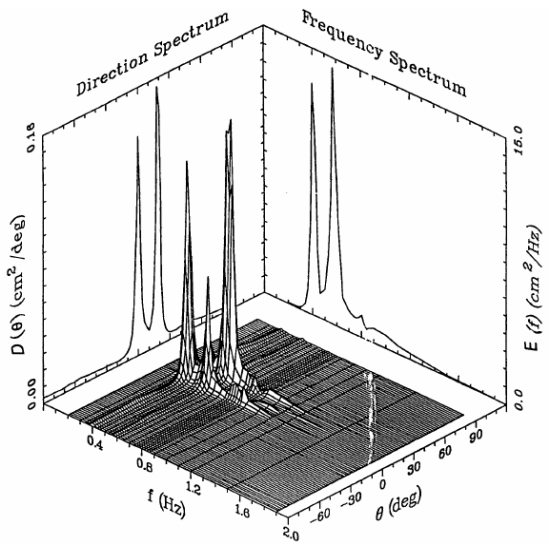

Figure2.21: 2D Spectrum, source Coastal Engineering Manual.

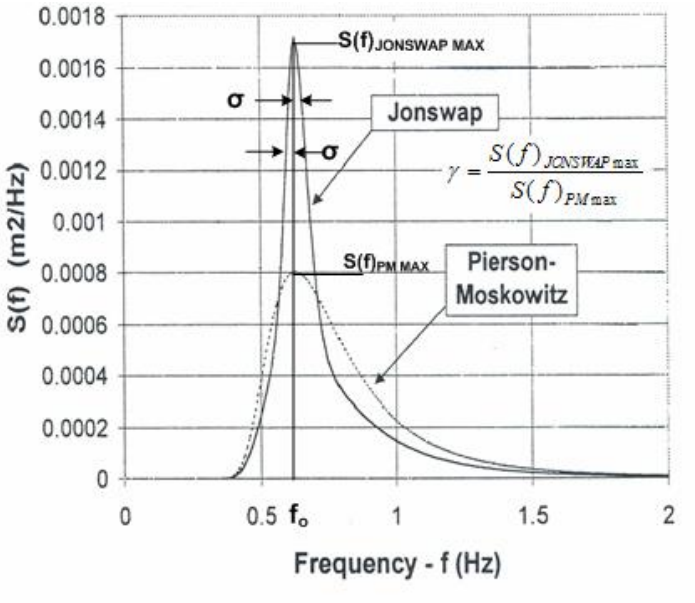

Figure2.22: Pierson-Moskowitz and JONSWAP spectrums, source C.E.M.

In the real sea there is a last aspect to considerate, in particular as the waves approach shallower waters begin to feel the bottom and the wavelength decreases while the wave height increases. This result in increased wave steepness. When wave becomes so steep that it can no longer remain stable, it breaks. Since wave breaking is related to water depth, the height of a breaking wave can be estimated from the following equation: $H_b = 0{,}78 * h_w$

Where:

- H_b= breaking wave height;
- h_w= water depth.

The shallow water breaking wave height is dependent on seabed slope and bed characteristics, and can be affected by strong winds or currents in the direction of the wave propagation. Breaking waves are classified as spilling, plunging, or surging.

The kinematics of breaking waves are not as well understood as the kinematics of non-breaking waves. Since kinematics are the prime factors that control wave induced loads, the loads due to breaking waves are also not as well understood. Reasonable approximations of the forces from a breaking wave are on order of two to four times that of a non-breaking wave.

For that reason the breaking cases won't be study in this project.

2.3- Wave Energy Converter

The potential global wave power has been estimated to be 8^{6}-8^{7} kWh/year (which is equivalent to an installed power generation capacity of 1 to 10 million MW), which is of the same order of magnitude as world electrical energy consumption in the 70's (Isaacs and Seymour, 1973; WEC, 1993).

Next image illustrates the highest wave power zones. In the zone from 30° to 60° north and south latitude is found the highest annual average power level, that is between 20 to 70 kW/m or more. However, significant wave climates are still found within ± 30º latitude where regular trade winds blow; the lower power levels being compensated by the smaller wave power variability.

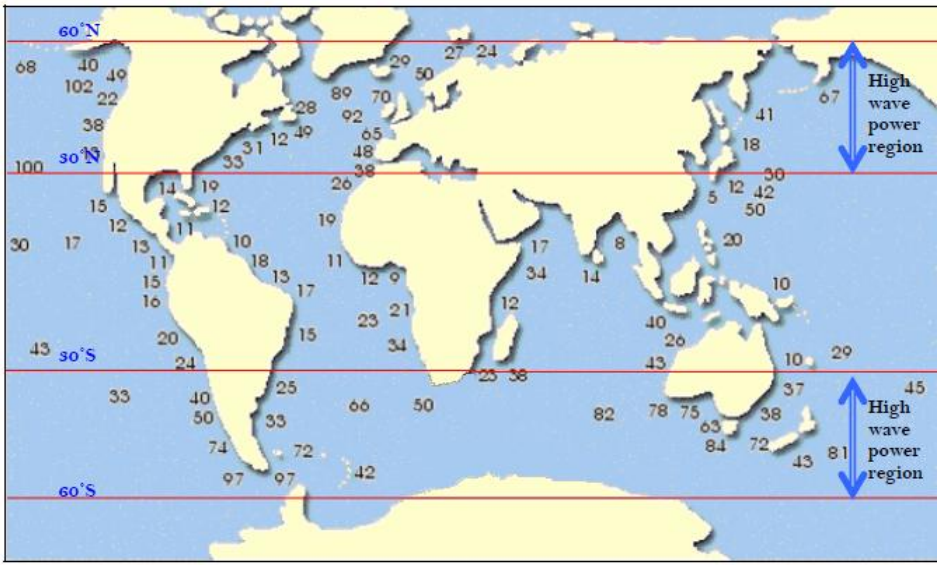

Figure2.23: Average annual ocean wave power in kW/m, source ww.oceanpd.com/Resource/Worldresourcemap.html

The map illustrates that the most energy rich coastlines in the world are Chile, South Australia, New Zealand as well as parts of Western Europe, notably Ireland, Scotland and Iceland as well as western Canada and South Africa.

This does not necessarily mean that these areas have the highest potential for wave energy exploitation. Several of these areas are isolated with poor communications. The highest potential at the first stage for wave energy is probably areas such as islands in the trade wind belt of the Pacific, where overall wave energy is much lower but considerably more steady both in strength and direction.

North-east Atlantic area (including the North Sea) offers the availability of wave power of 290 GW, with annual variations ranging between 25 kW/m in the area further south on the Atlantic coast, to 75 KW/m corresponding to the Irish and Scottish coasts. In the North Sea, the energy source undergoes strong fluctuations, ranging from 21 KW/m, in the most exposed (north) to a level of 10 kW/m.

Figure2.24: Europe: Average annual ocean wave power [kW/m]

Wave energy conversion is not a new concept, in fact, the first patented Wave Energy Converter (WEC) is dating back to the early 18th century. As presented in the previous chapter, the high oil prices in the 1970's forced governments of the world to consider alternative sources of energy. During this period ocean energy was identified as one of alternative extractable sources. This lead to world-wide research to the field of wave energy conversion.

However until post-2000 there existed few large-scale sites where wave energy machines could be tested, and only two sites were available pre 2000: both of these were in Denmark and at that time they were not registered externally as official test centres.

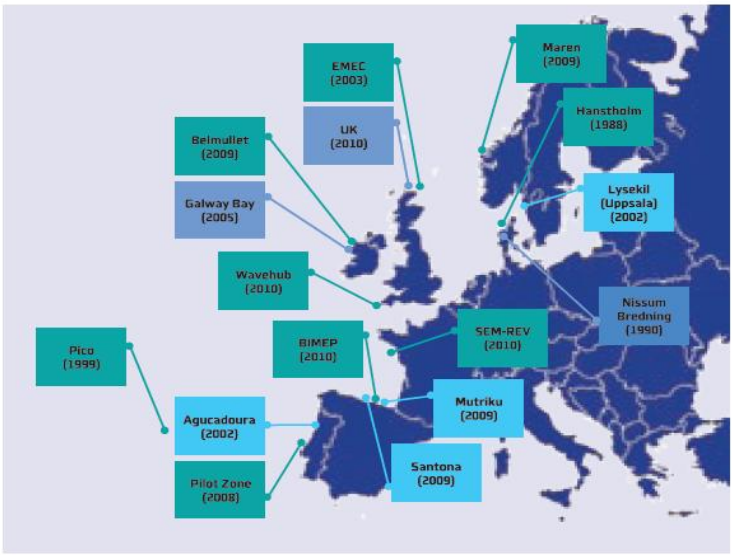

Figure2.25: Europe's map: Wave Test Centres

Even though wave energy is not a new search field, non formalised guidelines or recommended procedures or best practice manuals appeared until 2003. Until that time the vanguard companies had to design their own development schedules and test programmes on an ad hoc basis, and usually in isolation from each other.

Most of the initial investigation took place in the UK, and in the early 1990s the European Union became interested in the potential of ocean power supplying electricity into the member states energy portfolios. One of the first proposals supported was the Offshore Wave Energy Converter Project (OWEC1). A test programme was documented in 1995. However, nothing was advanced on this report and the schedule did not become a standard approach to be applied throughout the member states researching the area.

The OWEC1 development schedule was used as the framework for the Irish Wave Energy Development & Evaluation Protocol published and implemented in 2003 and the Danish wave energy programme, 1998-2002.

Now in Denmark there is a particular and standardized assessment to determine the benefits and the performance of new wave energy converters. This evaluation is constituted by four phases, and it is used in the next chapters. These phases are:

1- Phase 1: Proof of concept. Rough estimates of energy production in five specified wave states leading to an estimate of a yearly energy production. Suggestions for further development of the device. Typical small indicative laboratory tests followed by a 10 page report. Cost 10.000 €.
2- Phase 2: Design and feasibility study. Typically through detailed laboratory tests in scale 1:50 to 1:20. Detailed Numerical calculations, estimates on cost, feasibility studies, Power take-off (PTO) design, etc. Typical intensive laboratory tests (optimizations) or intensive numerical modelling. This phase can consist of detailed investigations followed by 100 page reports. Cost 25.000-50.000 €.
3- Phase 3: Testing in real seas in scale 1:10 to 1:3. Normally Nissum Bredning where a “small” benign piece of inner sea, a part of the Limfjord in the northern part of Denmark , has been used for this purpose. Cost 0.5-5 million €.
4- Phase 4: Demonstration in half or full scale. Cost 5-20 million €.

The main instrument used under phase 1 and phase 2 to assess the wave energy devices is small scale testing in a hydraulic laboratory. These tests are performed in order to gain knowledge on the devices before they actually are built and deployed in the sea. The laboratory tests will give information on:

a. Loads on the device
b. Movements of the device
c. Run-up / overtopping of the device
d. Energy production

In phase 1 assessment, the test will give rough estimates (± 20%) on energy production. The main idea of the Danish practice is that each of the phases should provide valuable information for the developers and investors, before the project is taken to the next phase. Thus, the risk of using unnecessary resources on a device before reliable estimates of the concepts potential is known and it is thereby minimized. Furthermore, it eases the comparison of various projects at the same phases of development.

2.3.1- Classification of the Wave Energy Converters

There are various ways of classifying WEC's. The most common classification in literature is to describe a WEC in terms of its deployed location. The three main location categories are ***on-, near-*** and ***offshore***.

It has been suggested that a distance of almost 23km (12 miles) from shore is the distance within which a device is said to be near shore. Installations of devices near-shore operations should consider the aesthetic influence that they will have on what could be a picturesque area, moreover they also will have a definite impact on shipping and marine life, but this will be no greater than the offshore installations.

It has been suggested that a depth greater than 50m will constitute an offshore device. Any devices off shore can have an effect on the aquatic life in that area, but this is very site specific and hard to predict. But anchoring systems can become almost like artificial reefs, creating a place for new colonisation.

On shore wave power will have a marked effect on the area it is deployed. There are ways of incorporating it into existing structures to minimise the effect, such as harbour walls. Wave devices that are on-shore have social implications for the surrounding area. They can create employment in the area and attract visitors. Devices that are on-shore can have environmental benefits, such as helping to reduce the erosion of the landscape.

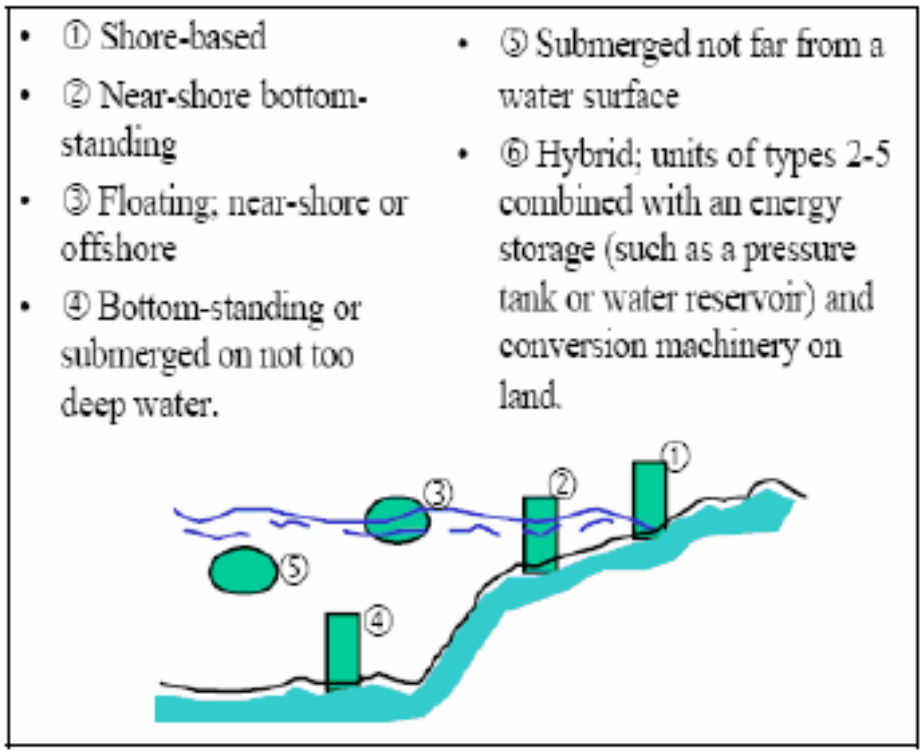

Figure2.26: Cataloguing of the WEC based on the location (Falnes, 2005)

Another classification method is to describe the WEC in terms of its size and orientation. In this classification type there are three categories. A WEC can be classified as a ***point absorber, attenuator*** or ***terminator***.

A point absorber is a relatively small device compared to a typical wavelength. A point absorber is a floating structure which absorbs energy in all directions through its movements at/near the water surface. The power take-off system may take a number of forms, depending on the configuration of displacers/reactors.

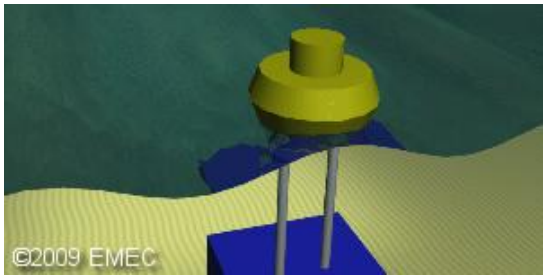

Figure2.27: Point Absorber, source EMEC

An attenuator is a floating device with a length equal to/ or greater than one wavelength. This type of device is aligned in the direction of wave propagation, so it works parallel to the wave direction. If this same device is aligned perpendicular to the direction of wave propagation it is called a terminator device.

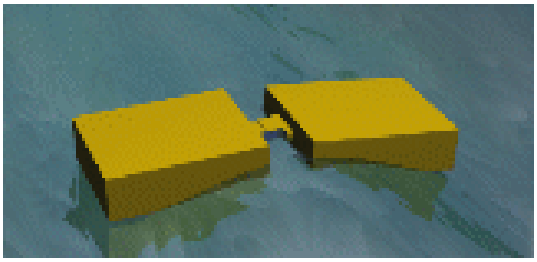

Figure2.28: Attenuator, source EMEC

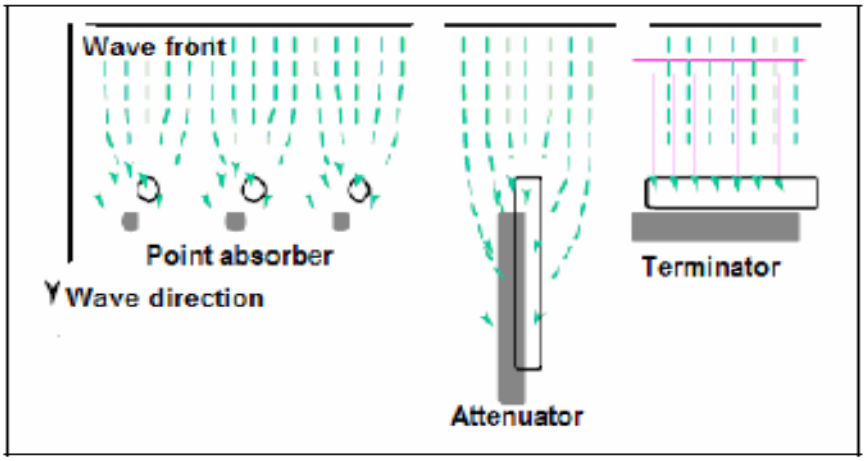

Figure2.29: Second classification of the WEC based on the orientation (Falnes, 2005)

A further classification of WEC units is based on technology with regards to its basic principle of energy extraction. The classification categories include:

1. **Overtopping Devices (OTD),** they are device able to convert the potential energy of the water in electricity, as a small hydro power scheme. The ocean waves are elevated through a ramp and focus into a storage reservoir above the sea level. As more water enters into the reservoir, an equal amount of water is forced through the turbines, that are usually low head Kaplan turbines. The water entrance causes the rotation of the turbines and consequentially the electricity generation. The difference water level between the reservoir and the sea is continuously annulled, because the water passing through the turbines returns to the sea. The efficiency of the hydro power plant component of the system is high (up to 80%) and this will minimise overall losses of the system.

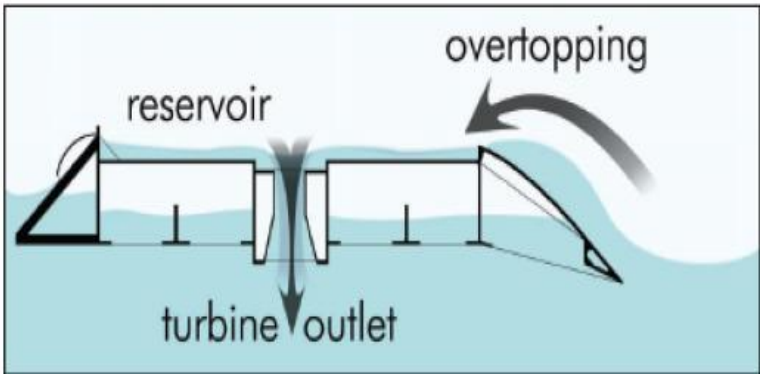

Figure2.30: Typical representation of a Overtopping Device

The overtopping devices can be allocated on-shore or off-shore. One example of on-shore OTD is the SSG, i.e. Seawave Slot-Cone generator.

Figure2.31: On the left: Section of the SSG, on the right: possible installation as a breakwater

Whereas one example off-shore is the Wave Dragon.

Figure2.32: Wave Dragon is an off-shore OTD

2. **Wave Activated Bodies (WAB) Device**, they are also called two-bodies devices, because the peculiarity of this kind of devices consists in the relative motion between the component parts of the devices themselves. The oncoming waves activate the oscillatory motions between the parts, or one part relative to another fixed part. By using an hydraulic system it is possible to convert the relative motion into electricity by a turbine activated by the pressured fluid, who comes from the hydraulic system. If this kind of devices is placed in a perpendicular direction with the wave direction it becomes even a terminator, while if it is parallel it is even an attenuator. Common examples of Wave Activated Body (WAB) are Pelamis, AquaBuoy, DEXA.

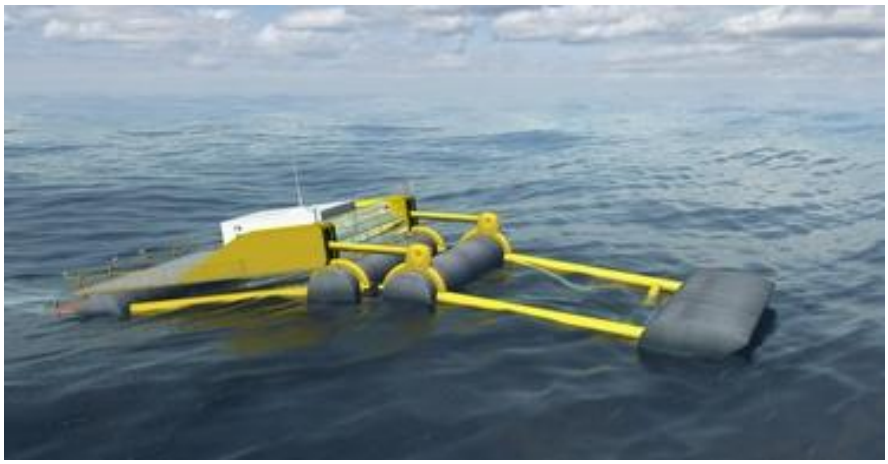

Figure2.33: DEXA is an example of Wave Activated Body, source www.dexawave.com

A subset of the Wave Activated Body is the **Submerged pressure differential**. These devices are typically located near-shore and attached to the seabed. The motion of the waves causes the sea level to rise and fall above the device, inducing a pressure differential in the device. The alternating pressure can then pump fluid through a system to generate electricity.

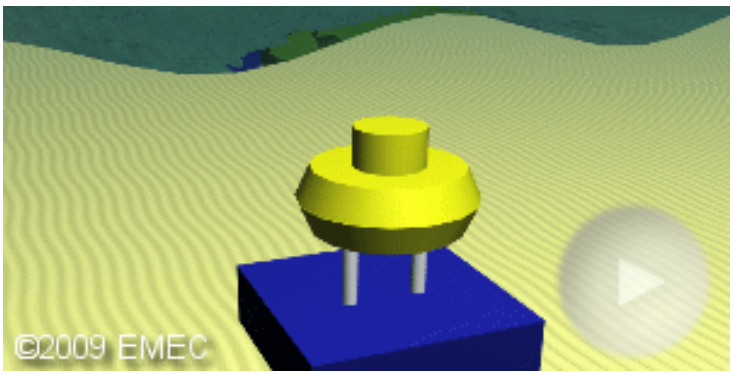

Figure2.34: Submerged pressure differential, source www.emec.org.uk

3. **Oscillating water column (OWC) Devices**, they are one of the most common devices for the energy production, because since 1980's some prototype of OWC are developed in several places in the world, so the engineers have for this technology a great experience. The study of this category is well delved because the device under consideration belongs to this category. Usually an oscillating water column is a partially submerged and hollow structure. It is open to the sea below the water line, enclosing a column of air on top of a column of water. Waves cause the water column to rise and fall, which in turn compresses and decompresses the air column. This trapped air is allowed to flow to and from the atmosphere via a turbine, which usually has the ability to rotate regardless of the direction of the airflow. The rotation of the Wells turbine is used to generate electricity. The main benefits of OWC technology include the following:
    - shore based OWC devices provide easy access for operation and maintenance work;
    - the near shore location reduces transmission costs;
    - OWC devices can be incorporated into breakwaters and can be used to create calm sea areas.

    Some disadvantages associated with OWC devices are:

    - the available wave power resource is less in the near-shore zone compared to off-shore one due to energy dissipation processes;
    - an OWC being a terminator device can disrupt sediment transport processes by reducing the wave power reaching the shore;
    - most OWC devices are non-tuneable and this reduces the system's overall efficiency;
    - shore based OWC structures can have a visual impact if they are not submerged.

    Familiar Oscillating Water Column (OWC) Device is the Limpet.

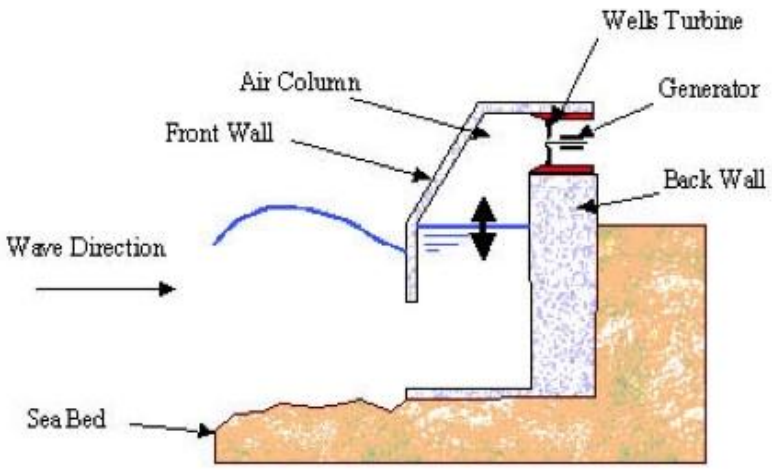

Figure2.35: Oscillating Water Column, source renewable energy journal, mechanical ocean energy conversion, part II

A subset of the Oscillating Water Colum is the **Oscillating Wave Surge Converter (OWSC)**. This is a new shore-line or near-shore wave energy converter. The concept has developed from an analysis of the performance of the LIMPET shoreline oscillating column.

This analysis shows that the hydrodynamics of shoreline wave energy converter are highly non-linear, and they have a qualitatively different response to similar device that are sited in deeper water. In particular, the water particle motion in shallow water is predominantly horizontal. The OWSC are designed to use the horizontal particle motion, so permitting large amplitude of motion.

The larger horizontal water particle motion in shallow water suggests that the working surface of the wave energy converter should not move only in an approximately horizontal plane, and to minimise the required volume of displacement, this suggest a relatively thin paddle. The horizontally aligned slides and straight-line mechanisms are likely to be costly and difficult to maintain, hence the easiest choice can be between hinging the paddle at the top or bottom. If the hinge point is above the water surface it is possible to match better the average horizontal water particles motion, and in addition there are the benefits of having a power take off more accessible and the no "end-stop" of the paddle.

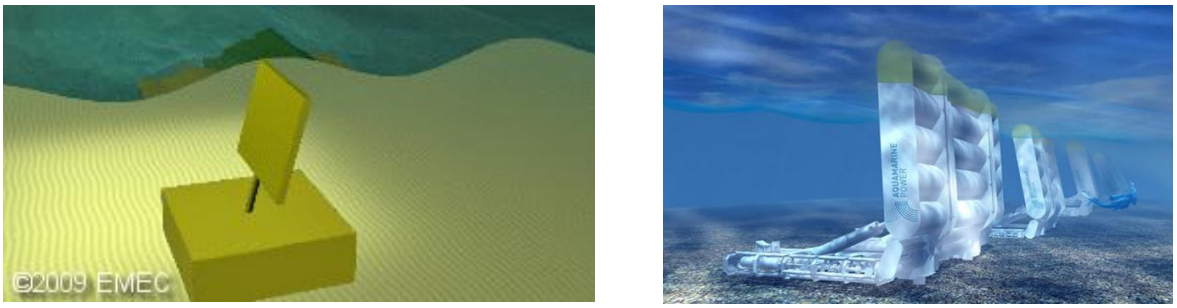

Figure2.36: Oscillating Wave Surge Converter: scheme with the paddle hinged at the bottom, source www.emec.org.uk

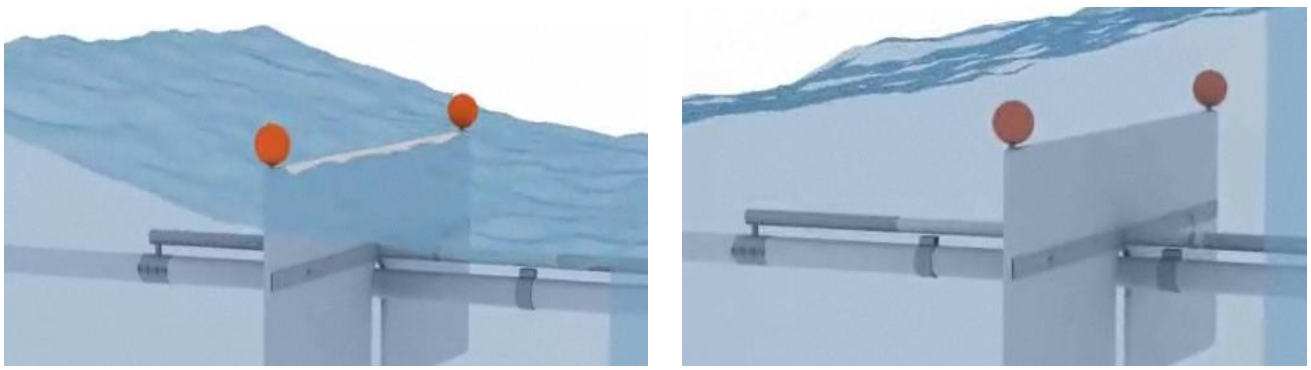

Figure2.37: Oscillating Wave Surge Converter: scheme with the paddle working with a straight-line mechanisms Units of the WavePiston Device, source www.wavepiston.dk

Furthermore the potential for the OWSC resides even in low construction and maintenance cost and in the price for generate the electricity; in fact even if the OWC technology is inviting for its simplicity, it has the problems in the low air turbine efficiency and in the not well-known hydrodynamic of the water column in shallow water. Consequently the wave energy research at Queen's University Belfast started to developed a new kind of device called OWSC. A number of distinct embodiments of the OWSC can be envisaged. These different embodiments all exploit the beneficial hydrodynamics of the paddle and the water column, but differ in how this is achieved and consequently in their construction and performance.

Even though there are many classes to which a device can belong, there are some device that due to their unique different design or characteristics cannot be included in any class.

Regardless of the class, to design a device is necessary to take care in the material choice. The durability aspect is crucial, the device have to withstand storm, high seas and corrosive salt water and their maintenance cost are really high.

2.3.2- Examples of the Wave Energy Converters

2.3.2.1- LIMPET

LIMPET stands for "Land Installed Marine Powered Energy Transformer". The LIMPET is a 500 kW OWC developed by the Queen's University of Belfast and Wavegen Ltd in the United Kingdom. It was installed on the Isle of Islay off the west coast of Scotland and was commissioned in November 2000.

The collector structure consists of reinforced concrete chamber and it has cross sectional dimensions of 21mx 7m. The structure is very robust in order to survive extreme loadings with 0.75 m thick walls. The airflow caused by the oscillating water column drives two Wells turbines each with a 250 kW capacity and a blade diameter of 2.6 m. The turbine has to be able to generated energy turning regardless of the direction of flow of air.

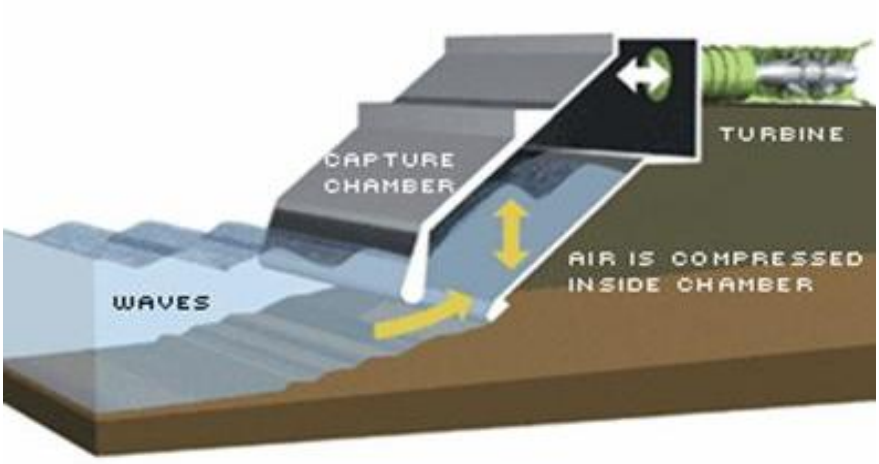

Figure 2.38 : LIMPET's section

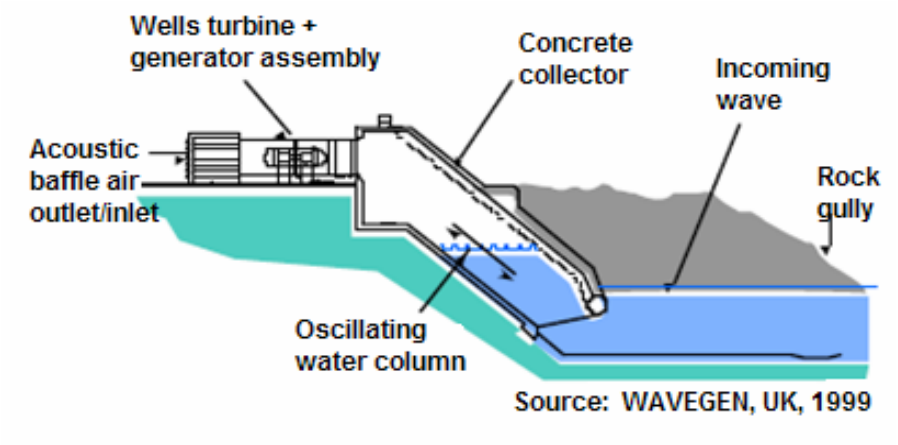

Figure 2.39 : Cross sectional view of LIMPET

Figure 2.40 : Real view of LIMPET

The available annual average wave power resource in the deployment area is 20 kW/m and the water depth is six meters.

This device is currently generating 0.5MW of power that it supplies to the grid on the Island of Islay off the west coast. This is an example of how this technology can be used to meet small-scale local needs. Wavegen have said that at present the answer lies in not huge operating plants but small ones such as these, which can concentrate on meeting local or regional needs.

It is possible to calculate how many homes it will supply, in following calculations were made with this aim.

max electricity generated [kWh/year]	500
max electricity generated [MWh]	=500*8760 = 4380
Load factor or capacity factor	0,40
Electricity generated per year [MWh]	=4380*40%= 1752
Average annual household consumption [kWh/day]	12
Average annual household consumption [kWh/year]	4377
Number of houses	$=1752*10^3/4377= 400$

Table 2.1: Quick overview of the LIMPET performance

2.3.2.2- PENDULOR

The “Pendulor” consists of a caisson with a top hinged paddle at the mouth of a water chamber. The length of the chamber is ¼ of a wave length to produce harbour resonance. Unfortunately, typical wave periods where wave energy converter are likely to be sited, would result in un-economically long water chambers.

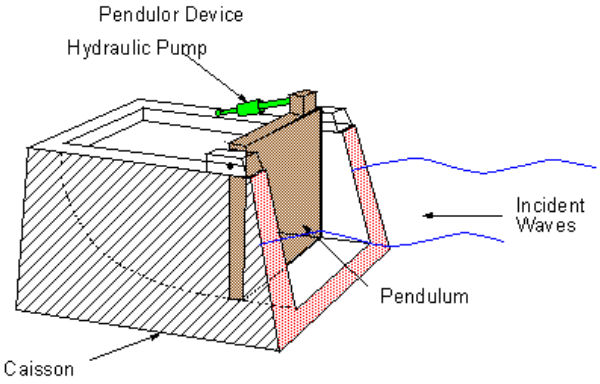

Figure 2.41 : Pendulor’s scheme

2.3.2.3- WAVE DRAGON

The Wave Dragon is an off-shore reservoir storage WEC. This typology focus waves into a storage reservoir and from here the stored water flows through low head turbines to generate power, similar to a small hydro power scheme. The WAVEDRAGON is a floating and overtopping WEC device. It consists of two parabolic reflecting arms, a double curved overtopping ramp, a storage basin and multiple low head turbines. The reflecting arms focus waves onto the overtopping ramp and into the storage basin above sea level. From the basin the water flows through modified Kaplan-turbines and generates electricity. This device is slack moored and can orientate itself to face into the dominant wave direction. The structural components of the WAVEDRAGON consist out of steel and reinforced concrete. The reservoir storage ranges from 5000 to 14000 m^3. It is designed to operate in water depths greater than 25 m.

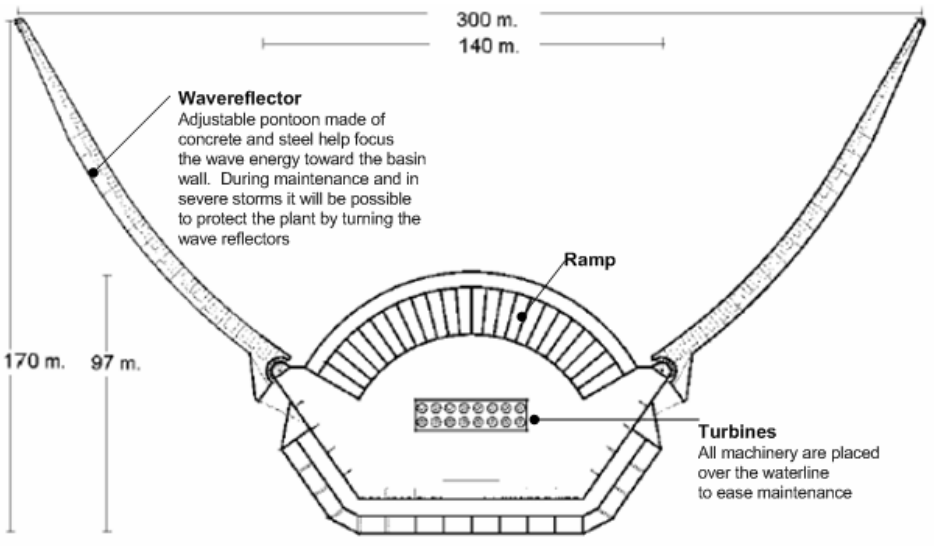

Figure 2.42 : Wave Dragon representation

2.3.2.4- PELAMIS

The PELAMIS is a WAB device. Usually the WAB device generate energy giving pumped fluid to a turbine. The pumped fluid is obtain by the relative motion of a component relative to another device component. The word “pelamis” is Latin for sea snake. The PELAMIS WEC is a floating device consisting of four tubular sections connected at three hinges. These tubular sections move relative to each other as a wave crest passes under it and power is generated through a digitally controlled hydraulic power conversion system. The device is slack moored enabling it to orientate itself into the direction of the most dominant wave conditions. The PELAMIS unit has a diameter of 4.6 m and a length of 150 m. It is designed to be deployed in water depths deeper than 50 m.

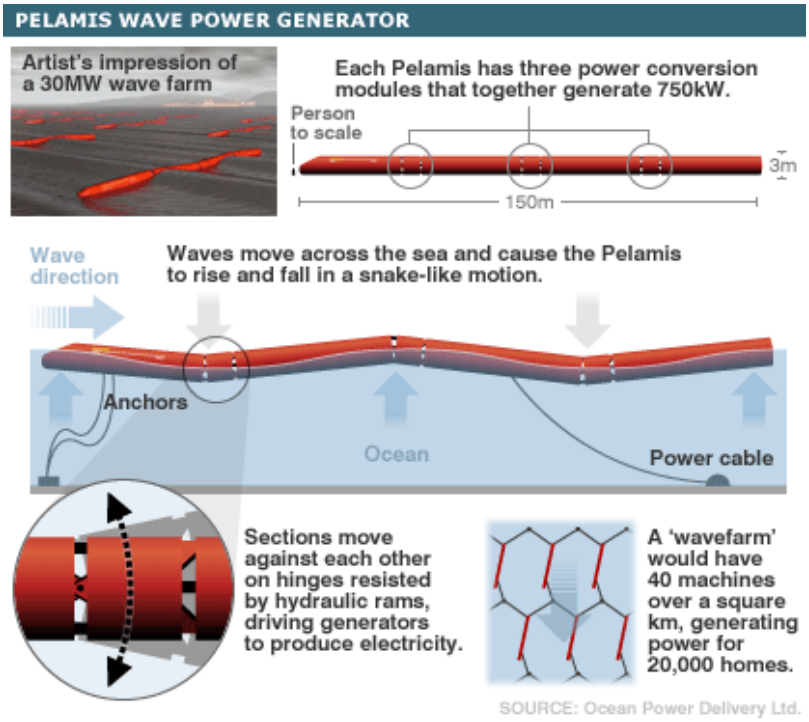

Figure 2.43 : PELAMIS – Schematic representation

2.3.2.5- SWEC

The SWEC comprises of a pair of collectors (arms) coupled in a V-formation to a single air turbine and power generator mounted above water level in a tower at the apex of the V. Each collector arm has OWC chambers and the pressurised air is send along the arm to the power generator in the tower. This is a near shore system founded on the seabed in water depth of between 15 to 20 m.

The design length of a collector arm is 300m with a 30° inclination angle to the shore. This gives the system an effective width of 350m for power extraction.

The SWEC looks like the LEANCON, the main difference is that the LINCON is a floating device.

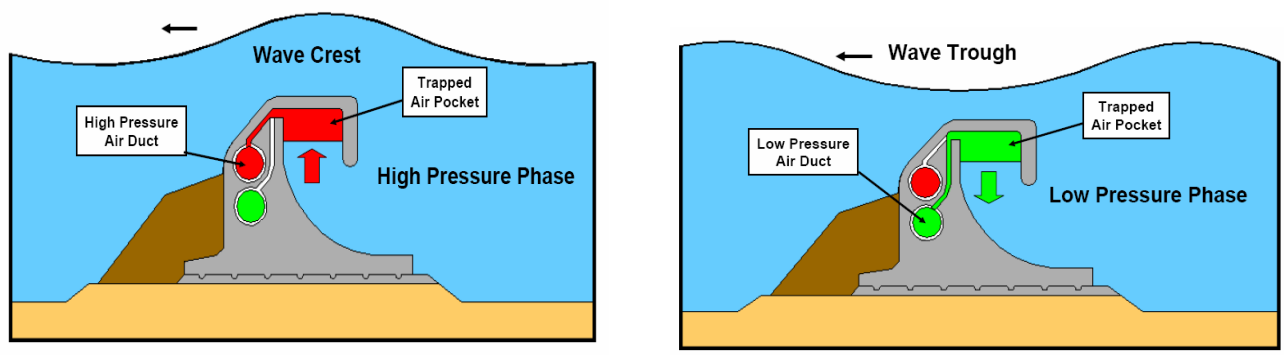

Figure 2.44 : SWEC's pressure system

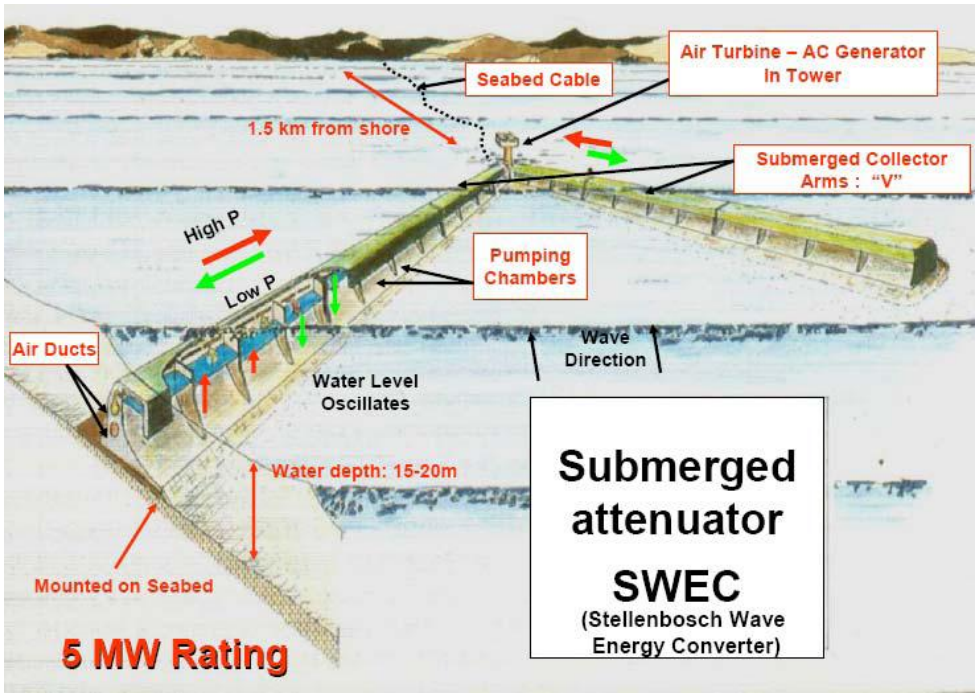

Figure 2.45 : Overview of the SWEC

3- WavePiston Device

3.1- The real WavePiston

The WavePiston is a new wave energy converter(WEC) and belongs to the category of the oscillating wave surge converter (OWSC).

Usually, for the WECs belonging to the OWC, the way to harness energy consists in using a device that makes a vertical translational motion as a normal floating point.

The particularity of the WavePiston lies in the type of displacement that it uses to produce energy: an horizontal translational motion. The WavePiston harvests energy along a string having a length equal to or larger than a typical wave length.

In the water, in a vertical plane perpendicular to the wave movement, the motion of all the particles in this plane is parallel within a reasonable depth range.

Whereas, if the plate in a plane not vertical, for example horizontal, the motion of the particles in the plate will be multidirectional, and the overall movement of the device is not a simple horizontal translation.

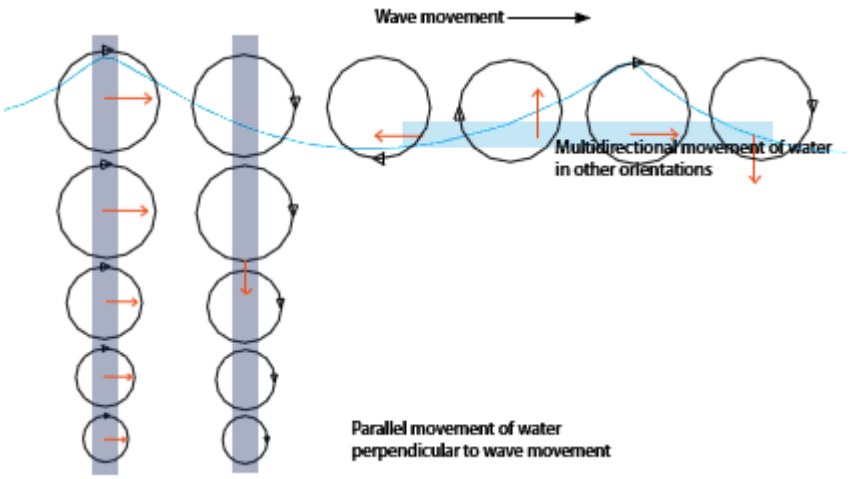

Figure 3.1: motion of the water particles

Hence, in the WavePiston there is a large, but thin plate in the vertical position and that plate will make a motion back and forth in a linear way, and so the forces are all pushing in the same direction.

In the reality, the WavePiston works by the mechanical movement of the collector elements pumping pressurized sea-water into a string upon which the collectors are mounted, and the pressurized water can easily be used for power generation.

Furthermore, the water pressure can be controlled on shore by shunting the flow from the incoming pipes.

If the WavePiston system is deployed in coastal waters, the necessary turbine and power conversion systems (PTO) could be placed in the same structure onshore, so that the system can be controlled under all conditions and even more, that will reduce the total cost.

The WavePiston system should be build from prefabricated modules that can be mass-produced at a low cost. Each module consists of an energy collector and a piece of the static structure (pipe).

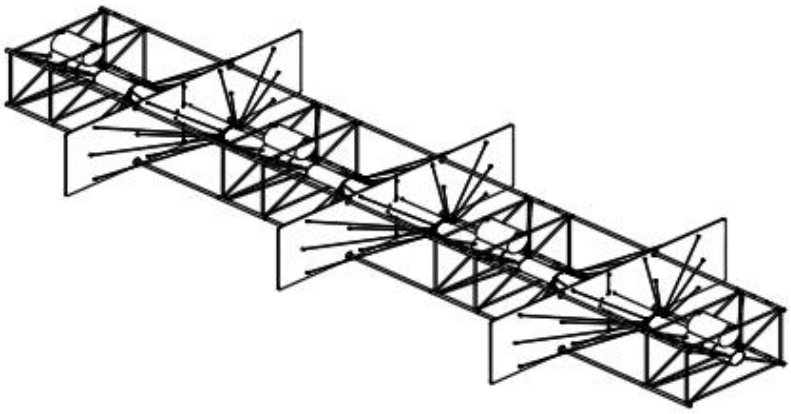

Figure 3.2: WavePiston envisaged design, it is possible to note the whole structure composed by a multitude of plates united in a unique moored frame

The energy collector is a plate that can slide back and forth along a pipe in a static structure. The interface between the plate and the pipe is a pump that pumps water into the pipe in both sliding directions. When an energy collector gets near the limit movement, a spring will slowly close the pump valves to avoid sudden bumps.

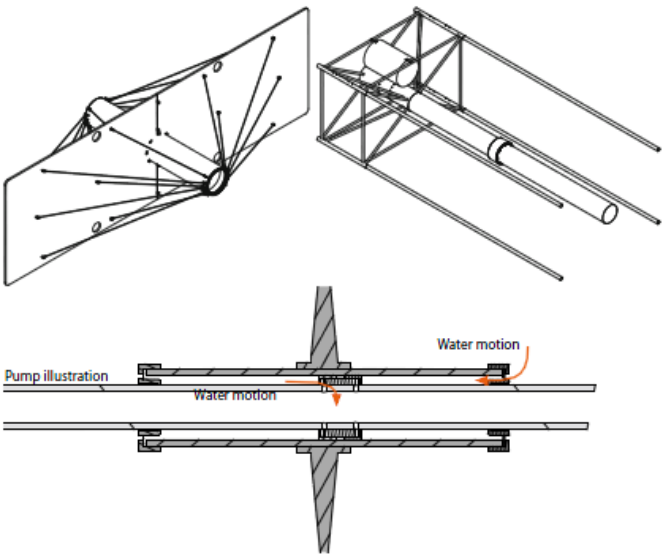

Figure 3.3: single module design: in the pictures you can see the single plate and the pipe that connects two sequent plates, that is the mainly part of the device because it transports the seawater pressured to the turbine station.

Building the system from modules makes it easy to transport, deploy, and repair.

If a module fails, it will not compromise the entire system.

Faulty modules can be replaced or fixed on the spot, when weather allows it.

Due to the oscillatory nature of the water movement along the WavePiston, the forces on the individual collectors will tend to cancel each other out, with the result that even very long WavePiston systems can be moored using only moderate means.

The nature of the water movement also means that there is not a unique depth to put this device, but the optimal depth range for a wave energy farm depends only on the nature of the sea condition.

The key for the efficiency is only the width and the depth of collector. As the amount of energy that can be harvested is proportional to the available collector area, the collectors should be made as large as possible.

In view of the fact that the WavePiston concept is based on connecting multiple vertical energy collectors, it is important to study the mutual distance between them; ideally, if two vertical plates are positioned exactly at the distance of a half wave length from each other, they will move in opposite directions all the time, hence they will work with the maximum efficiency.

Although most forces from the collector elements are cancelled out, the system still needs to be moored to the seabed to compensate for residual forces, such as currents and winds. Moreover, at a certain energy level, the waves will start breaking and the speed and force of water increases dramatically at surface level, but anyway the mooring will be minimal, also because the Wave Piston system is almost fully submerged and therefore less vulnerable to storms.

3.2 - WavePiston prototype

3.2.1 – Aalborg laboratory

The University of Aalborg is one of the most important universities in Denmark, and its particularity consists in the way of teaching and developing the subjects. The idea is to give the students the possibility to solve themselves different problems with group projects and that's why this university has a lot of laboratories. Specifically, the wave energy converters are studied in the wave laboratory that belongs to the Water and Environment Department of Structure Engineering.

This laboratory is equipped with a reinforced concrete tank, with a rectangular shape of the dimensions of 15.7m x 8.5m and a maximum depth of 1,5m, where it is possible to reproduce 3D waves.

The tank is supplied with a paddle system as a snake-front piston type with a total of ten actuators to simulate the sea wave, and an absorbent shore composed by gross gravel with a 1:4 slope. The motion of each actuator is independent from one another, and this permits the generation of longitudinal waves as well as oblique ones.

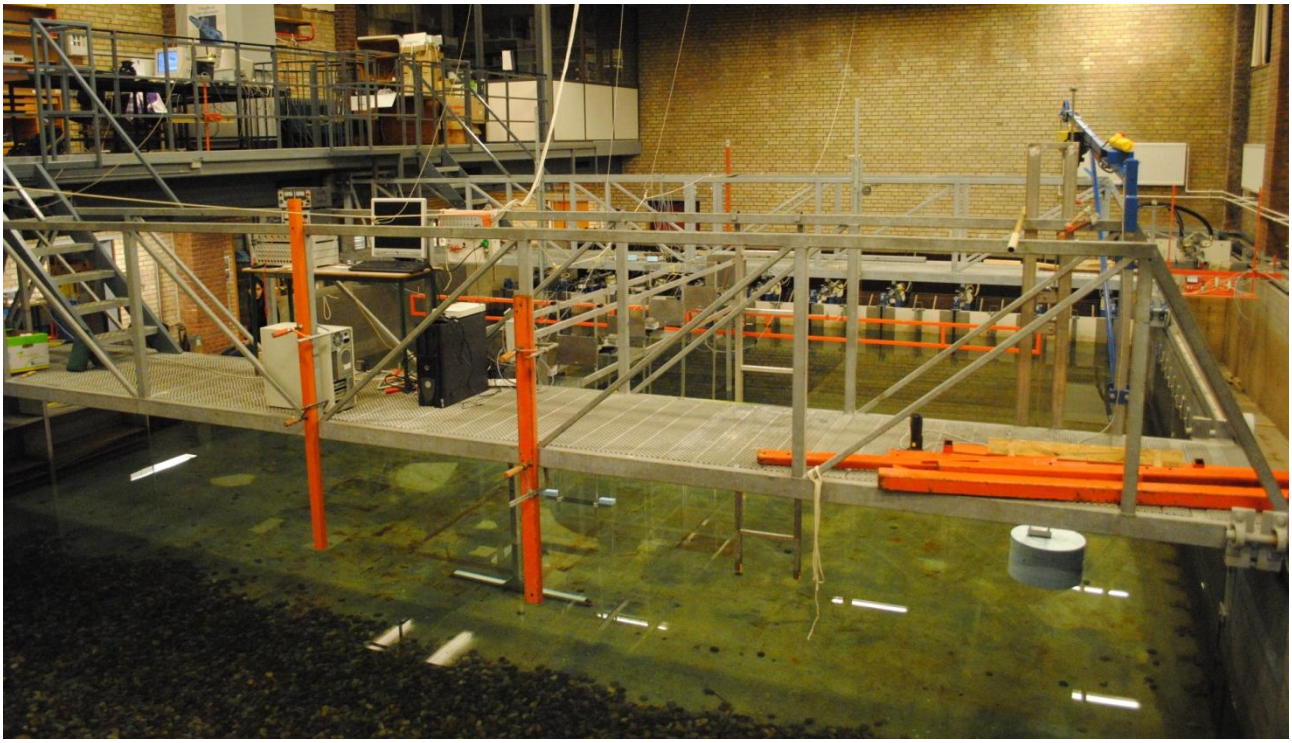

Figure 3.4: Overview of the laboratory in Aalborg University:
On the left you can see a part of the absorbent shore, and in the background the paddle system as a snake-front piston type, whilst between the two piers there is the device in the configuration with four wings. Finally in the left background, there are computers to make and analyze the waves.

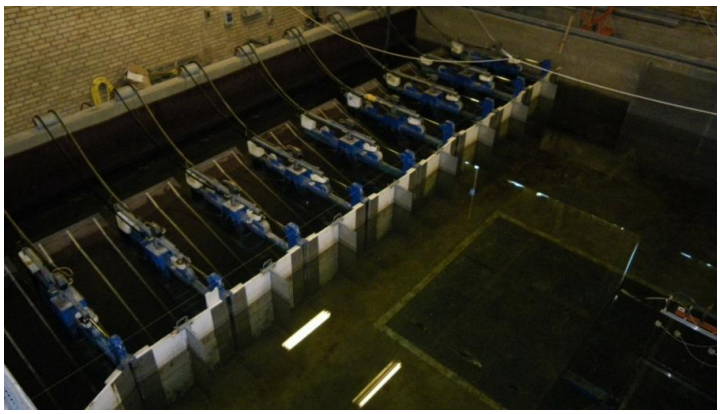

Figure 3.5: Detail of the paddle system as a snake-front piston and of the gauges on the left part. Since the paddle system is not provided with its own system of absorption of the reflection waves, on the sides of the tank and on the blades of the paddle system, there are metallic breakwater.

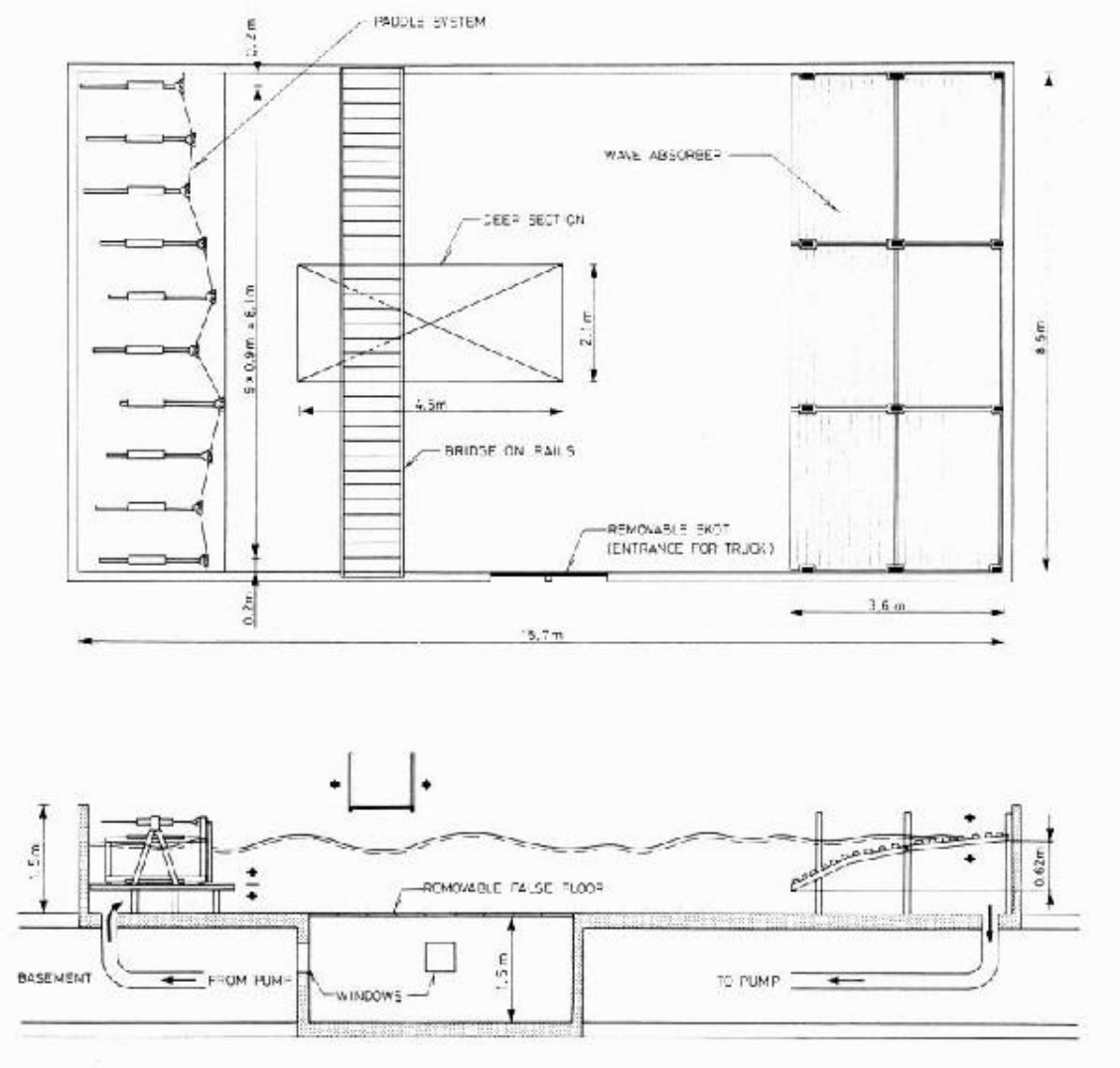

Figure 3.5: Section and top view of the laboratory of Aalborg University

To control the paddle system, the university research group invented a software on purpose and it is called AWASYS5. To create the different wave states, the program needs different parameters as:

- kind of the wave (regular or irregular wave)
- wave height
- wave period
- water depth
- duration of the test
- choice of the spectrum for irregular waves and peak factor

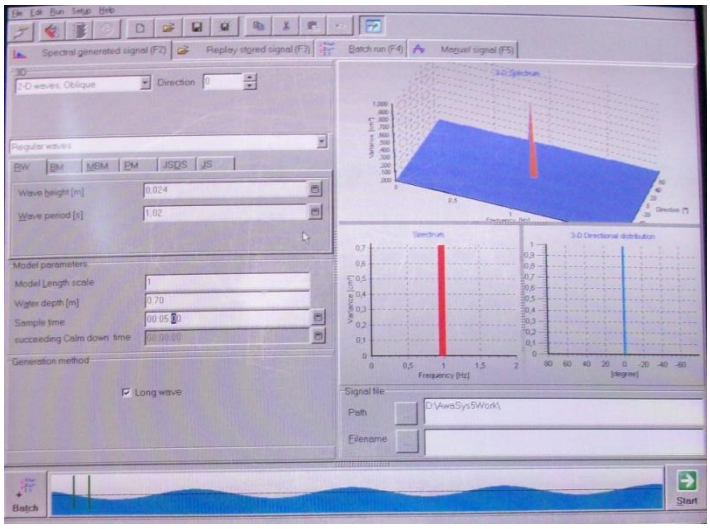

Figure 3.6: Screen of the AWASYS5 for the generation of a regular wave of 0,024m wave height and 1,02s of wave period, corresponding to the first wave state, and for the duration of 5 minutes.

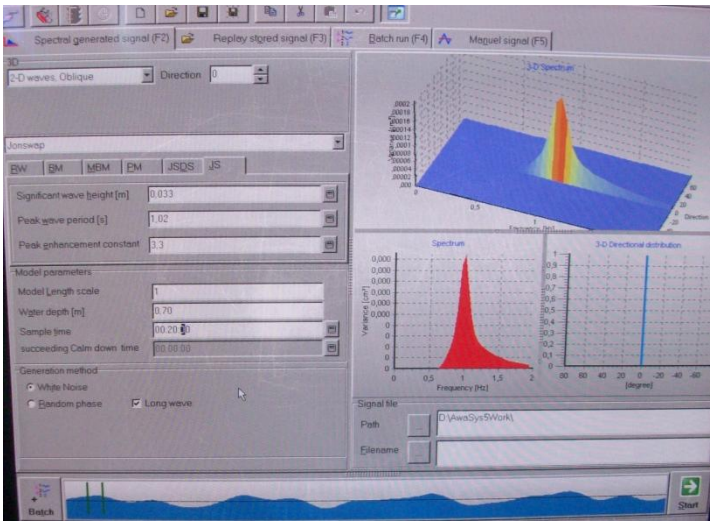

Figure 3.7: Screen of the AWASYS5 for the generation of an irregular wave of 0,033m wave height and 1,02s of wave period, corresponding to the first wave state, and for the duration of 20 minutes. JONSWAP Spectrum has been used.

All the data were acquired and analyzed using a software called WaveLab3.33. The acquisition system works at the sampling frequency of 20Hz.

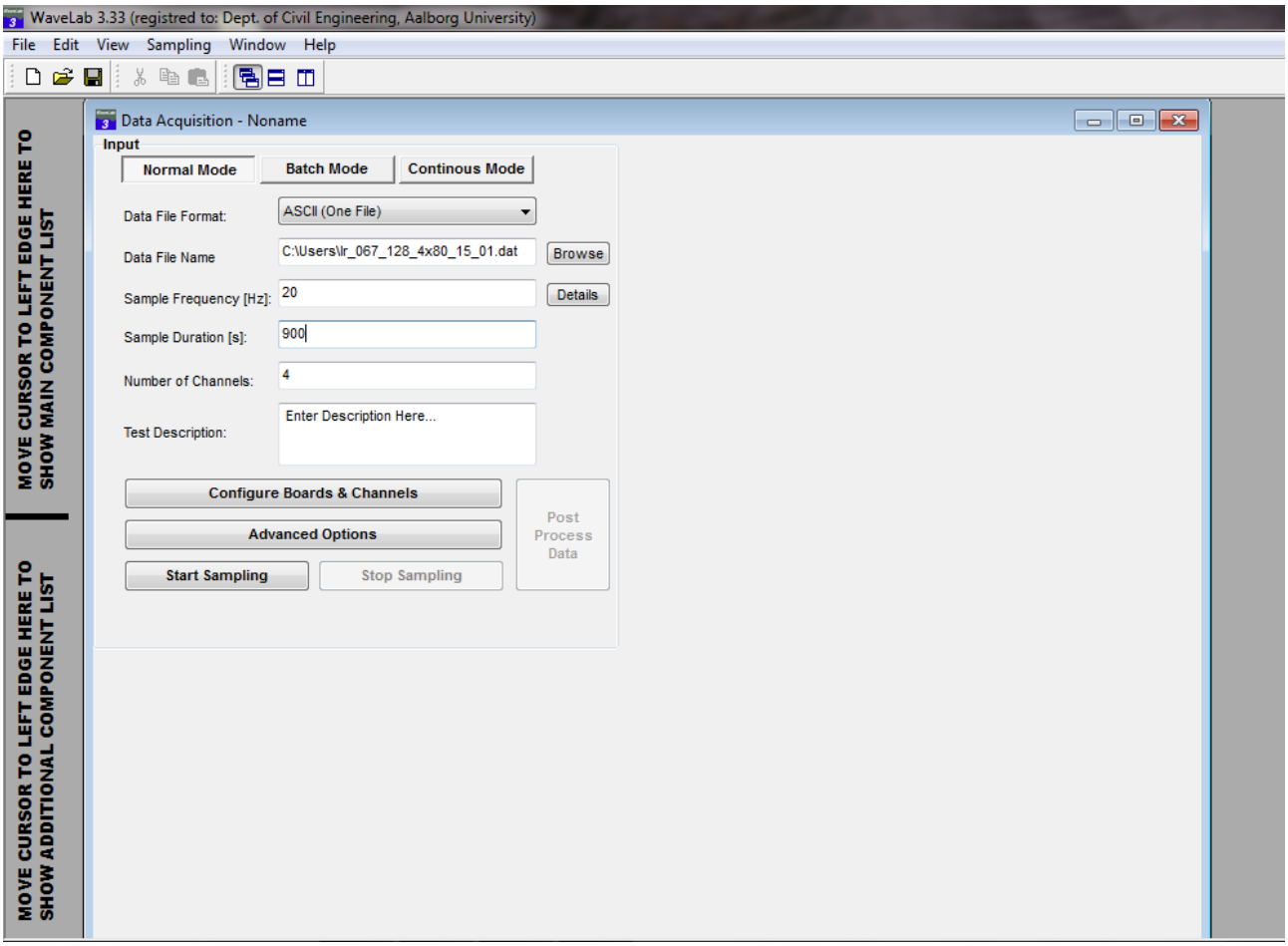

Figure 3.8: Screen of the WaveLab3.33 "Acquisition Data"

The data acquired by WaveLab3.33 come from the connection with the gauges.

Indeed, for the measurement of the wave height, four wave gauges were collocated in the tank in front and in line with the device and particularly between the device and the paddle system. Usually, to have the most accurate representation of all the waves both incident and reflected, the wave gauges are collocated in front and behind the device, but due to space, in the laboratory configuration it is permitted only the positioning in the front part.

A wave gauge is an instrument that measures the fluctuations in the surface level; an ordinary instrument in its type is the step-resistance wave gauge. This consists of a series of electrical contact points. The gauge is attached in a vertical position to a supporting structure such as a pier, with the bottom below the lowest expected wave trough. It's essential to calibrate these probes every day, before starting with the sampling and even more frequently during the same day, if the tests are stopped for more than two hours. The calibration is necessary to prevent errors due to the different water temperature or conductivity.

For all the tests their configuration is at a distance of 1,5m from the paddle system, and the distance between gauge1 and the subsequent is 0,15m; 0,40m; 1,0m, as it is shown in the configuration in the figure n. 3.14 at page 56.

It is important that the relative distances between two probes are such that they are not among multiples or dividers, to allow the separation of incident and reflected waves.

As you can see from figure 3.8, to save the data from the wave gauges, the software WaveLab3.33 needs some parameters into account, such as: the sample frequency, the number of channels, the sample duration, and the data file name. For each test, the data file name structure was AA_BB_CC_DD_EE_FF.dat where:

- AA indicates if the wave is regular (RW) or irregular (Ir);
- BB indicates the wave height;
- CC indicates the wave period;
- DD indicates the distance between the wings in a particular configuration test;
- EE indicates the load;
- FF indicates the number of the test.

Under particular conditions, there is something else added at the end of the name, and this occurs when the study is aimed to the importance of a particular parameter as the angle, or the wave period variation.

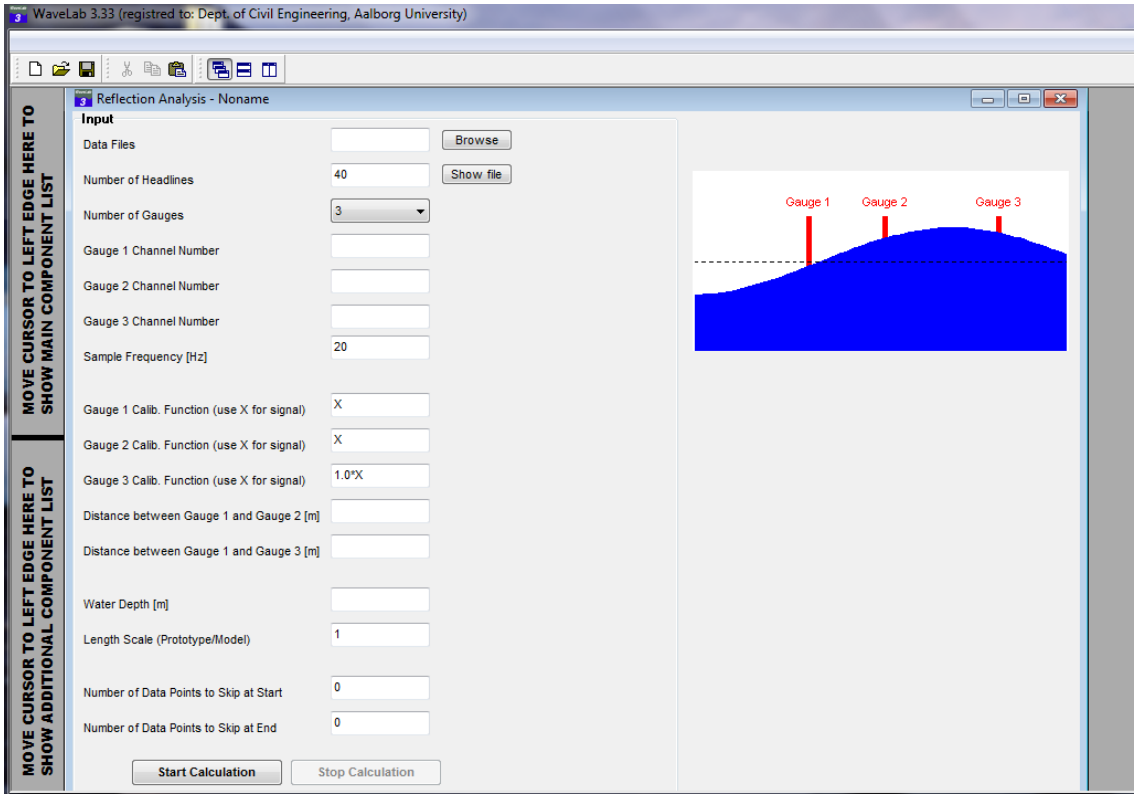

Figure 3.9: Screen of the WaveLab3.33 "Reflection Analysis"

As it is exposed in the figure 3.9, to obtain the main results for the incoming and reflected waves (for example: the significant wave height, the wave period and the power per meter wave) the software WaveLab3.33 needs some parameters into account such as: the data file, the three gauges channels, the relative distance between the gauges under consideration and the water depth.

WaveLab3.33 analyzes the wave gauges data through the reflection analysis, using a numerical procedure which implements the method of Mansard & Funke for the separation between incident and reflected waves from the data of three level probes.

The method presented by Mansard & Funke assumes that the wave elevation is a sum of regular waves travelling with different frequency and phase. Hence, using the Fourier analysis, the amplitude of the incident and reflection waves for a given frequency can be estimated and moreover, it gives the variation of the measured noise from wave gauge to wave gauge.

Further WaveLab3.33 has different main component as:

- the show and compare signal procedure: where it is possible to see the overview sampling signal from only one sampling or from more than one samplings;
- the filtering component;
- generate and analysis of time series.

Moreover, at the time of the experiments, the laboratory was also equipped with an additional computer, where runs the software “National Instruments LabView 8.5” that includes “WavePiston.vi”.

WavePiston.vi is a software appointed to harvest the data from the device, that transmits through four cables the values of the linear displacement sensors, and of the force transducers.

That software saves the data with a sampling frequency 10Hz, hence this data are used for the calculation of the power take off (PTO).

Before the sampling, a name is chosen to save the data, following the same criterion as for the one in WaveLab3.33. The sampling gives a file.txt of the results that is composed of four columns, of which the first two contain displacement information, while the last two contain force information.

The figure 3.10 shows what happens during the sampling, on the left part it is possible to see the trend of the measurements, and on the right part their values, so that through the graph it is easy to understand, even during the record, if there are some kind of problems.

The water depth during all the tests was 0.70m.

Figure 3.10: Screen of the WavePiston.vi "Sampling Graph". On the left the picture shows the graph of the recording of the four channels, and on the right the values of these sampling.

Figure 3.11: Box that connects the device and computer

3.2.2 – Model and experimental activity

The WavePiston prototype is invented by a Danish group including Martin von Bülow and Kristian Glejbøl, both from Copenhagen.

That prototype was then studied in the laboratory of Aalborg University, Department of Civil Engineering, in February and March 2010.

The peculiarity of the horizontal translational motion was difficult to reproduce in the laboratory, so the prototype used was slightly different from a real world scenario.

Hence, the whole device, including the power take off unit(PTO), is modelled in a different way.

The main change made was to add a structure that supported the floating devices.

This structure was built very high compared to the size of the parties that constitute the core of the device, in order to reduce the effect of an arm rotating around a fixed pivot.

As already reported in the presentation of the real device, every plate is connected to a unique power take off system, while in the laboratory state, each plate has a singular power take off unit.

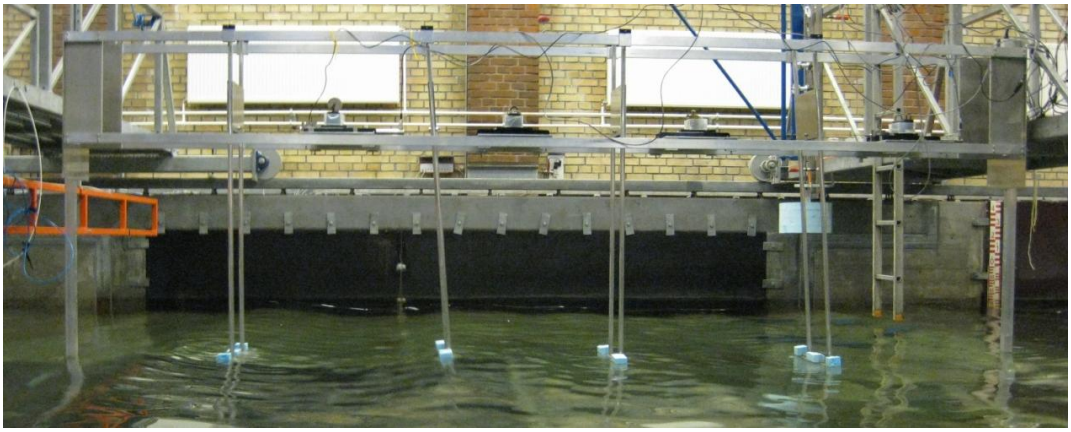

Figure 3.12: Support structure added

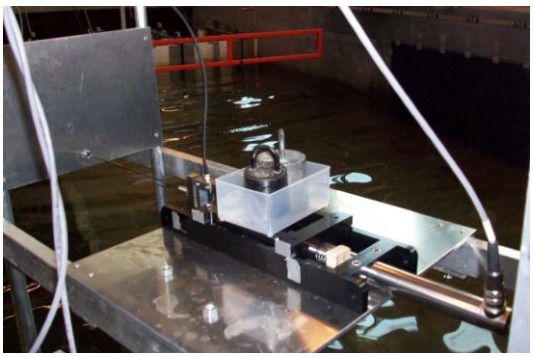

Figure 3.13: Single PTO for each energy collector plat, including the sliding rail with the load, the force transducer and the LVDT

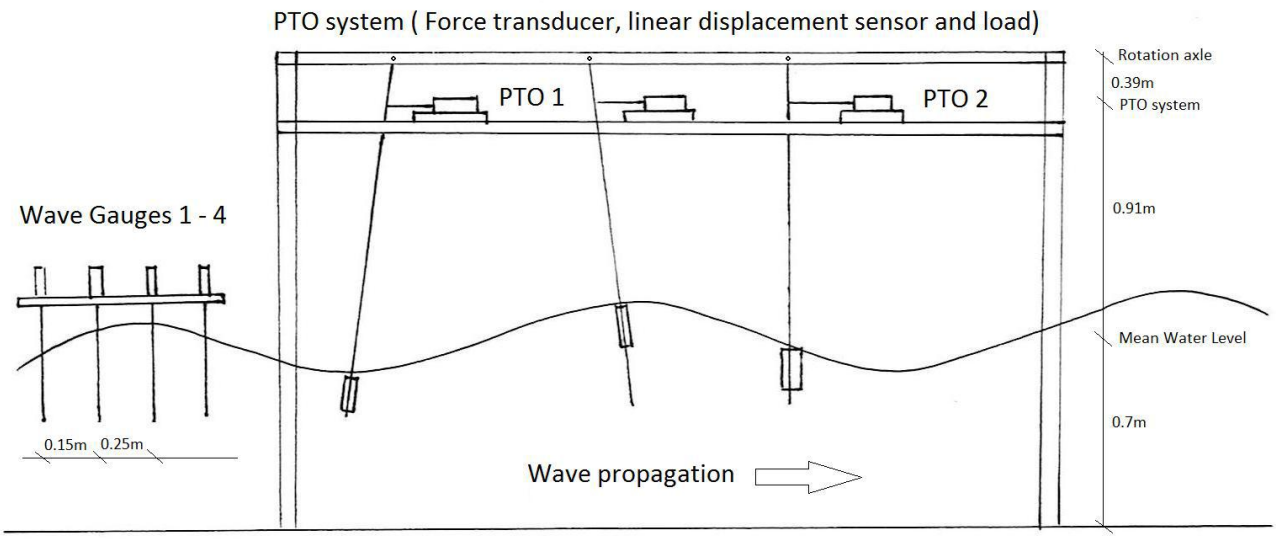

Figure 3.14: WavePiston Prototype and its configuration in the laboratory

Thanks to the support structure added it was also easily feasible the design configuration of the real WavePiston, i.e. to have one moored reference frame supporting a multitude of working plates that are placed in parallel and in line relative to the incoming wave. Further, this structured includes in itself the mooring of the device, that is not a part to be designed.

The model was first designed in scale 1:20, but in the early tests, it was decided to change the scale in 1:30, modifying neither the dimension of the device, nor the water depth. This means that, in the reality, the device will become bigger than it was designed and it needs to be located more offshore.

In the examined prototype, only two of the plates can take measures, and in each of them there is the measure of the displacement (LVDT), through a linear displacement sensor, and a transducer for the force; the reason why only two water wings have measurements is due to the limited availability of measuring instruments at the time, so they are located in the front and in the back position, with intent to put them also in the middle positions. The load system consists of a rail on which weights were applied, from 0 kg to 5 kg, in order to change the friction.

As you can see in the figure 3.13, the PTO of the model consists of a friction wagon for the loading, a sensor to measure the displacement and a force transducer to measure the force.

From these measurements the mechanical power (P) of a device can be defined by:

$$P(t) = |\boldsymbol{F}(t)| \cdot |\boldsymbol{v}(t)|$$

The velocity (v) of the device was calculated taking the difference of the displacement values of the plate in two successive record instants and then multiplying this by the frequency of data acquisition.

For the force F(t) it is appropriate to consider not the values that the transducer gives moment by moment, but this values subtracted by its offset, because the plates don't come back at the original positions.

The device was tested with varying "PTO loads" on the plates. These loads apply a force that resists the movement of the wings. This is done to find the ideal PTO loading, which corresponds to the highest amount of energy that it is extractable from the device. The load itself was set by putting real weight on the friction wagon, and the choice of the load range was from the situation without load (free movement) to 5,0kg of maximum load, hence maximum resistance to the movement for the plate.

To have an idea of the overall behaviour of the device, it is necessary to fill in a table that includes the efficiency, the average mechanical energy available to the PTO system of the device, the yearly mechanical energy production of the device and the load factor.

These values are given for the average of the two instrumented plates, because the two energy collector plates feel different wave incident force, decreasing from the front to the back.

The wave parameters of these wave states, such as the H_s, and T_p are based on the standardized Danish North Sea, Kofoed & Frigaard (2009), at a scaling ratio of 1:30, and on 30m deep location.

The parameters of the table are defined as:

- the "efficiency" is the ratio between the power generated and the available power from the waves relatively to the same width crest. The power generated is the converted energy from the waves into useful mechanical energy. In the laboratory the efficiency was found for each wave state dividing the average power generated, calculated as the equation showed before as multiplication between the force and the velocity, by the wave power of the same wave state and relative the same width.

$$Efficiency_{WS} = \frac{Power_{Mechanical}}{Power_{Wave}} \quad [\%]$$

- the "overall efficiency" is the efficiency corresponding to the device in the whole year, and it is calculated as:

$$Efficiency_{Average} = \sum_{WS=1}^{5} Efficiency_{WS} * Probability\ of\ occurance_{WS} \quad [\%]$$

- the "Generating Power" corresponds to the efficiency of the device multiplied by the average available power in the waves in a particular wave state. The maximum of these generating power values is taken as the rated/installed capacity of the PTO system.

$$Power_{installed} = max_{WS}\left(Power_{wave_{WS}} * Efficiency_{WS}\right) \qquad [kW]$$

- the "power production" represents the average generated power of a wave state set on a year base. This corresponds to multiplying the average product power in a wave state by the probability of occurrence of that wave state.

$$Power_{product} = Power_{generated_{WS}} * Probability\ of\ occurance_{WS} \qquad [kW]$$

$$Power_{product} = Power_{wave_{WS}} * Efficiency_{WS} * Probability\ of\ occurance_{WS} \qquad [kW]$$

- the sum of the power production of every wave state gives the yearly average available of mechanical power to the PTO system. From this yearly average power production, the yearly total energy production can be calculated.

$$Power\ production_{Average} = \sum_{WS=1}^{5} Power\ product_{WS} \quad [kW]$$

$$Yearly\ Energy\ Product = Power\ production_{\ average} * 365 * \frac{24}{1000} \qquad \left[\frac{MWh}{year}\right]$$

- the "factor load" represents the average usage of the installed capacity, here set to the average generated power in the highest of the tested wave states.

$$Load\ factor = \frac{Power\ production_{average}}{Power\ production_{max}} \qquad [\%]$$

The summarizing table is showed at page 74 and following.

3.2.2.1- Test Program

The purpose of these tests is to find the efficiency of the device and a yearly average energy production.

3.2.2.1.1- Overview

The WavePiston prototype was subjected to different tests.

At the beginning the aim of the tests was to understand the mainly behaviour of the device and the optimal configuration for the further tests, and for this plan some tests in regular wave were completed.

Subsequently to have a reasonable behaviour of the model several tests in irregular wave were done.

The regular wave tests were normally carried out over a period of 3 minutes, whereas the irregular test were done for 30 or 15 minutes. All the irregular tests were performed following the JONSWAP Spectrum with the coefficient factor peak of 3,3.

The table below shows an overview of all the assessments carried out.

TEST PROGRAM	Configuration with 2 wings	Configuration with 4 wings
Regular Wave		
Choice of the best load	X	-
Different incident angle wave	-	X
Variation of wave period	X	X
Variation of wave height	-	X
Relative distance between plates	X	-
Irregular Wave		
Choice of the best load	X	X
Different incident angle wave	-	X
Relative distance between plates	-	X
Different shape plates	X	-

Table 3.1: Summary of the laboratory experiments

3.2.2.1.2- Description of the wave state

In order to evaluate the performances of the device, regular and irregular wave states were made, as described in "Assessment of Wave Energy Devices. Best Practice as used in Denmark", Kofoed and Frigaard et al.,2008.

The Danish part of the North Seas is characterized by five wave state, and for each one there is the probability of occurrence.

Sea State	H_s	T_z	T_p	Energy flux	Prob. Occurrence
	[m]	[sec]	[sec]	[kW/m]	[%]
1	1.0	4.0	5.6	2.1	46.8
2	2.0	5.0	7.0	11.6	22.6
3	3.0	6.0	8.4	32.0	10.8
4	4.0	7.0	9.8	65.6	5.1
5	5.0	8.0	11.2	114.0	2.4

Table 3.2: North Sea Wave state from Kofoed and Frigaard (2008). In the table H_s means the significant wave height, T_z is the average zero-crossing wave period, T_p is the peak period of the wave spectrum and the energy flux is the average wave available power per crest meter.

To relate the real situation to the laboratory situation there is the need to apply a scale Freud:

Parameter	Model	Full Scale
Length	1	S
Area	1	S^2
Volume	1	S^3
Time	1	$S^{0.5}$
Velocity	1	$S^{0.5}$
Force	1	S^3
Power	1	$S^{3.5}$

Table 3.3: Scale Freud

For the Danish part of the North Seas it is possible to obtain the five wave state to reproduce in the laboratory as the table below shows:

Scale 1:20 Regular Wave			Scale 1:20 Irregular Wave		
Sea State	H [m]	T [s]	H_s [m]	T_z [s]	T_p [s]
1	0.035	1.25	0.050	0.89	1.25
2	0.070	1.57	0.100	1.12	1.57
3	0.105	1.88	0.150	1.34	1.88
4	0.140	2.20	0.200	1.57	2.20
5	0.175	2.50	0.250	1.79	2.50

Table 3.4: Overview of the wave parameters for the regular and irregular waves in scale 1:20

The first scale decision was the scale 1:20, because the device was built up for that scale, but soon it was possible to see that it was better to change scale from 1:20 to 1:30, without changing the water depth and the size of the device.

In scale 1:20 the real dimensions of the device becomes 10m for the width and 2 m for the depth, while in scale 1:30 these dimensions would be 15m for the width and 3m for the depth.

Scale 1:30 Regular Wave			Scale 1:30 Irregular Wave		
Sea State	H [m]	T [s]	H_s [m]	T_z [s]	T_p [s]
1	0.024	1.02	0.033	0.73	1.02
2	0.047	1.28	0.067	0.91	1.28
3	0.071	1.53	0.100	1.10	1.53
4	0.091	1.79	0.133	1.28	1.79
5	0.118	2.04	0.167	1.46	2.04

Table 3.5: Overview of the wave parameters for the regular and irregular waves in scale 1:30

The values in the table are the ones used to generate the waves. In reality, the realized waves might be different due to all the influential parameters, such as the margin of uncertainties of the generating equipment, the reflection in the tank and other details. This difference is showed in the figure below.

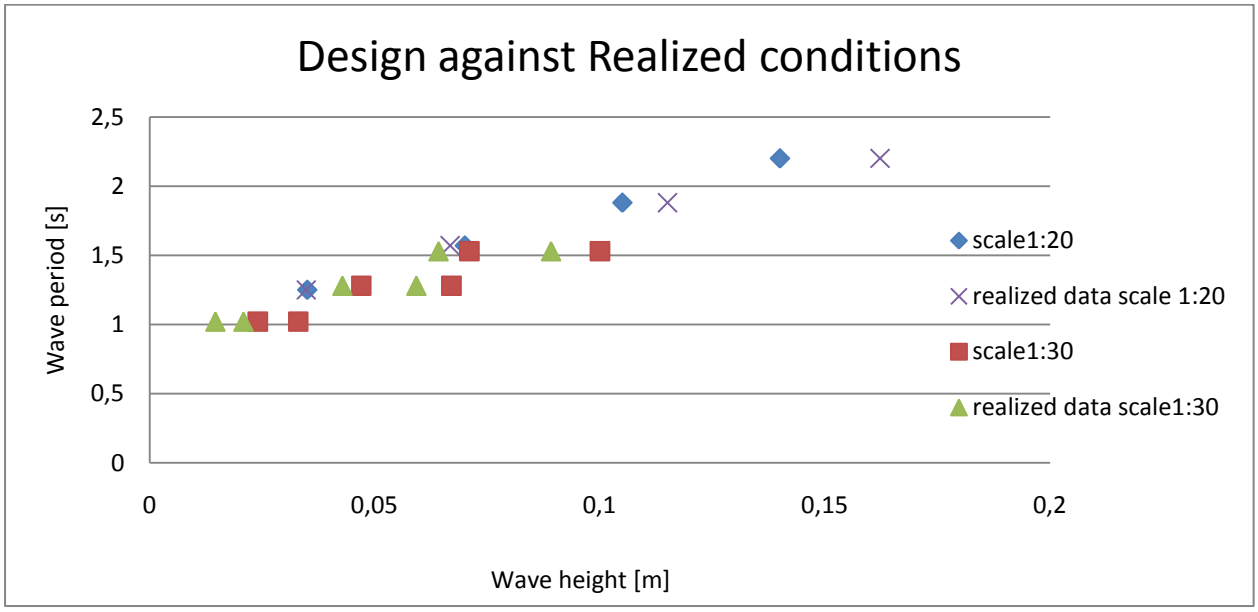

Figure 3.15: Plot of the different design conditions and the observed conditions. The observed conditions are calculated by the reflection analysis of WaveLab3.33

All the results of the test have been analyzed on the same way, by the reflection analysis of WaveLab3.33 and by a Matlab Editor. Thanks to that analysis it is possible to note that the values of the reflected wave are smaller than 5% of the values of the incident wave, hence they were neglected.

3.2.2.1.3- Research of the reference configuration

The first configuration of the device is with only two wings, one on the front and one on the rear part of the device, and these two plates were positioned at a distance of 2,40m. Each wings is constituted of a thin plate, its shape is 0,5m of width and 0,1m of depth, that means in full scale 15m of width and 3m of depth.

The later lay out of the device is with four plates at the distance of 0,80m each other (with the same shape), even if only the front and the back plate take measurements as before.

In both the configurations, different tests, both in regular and irregular wave, were done. The goal of that part was choosing different load to simulate the friction effect. The load range was from 0kg, that means free movement of the plate, to 5kg that represents the prevented or limited movement.

Some tests were made with another layout, such as with four plates, but even closer. To put more than two plates gives the possibility to study a configuration nearer to the real installation, because it means that it is possible to harvest energy from more than two plates, but at the same time it means that the plates that are in the rear part of the device should be influenced by the damping made from the plates in the middle. The middle added plates are simply flat wing with the same shape and the same load of the other two.

For the full-scale device the load setting is design to be able to change in function of the incoming waves, however, in the laboratory configuration, a constant load was used for the different wave states.

The target of this step is the identification of the reference configuration and the possibility to do what was done in previous tests with regular wave, and in order to fine-tune the load even in the tests with irregular wave.

During all the tests, the configuration takes as reference was with only two wings at a distance of 2,40m, each wings of the shape of 0,5m x 0,1m in width and depth, with 1,5kg, except when the effect of inter-plate distance and/or the incident wave angle or other factors were investigated.

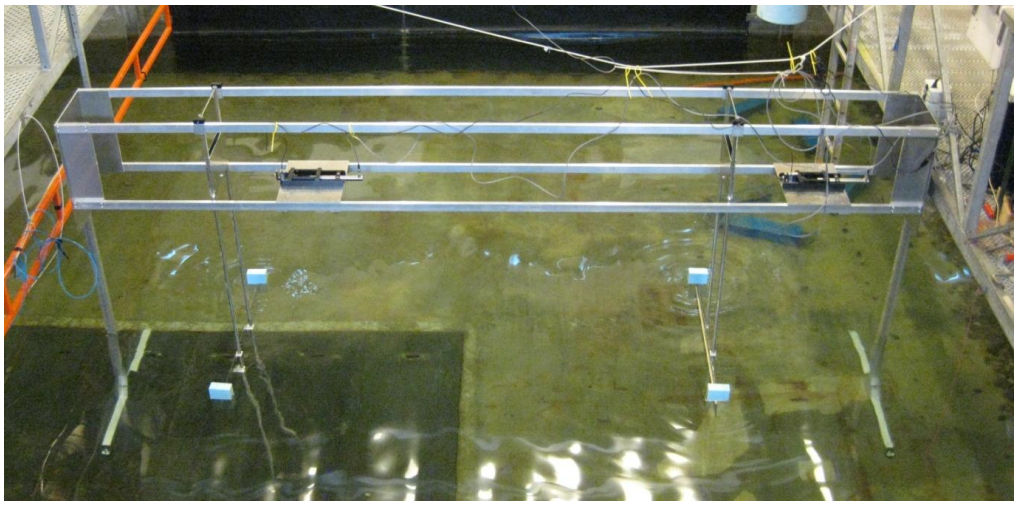

Figure 3.16: Reference configuration of the device: it is constituted by two energy collector plates, of the shape of 0,5mx0,1m in width and depth, at a distance of 2,40m and with the load of 1,5kg.

3.2.2.1.4- Wave Period and Wave Height variation

The aim of this investigation is to find out if there is a dependence of the device to either parameters.

To study the effects of changing the wave period with a fixed wave height of 0,06m, the testing set-up is with a wave period in the range between 0,6s and 1,8s with a step of 0,2s from one experiment to the subsequent.

Whereas, to study the effects of changing the wave height with a fixed wave period of 1,2s the testing set-up is with a wave height in the range between 0,03m and 0,11m with a step of 0,02m from an experiment to the subsequent.

To choose the range for the wave height and for the wave period it is necessary to considerate the limits of the equipments.

The highest wave parameters were chosen to assure a good behaviour of the device and, at the same time, prevent any kind of failure risk, while the lowest wave parameters are in relation with the limits of the instrumentations and the basin.

The constant wave height was chosen because its value is between the one of the wave state 1 and the one of the wave state 2, where the model performance is better and the instrumentation can provide qualitative measurements. The constant wave period of 1.2s was chosen for the same reasons as the wave height, but also because the results of the other test with the wave height constant seemed to have an strange behaviour around this wave period.

These tests were only run with regular waves in order to analyse the dependence of the model to one particular wave length and not to a whole wave spectrum.

3.2.2.1.5- Analysis of the influence of the incident wave angle

Several tests were performed for the second and third wave state to find out how the direction of the incident waves would affect the energy production of the model. This investigation could help the real mooring design, because the real device will be allowed to rotate to face the predominant direction of incoming waves.

The device was tested for three different incident wave angles of 10° 20° and 30°. The results are compared to a reference test performed at 0°.

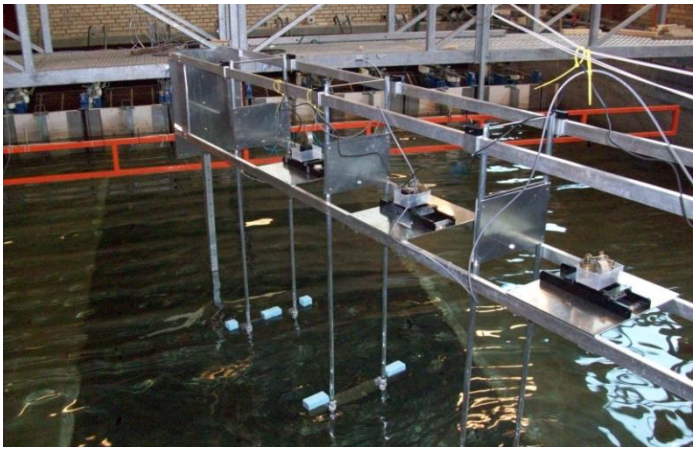

Figure 3.17: In this picture the device has an angle of 20° respect the incoming waves.

3.2.2.1.6- Number and shape of the energy converter plates

These tests were carried out with two targets: the first was to understand how the number and the distance between the plates, each one with the same shape, influence the efficiency of the device; whereas the second target was to note how the shape of each plate control the efficiency.

For the first aim the setup is with four plates mounted at a distance of 0,45m, then 0,55m and finally at 0,80m, and for the wave states number 2 and 3. Results are given for the first and rear plate, as only these were equipped with a PTO system and relative to the reference case, which is the 2 plates setup with 2.4m as inter-plate distance.

For the second aim the setup is with two plates mounted at a distance of 2,40m and for the irregular wave states number 2 and 3. The shape of the different plates are: 0,38m width and 0,13m depth; then 0,38m width and 0,10m depth; then 0,38m width and 0,07m depth; and finally 0,50m width and 0,10m depth with hole section. Results are given relatively to the reference case, which is the 2 plates setup with the plate shape as 0,50mx0,10m without hole.

Figure 3.18: In this picture the distance between two subsequent plates of the device is 0,45m.

3.2.2.2- Results

The results shown on this section are referenced to the overall efficiency of the device, it means that the values of the efficiency are the average of both the values sampling from the front plate and the rear one.

3.2.2.2.1- Research of the reference configuration

The first series of test were done for the configuration with two energy converter plates at a distance of 2,40m without load on the sliding box and for the scale 1:20. The figure below shows the trend of the efficiency for these tests.

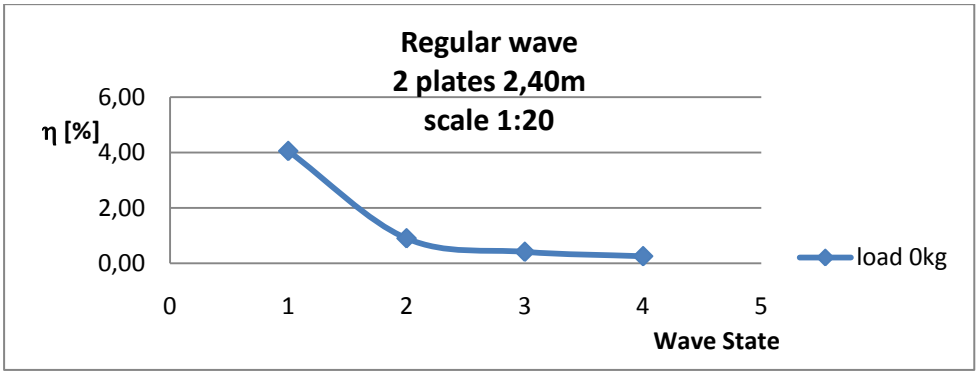

Figure 3.19: In this graph it is illustrated the trend of the overall efficiency of the device for the first four regular wave states in the scale 1:20.

The figure above proves that the efficiency decreases from the lower to the higher wave states. This means that a change of the ratio scale could increase the efficiency. If the focus is on a particular wave height, for example, a short one belonging to the highest efficiency zone and to lowest wave state, with a changing ratio scale, the same wave height will belong to a higher wave state, so that, the higher wave state has more wave energy and a high probability of occurrence, with the same efficiency.

However to be sure that this trend is representative of the real behaviour of the device further tests were done for different loads at the same scale 1:20.

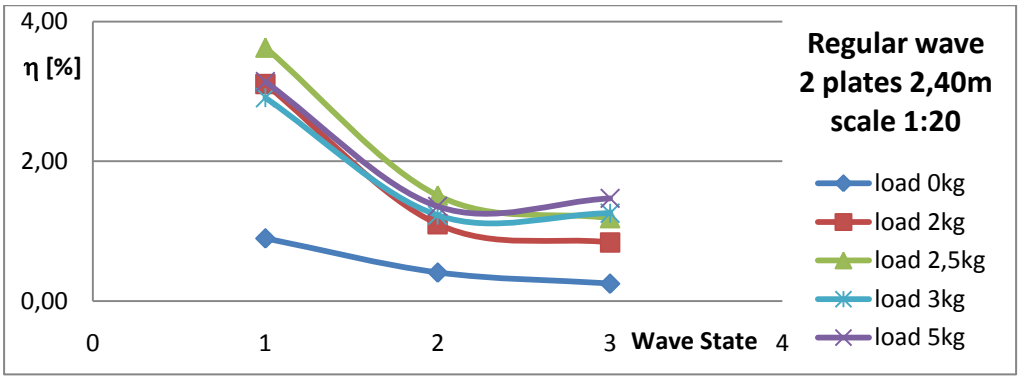

Figure 3.20: In this graph is illustrated the trend of the overall efficiency of the device for the first three regular wave states in the scale 1:20. It is possible to note that for each load the efficiency has the same trend.

Hence even if the device was built up for the scale 1:20, the great number of the tests were made increasing the scale until the scale 1:30. The graph below confirms that this decision is the right one.

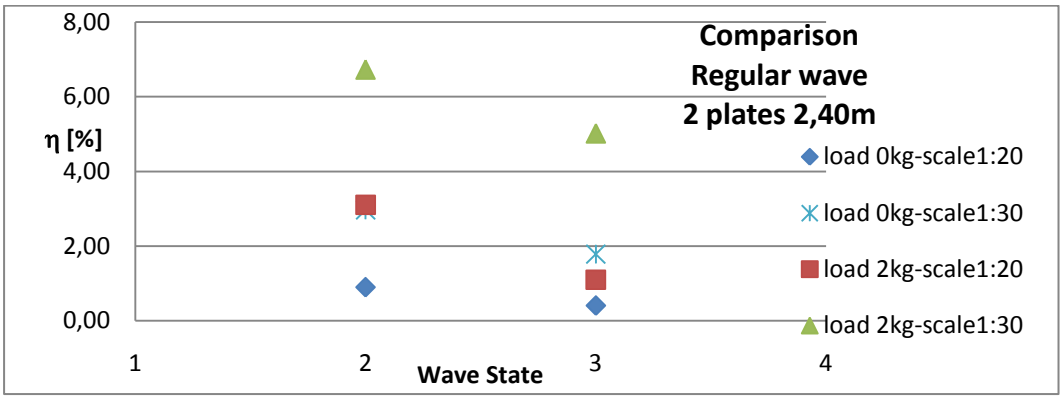

Figure 3.21: The diagram shows how the increase of the ratio scale implies an increase in the efficiency.

From the figure 3.20 it is possible to observe that the best load for the efficiency seems to be the 2,5kg. To fine-tune the finest load some tests in irregular states were done.

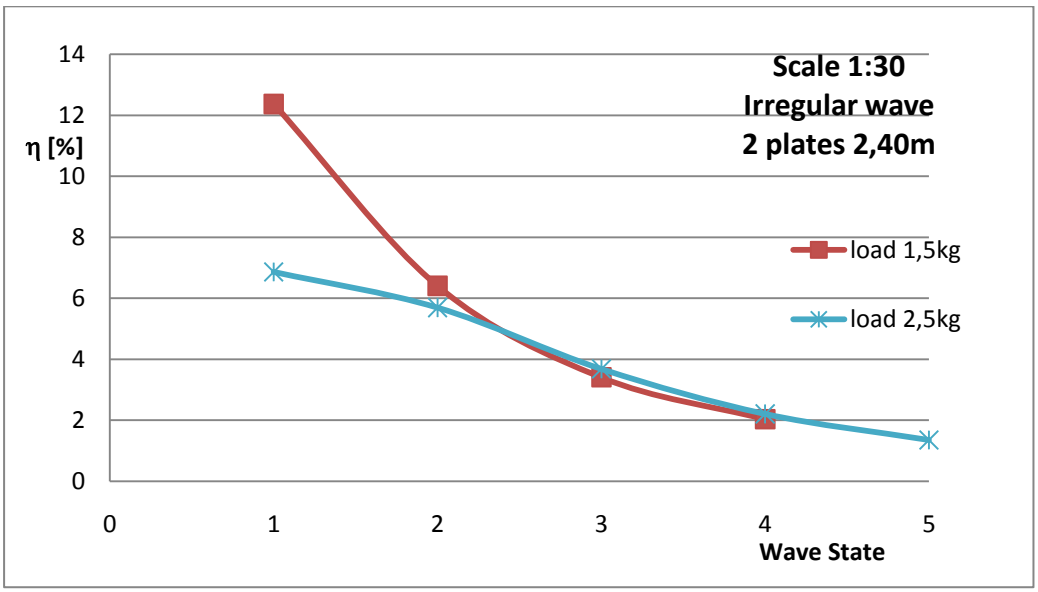

Figure 3.22: Representation of the efficiency of the prototype for the different irregular wave states, for the load of 2,5kg and 1,5kg. From the diagram it is possible to understand that the best load is 1,5kg and not 2,5kg.

The analysis of the best load with the irregular waves tests articulates that the best load is 1,5kg instead of 2,5kg. This aspect is even better because for the high wave states with the load of 2,5kg the sliding box went several time out of range, this was the reason because no more tests were done for the fifth wave state. The load of 1,5kg is taken from design and reference load.

The next two graphs want to represent the relation between the standard deviation of the force impressed on the plates, and the irregular wave states for the two best loads.

Even the first graph asserts that is better the choice of the load 1,5kg rather than 2,5kg, hence its standard deviation fluctuation is included in the range from 5,85N to 7,12N, while the standard deviation variation of the load 2,5kg is included in a wide range from 6,79N to 10,70N.

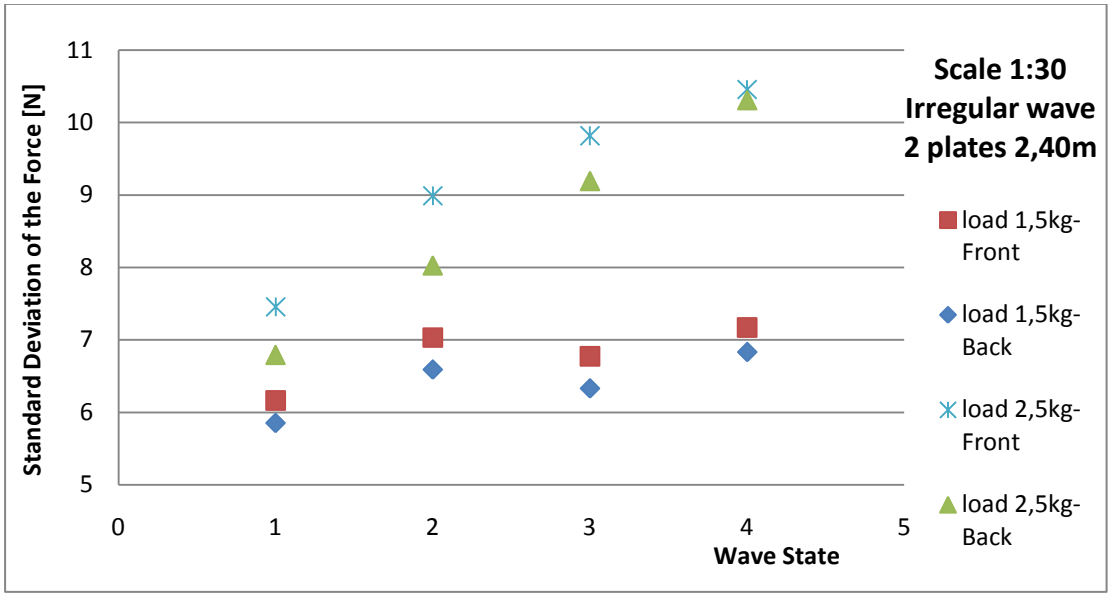

Figure 3.23: Correlation between the wave state and the standard deviation of the force. Even from this graph it is possible to declare that the load of 1,5kg is better than 2,5kg, indeed the standard deviation of the load 1,5kg is in a range between 5,85N and 7,12N for all the wave state, whereas the standard deviation of the load 2,5kg is in a wide range from 6,79N to 10 ,70N.

From the graph below it is again possible to observe that for the load 2,5kg, regardless of the wave states, the standard deviation values of the force is greater than the one of the load 1,5kg.

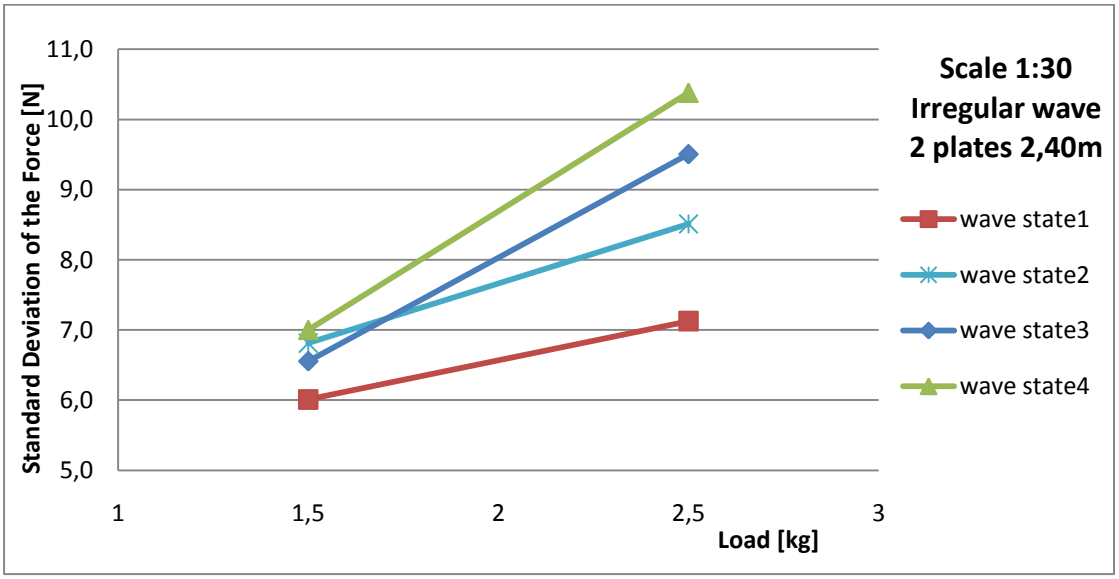

Figure 3.24: Correlation between the wave state and the standard deviation of the force. In this representation the standard deviation value is the average of the front and rear values.

Once decide that the design load is 1,5kg, the next step is to analyze the other parameters, such as the number and the relative position of the energy collector plates, the influence in the efficiency of the wave period, wave height and incident wave angle.

3.2.2.2.2- Wave Period and Wave Height variation

For these experiments the set-up is with the device with four energy converter plates at the distance of 0,80m each other and with the load of 1,5kg.

To study the effects of the variation of the wave period with a fixed wave height of 0,06m the range for the wave period is between 0,6s and 1,8s with a step of 0,2s between two subsequent experiments.

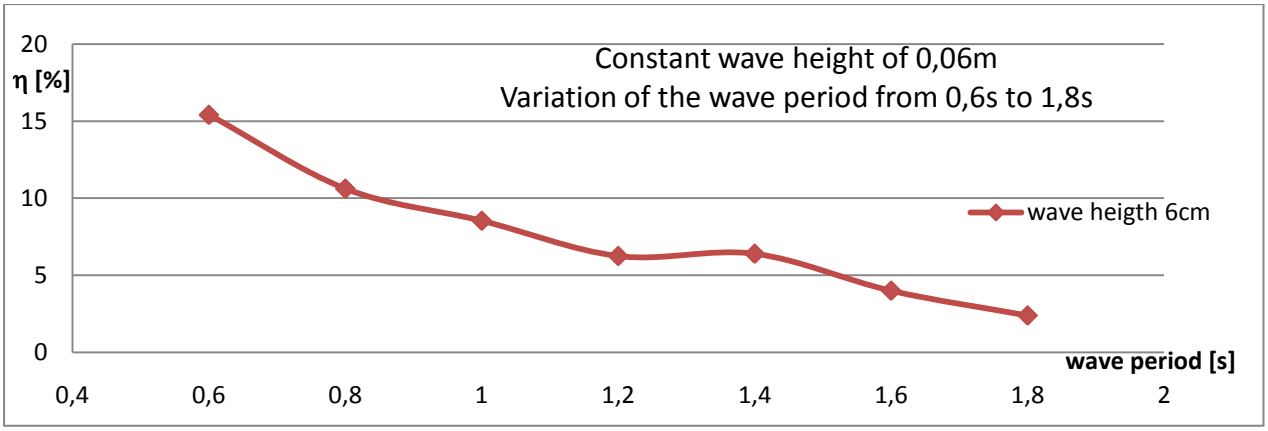

Figure 3.25: Relation between the efficiency of the device and the wave period. In this representation the efficiency value is the average of the front and rear values. The performance values are included in a range from 15,5% to 2,4%.

The image above shows that the efficiency of the device is between the range of 15,5% and 2,4%, and since the trend seems similar to go on as before, hence the efficiency decrease from the lower to the higher wave states.

This trend could be the sum of two aspect: the first is the intrinsic behaviour of the device having high efficiency for waves characterized by a small wave height and a small wave period; and the second depends on the load of 1,5kg.

Anyway, the trend suggests to focus more tests around the value of 1,2s. And for this reason, to study the effects of the changing of the wave height together with a fixed wave period, the set-up was with 1,2s for the wave period, and for the wave height in a range between 0,03m and 0,11m with a step of 0,02m from one experiment to the subsequent.

The next graph illustrates that, having a variation of the wave height, the efficiency of the device is between the range of 6% and 2,5%, and again the trend seems similar as before, hence the efficiency decreases from a wave state with a small wave height, to a wave state with a higher wave height.

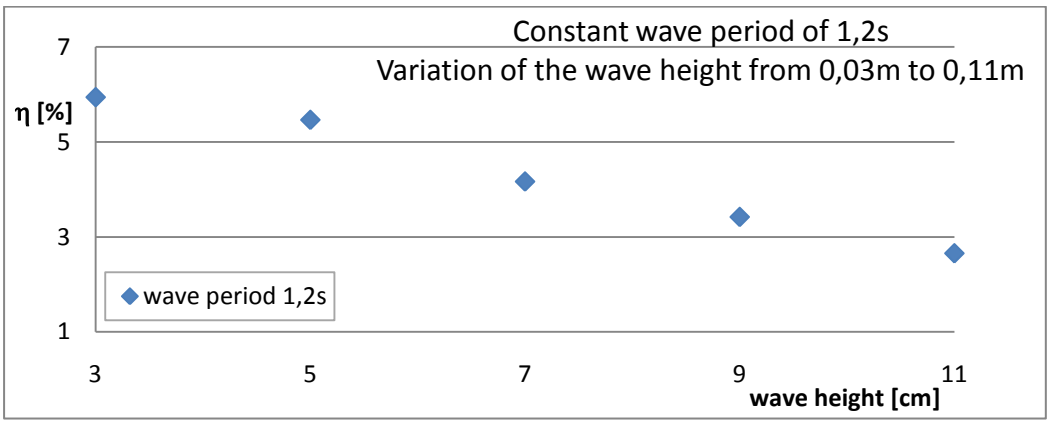

Figure 3.26: Relation between the efficiency of the device and the wave height. In this representation the efficiency value is the average of the front and rear values. The performance values are included in a range from 6% to 2,5%.

Both the graphs demonstrate that the performance of the device increases for a wave state characterized by a small wave height and a small wave period, rather than by a wave state with high values of wave height and wave period, where the efficiency decreases.

In addition, the graphs prove that the device is more influenced by the wave period than by the wave height, indeed changing the wave period, the efficiency changes from 15,5% to 2,4%, while changing the wave height, the efficiency changes only from 6% to 2,5%.

To understand better the strange behaviour around the wave period of 1,2s several tests were carried out to fine-tune the possible motivations. These tests were made with the reference configuration, i.e. the device with two energy collector plates at a distance of 2,40m each other and differently to the reference configuration, during these tests the load was of 2,0kg.

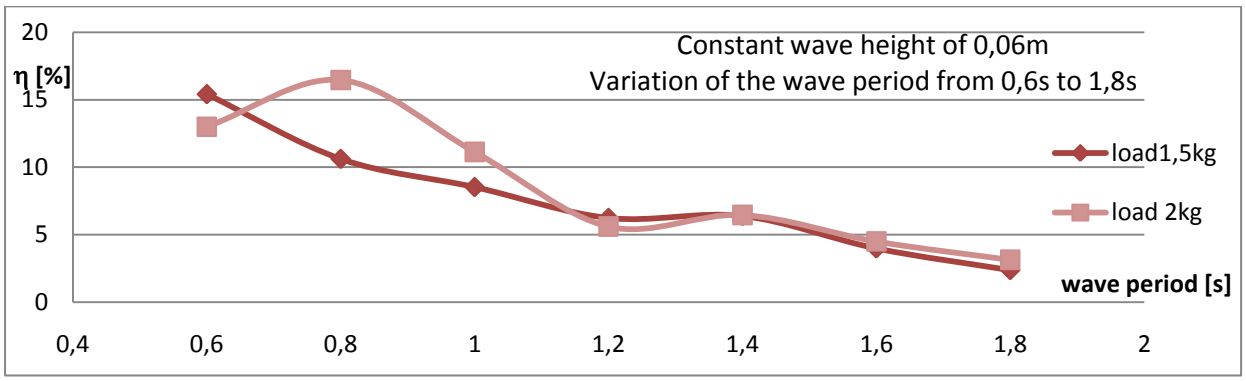

Figure 3.27: Relation between the efficiency of the device and the wave period. In this representation the efficiency value is the average of the front and rear values. The performance values are included in a range from 17% to 2,4%. Moreover this graph proves that this kind of curve is the sum of two contributions, in fact the peak moves to the left, increasing the load.

Even if all these tests were only run with regular waves in order to analyse the dependency of the model to a particular wave parameter and not to a whole wave spectrum, the results seem reliable.

3.2.2.2.3- Analysis of the influence of the incident wave angle

For this analysis the device configuration is with four plates at the distance of 0,80m each other and with a load of 1,5kg. The results are presented in reference to the configuration where the device is in line with the incoming wave, hence for an angle of 0°.

Few tests were performed both for regular wave states that for irregular wave states, to find out how the direction of the incident waves would affect the energy production of the model. The first set-up was with regular waves, and in particular for 10° and 30° incident wave angle. In this case the results are not given by reference.

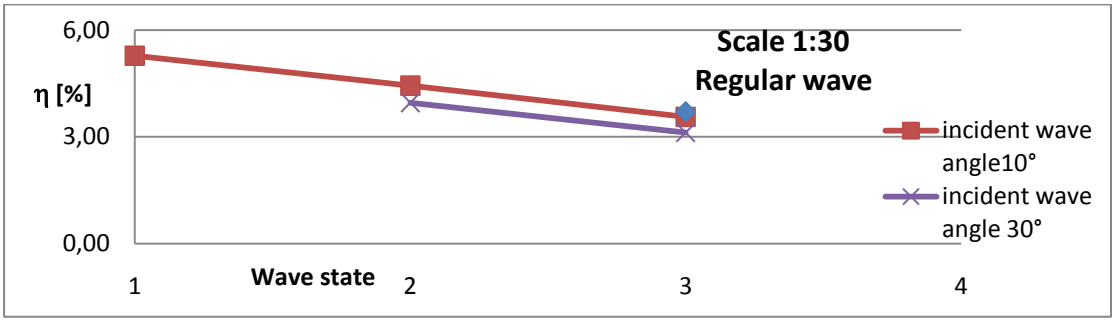

Figure 3.28: Ratio between the efficiency of the device and the incident wave angle. In this representation the efficiency value is the average of the front and rear values. The performance values are included in a range from 5,5% to 3%. The wave incident angle seems not decrease so much the efficiency.

The second study concerns the irregular wave state and in this section the configurations with 10° 30° and even 20° for the incident wave angle are analyzed.

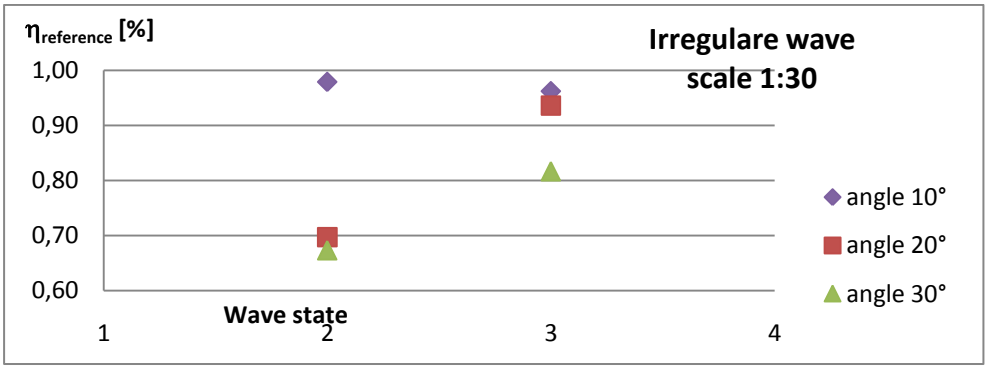

Figure 3.28: Ratio between the efficiency of the device and the incident wave angle. The performance values are referenced to the configuration where the device is in line with the wave propagation.

In the figure above, the results show that there is not a larger loss of efficiency, and furthermore that for every incident direction the loss is less for the wave state number three than not for the number two.

The same results is verified in the figure below, where there is the ration between the average of the efficiency of the device and the incident wave direction. The wave state number three presents a loss of efficiency minor than the wave state number two.

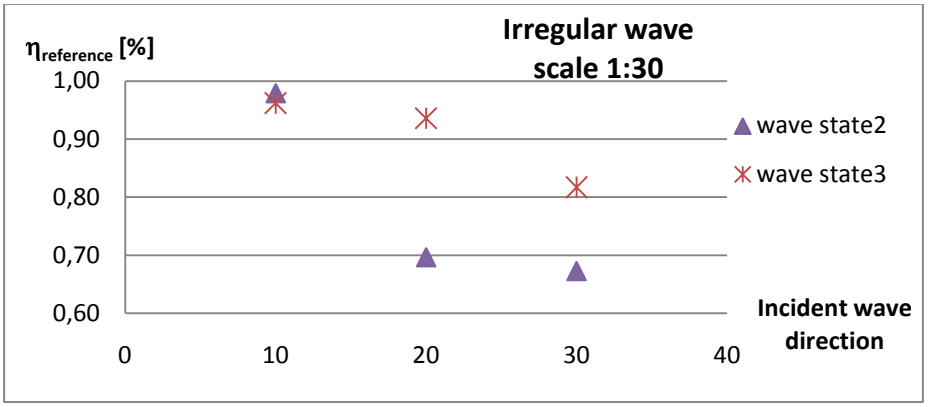

Figure 3.29: Ratio between the efficiency of the device and the incident wave angle. The performance values are referenced to the configuration where the device is in line with the wave propagation.

In conclusion, the angle of attack of the incoming waves doesn't have a significant effect on the efficiency of the device, indeed the greatest loss of efficiency is approximately the 30% and this was found for incoming waves with an angle of attack of 30 °.

3.2.2.2.4- Number and shape of the energy converter plates

The last step of the laboratory analysis is constituted by two part.

The first section is the study of the number and the position of the energy collector plates. For this analysis the usual shape of these plates is 0,5m in width and 0,1m in depth without hole. The results are represented even in reference with the standard configuration of only two plates.

The second sector is the study of the shape of the energy collector plates, in this case the configuration of the device is always with only two plates at a distance of 2,40m. The results are given in reference to the standard configuration.

In both situations, experiments were made only about the irregular wave states and all the measurements were taken from the front and the back plate, even in the configuration with four plates as before.

Hence for the first number and position aim the setup is with four plates mounted at a distance of 0,45m, then 0,55m and finally at 0,80m.

As the figure 3.30 and 3.31 show, the multi-plates configuration has a loss in efficiency, but this loss is less than the 20%, even in this case the wave state number three presents a loss of efficiency minor of the wave state number two.

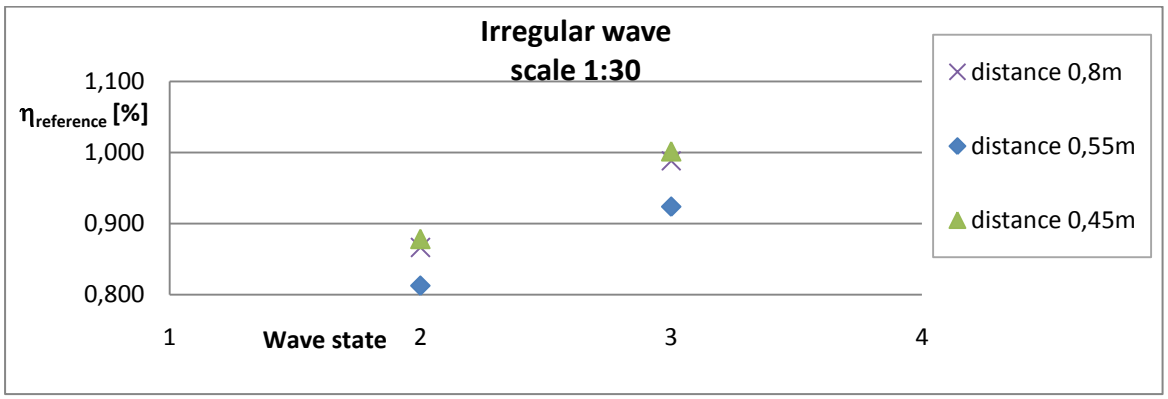

Figure 3.30: The performance values are referenced to the configuration where the device has two wings at a distance of 2,40m, from the graph it is possible to note that the main loss in efficiency is less than 20%, that value is the average of the values from the front and the back plate.

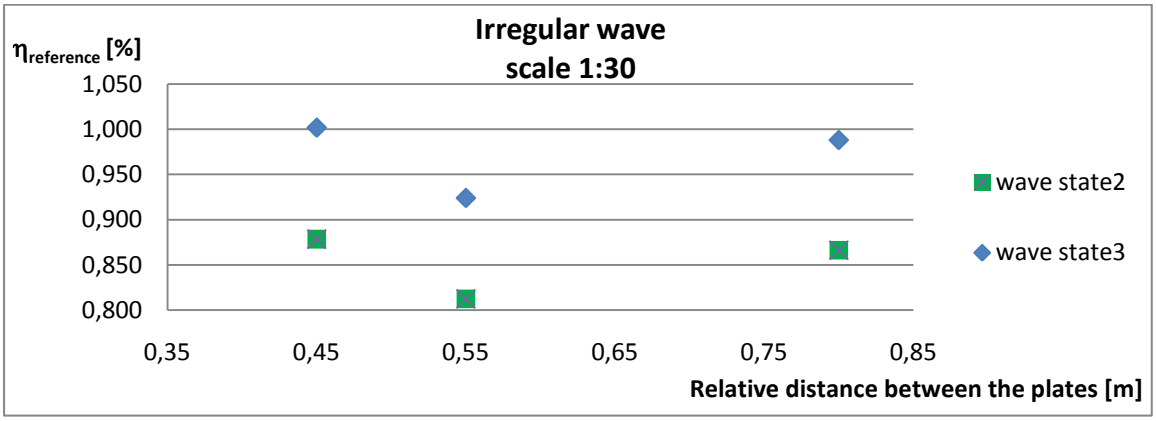

Figure 3.31: The performance values are referenced to the configuration where the device has two wings at a distance of 2,40m, from the graph it is possible to observe that the main loss in efficiency is in the wave state number 2.

Wave State	H_s [m]	T_p [s]	L [m]	Distance 2,40m	Distance 0,80m	Distance 0,55m	Distance 0,45m
2	0,067	1,28	2,42	6,41	5,55	5,21	5,63
3	0,100	1,53	3,21	3,41	3,37	3,15	3,42

Table 3.6: The values in the last four columns are the average of the efficiency among the values of the front and the back plate. These values demonstrate that the efficiency doesn't decrease so much with the increase of the number of the plate, this aspect is fundamental because in the real scenario the device is constituted to a multitude of plates. It can be noticed that the damping plates don't reduce significantly the efficiency of the device.

The table reveals that the loss of efficiency is greatest for the configuration of four winds at a distance of 0,55m, hence a possible configuration of the real device should be with the plates as closer as possible.

Whereas for the shape aim the setup is the device with two energy collector plates at the distance of 2,40m, the load is 1,5kg and different plates, and their shape are: 0,38m width and 0,13m depth; then 0,38m width and 0,10m depth; then 0,38m width and 0,07m depth; and finally 0,50m width and 0,10m depth with hole section. Results are given relatively to the reference case, which is the 2 plates setup with the plate shape as 0,50mx0,10m without hole.

When these shape experiments were carried out in the tank there was one more device, so the only way to have reliable results is to present them as reference between experiments of the same day. The reference configuration is with the shape of 0,50m width and 0,10m depth without hole.

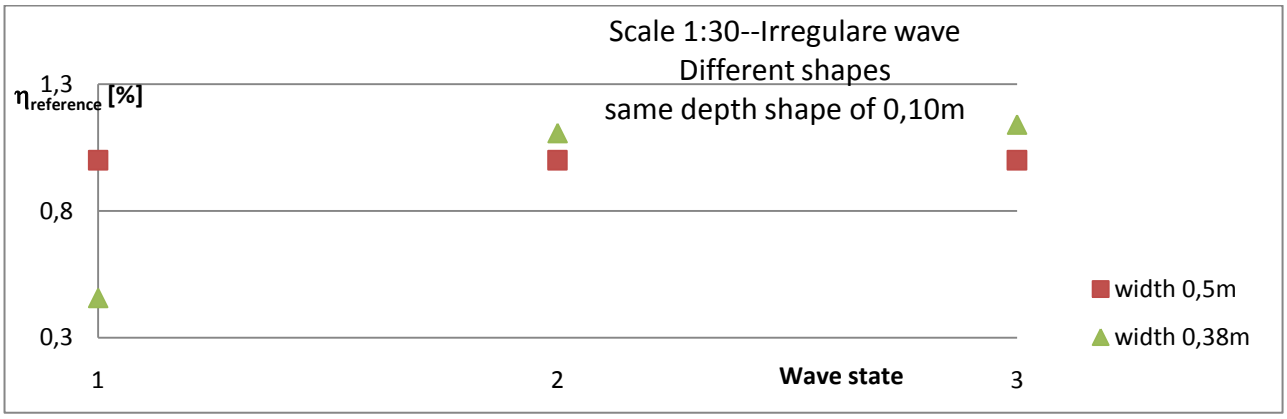

Figure 3.32: The graph shows how the efficiency increases with a decrease of the width of the plates, except for the first irregular wave state. The greatest increase of the efficiency is about the 20%.

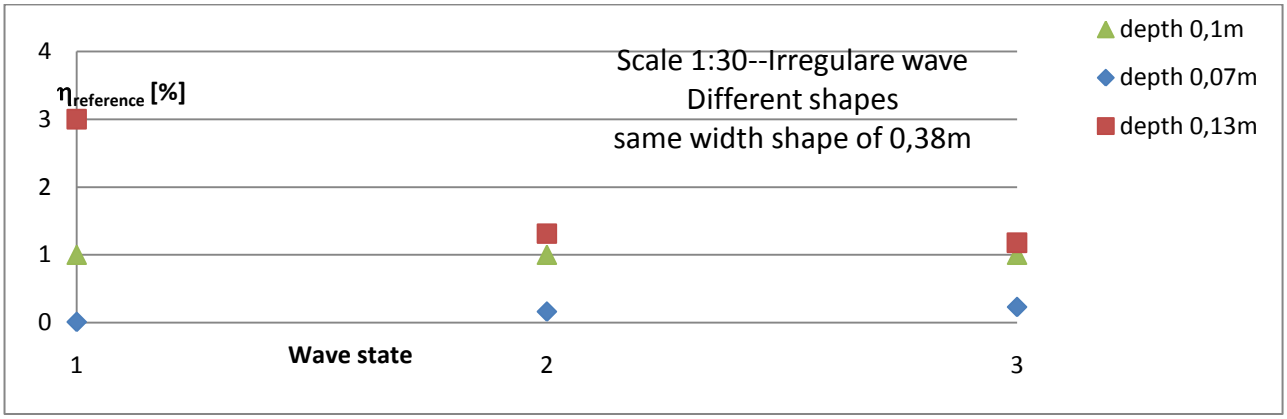

Figure 3.33: The graph shows how the efficiency increases with an increase of the depth of the plates for all the wave states. The greatest increase of the efficiency is about the 300% reported to the shape of 0,38m x 0,10m that was just more than the reference one of 0,50m x 0,10m.

Figure 3.34: The graph shows how the efficiency decrease even if the shape of the plates doesn't change. In this case the two plates differ for the presence of the hole.

The most important cause of the efficiency decrease is the different density of the two plates: in fact the plate with the hole is heavier respect the normal plate. However, it is possible to consider unreliable the values of the first wave state, while it seems correct the value of the third wave state and that means a loss of 70%.

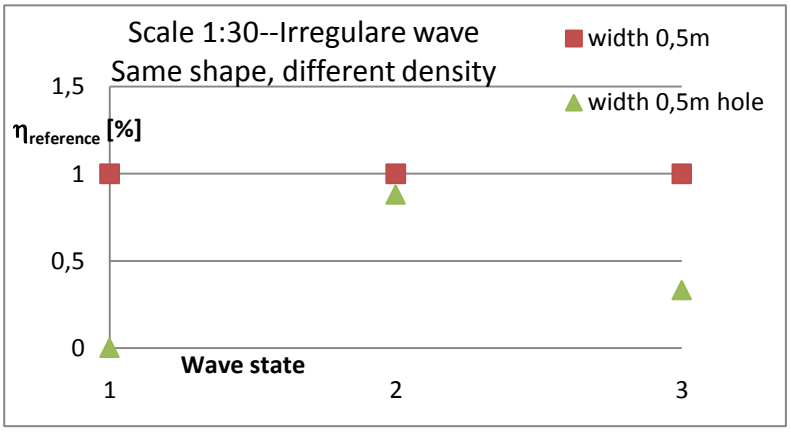

3.2.2.2.5- Summary of the performance of the device

The main aim of this work is the determine the efficiency assignable to the device for all the yearlong and of the yearly energy production, which is the quantity of energy that in a year the WavePiston can transform from wave energy in mechanical energy.

Firstly it is presented a table to summarize the wave parameters, and particularly the wave height and the wave power. The table 3.7 shows that there is different among the wave height corresponding to the real wave state and the wave height observed, consequently a similar different is in the wave power. For the following calculation the wave height corresponding to the real wave state and the wave power realized are taken as a reference.

Wave state	Tp [s]	Tz [s]	Hs wanted [m]	Power wave theoretical [W/m]	Hs realized [m]	Power wave calculated [W/m]	Power wave realized [W/m]
1	1,02	0,73	0,033	0,42	0,021	0,17	0,22
2	1,28	0,91	0,067	2,17	0,059	1,69	2,20
3	1,53	1,09	0,100	5,77	0,089	4,58	6,31
4	1,79	1,28	0,133	11,94	0,133	11,94	16,32
5	2,04	1,46	0,167	21,46	0,185	26,33	35,75

Table 3.7: Summary of the reference irregular wave states. The table shows the difference between the wave height and the wave power wanted and realized. The wave height corresponding to the real wave state and the wave power realized are taken as a reference.

A second problem is to determinate the power generated for all the wave state, because to preserve the model the fifth wave state was not carried out. So to have the value of this wave state an interpolation was done. To make this interpolation was possible to use the values regarding different test in irregular wave as

the ones with the same load of 1,5kg, but with the paddle at a diverse distance between them, finally the values concerning the four plates at a distance of 0,80m were chosen.

	Wave power generated [W/0,5m]		
Wave state	Front	Back	Average
1	0,0119	0,0153	0,0136
2	0,0731	0,0782	0,0756
3	0,1164	0,1133	0,1149
4	0,1640	0,1612	0,1626

Table 3.8: The table illustrates the values of the power generated used to the interpolation. These values are referred to the reference condition of the model.

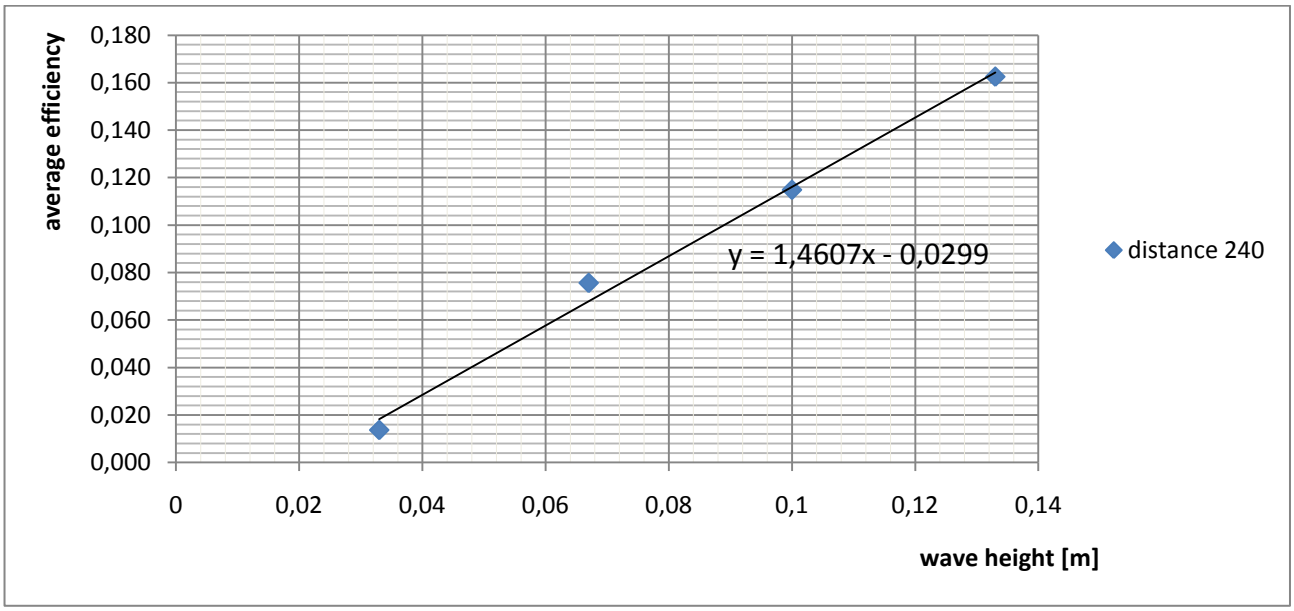

Figure 3.35: The figure illustrates the interpolation equation for the power generated.

Wave state	Tp [s]	Hs [m]	Power wave [W/m]	Prob [%]	Prob*Power wave [W/m]	Power generated [W/0,5m]	Efficiency	η*Probability	Prob*Power generated [W/m]
1	1,02	0,033	0,22	47	0,101	0,014	0,13	0,0590	0,013
2	1,28	0,067	2,20	23	0,498	0,076	0,07	0,0155	0,034
3	1,53	0,100	6,31	11	0,682	0,115	0,04	0,0039	0,025
4	1,79	0,133	16,32	5,1	0,832	0,163	0,02	0,0010	0,017
5	2,04	0,167	35,75	2,4	0,858	0,214	0,01	0,0003	0,010

Table 3.9: Summary of the performance that can be converted from the waves into useful mechanical energy by the WavePiston model. The reference configuration of the device is with two energy converter plates at the distance of 2,40m and with a load of 1,5kg. The device is subjected to irregular wave.

To identify the yearly values is feasible do a sum of the values multiplied to the probability of occurrence.

yearly average wave power [W/m]	2,9708
overall efficiency	0,080
yearly average power production [W/m]	0,0986
max power generated [W/m]	0,4281
yearly energy production [kWh/year/m]	0,8636
Load factor	0,23

Table 3.10: Estimation of the energy that can be converted from the waves into useful mechanical energy by the WavePiston device subjected to irregular wave.

The table above explains the output energy of the device for assumed 1:30 scaling lengths, the yearly average wave power is of 2.97 W/m, and the yearly power generated is almost 0,10 W/m, corresponding to a yearly energy production per meter of 0,86 kWh/y/m.

It is not possible to have a comparison between scale 1:20 and the 1:30, so it is not possible to know the improve of the yearly energy production.

Although the study regarding a scale model is on purpose to realize a real installation, it is more fruitful have the yearly power generated and consequently the yearly energy production of the real device.

The tables below show the output energy of the WavePiston wave energy converter, the yearly available average wave power is relative to the Danish part of the North Sea and is of 12,0 kW/m, and the yearly power generated is about 0,55 kW/m, corresponding to a yearly energy production per meter of 4,24 MWh/y/m.

Wave state	Hs [m]	Tp [s]	Power wave [kW/m]	Probability [%]	Prob*Power wave [kW/m]	Efficiency	η*Probability	Power generated [kW/m]	Prob*Power generated [kW/m]
1	1,00	5,60	2,11	46,8	0,988	0,13	0,061	0,275	0,128
2	2,00	7,00	10,56	22,6	2,387	0,07	0,016	0,739	0,167
3	3,00	8,40	28,51	10,8	3,079	0,04	0,004	1,140	0,123
4	4,00	9,80	59,14	5,1	3,016	0,02	0,001	1,183	0,060
5	5,00	11,20	105,60	2,4	2,534	0,01	0,000	1,056	0,025

Table 3.11: Summary of the performance of the WavePiston wave energy converter. The value of the power that can be converted from the waves into useful mechanical power by the WavePiston model is referred to one plate of 15m of width . The device is subjected to irregular wave.

In the next table, for a more immediate comprehension the same values are reported even referred to the width of the plate, of 15m.

Wave state	Hs [m]	Tp [s]	Power wave [W/plate]	Probability [%]	Prob*Power wave [W/plate]	Efficiency	η*Probability	Power generated [W/plate]	Prob*Power generated [W/plate]
1	1,00	5,60	31,68	46,8	14,826	0,13	0,061	4,12	1,927
2	2,00	7,00	158,40	22,6	35,798	0,07	0,016	11,09	2,506
3	3,00	8,40	427,68	10,8	46,189	0,04	0,004	17,11	1,848
4	4,00	9,80	887,04	5,1	45,239	0,02	0,001	17,74	0,905
5	5,00	11,20	1584,00	2,4	38,016	0,01	0,000	15,84	0,380

Table 3.12: Summary of the performance of the WavePiston wave energy converter. The value of the power that can be converted from the waves into useful mechanical power by the WavePiston model is referred to one plate of 15m of width . The device is subjected to irregular wave.

yearly average wave power [kW/m]	12,00
yearly average wave power [kW/plate]	180,07
overall efficiency	0,080
yearly average power production [kW/m]	0,504
yearly average power production [kW/plate]	7,570
max power generated [kW/m]	1,183
max power generated [kW/plate]	17,74
yearly energy production [MWh/year/m]	4,42
yearly energy production [MWh/year/plate]	66,3
Load factor	0,39

Table 3.13: Summary of the performance and the estimated energy that can be converted from the waves into useful mechanical energy by the WavePiston device subjected to irregular wave.

The tables are filled in following the explanation reported at page 57.

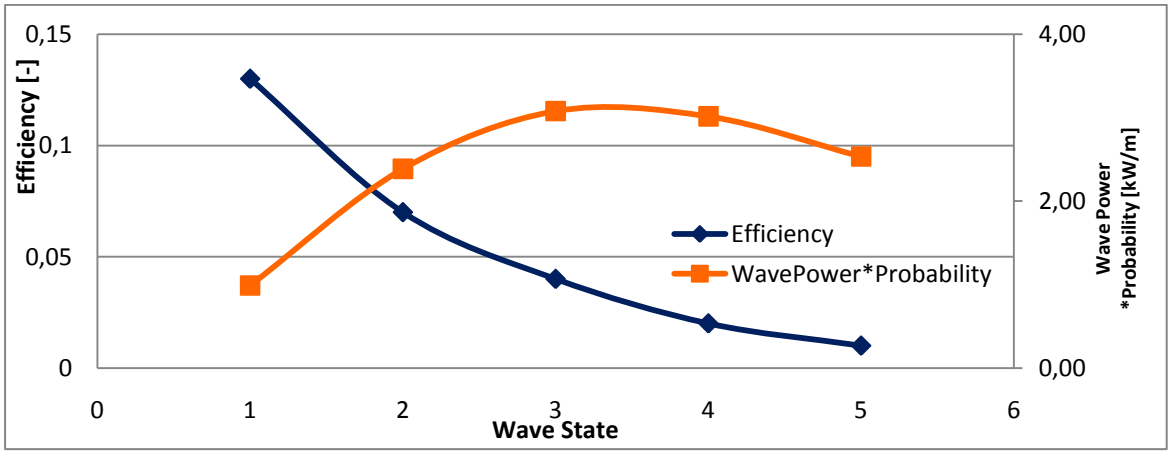

Figure 3.36: Representation of the average efficiency of a plate of 15m width of the WavePiston device in the blue line, instead the orange line is the product of the probability of occurrence and the available wave power.

4- Future Installation

4.1- Italian Installation basing on laboratory results

The aim of this part is to understand the performance of the WavePiston device in the Mediterranean Sea.

The font of every sea data in Italy is the *Rete Ondametrica Nazionale* (Wave meters National Network). The information are extremely useful for the design of engineering coastal works as ports, breakwaters, etc. Furthermore the same data are essential to analyze the coastal erosion, to determinate the actual occurrence of natural disaster, to predict the wave state in the Mediterranean, to enhance safety of the navigation. The *Rete Ondametrica Nazionale* (RON) is active since July 1989. The RON was originally composed of eight directional buoys, located off the coast of LaSpezia, Alghero, Ortona, Ponza, Monopoli, Crotone, Catania and Mazara del Vallo. Each buoy was anchored in the deep water, at 100m of depth. Each buoy is able to following the surface motion and is equipped with a satellite system to monitoring its position. In the 1999 two more buoys were added in Cetraro and in Ancona. And at last in 2002 four more buoys were added in Capo Linaro, Capo Gallo, Punta della Maestra and Capo Comino. Thus for now the Ron is composed by 14 buoys. The sampling station are completed of a receipt and elaboration centre where each bouy send the data by radio. Each buoy registers data about elevation, inclination, H_x, H_y, H_z. The data are usually acquired every three hours for a period of 30 minutes. In significant storm surges the data acquisition is automatic and continuous every half hour. In early 2002 work began for enhancement RON, for example with the addition of the processing in the time domain(zero-crossing analysis). From the elaboration centre some parameters are made as the significant wave height (H_s), the peak wave period (T_p), the medium wave period (T_m), the main wave direction, etc.

Figure 4.1: Position of the 15 Italian buoys

4.1.1- Italian Wave State

It is been decided to study the performance of the WavePiston in Mazara del Vallo.

Figure 4.2: Mazara del Vallo buoy. Each buoy has a diameter of 1,7m and it is positionated at an height of 2,8m from the waterline. The source of the picture is Idromare, web site www.idromare.it

Figure 4.3: Mazara del Vallo position. The source of the picture is Idromare, web site www.idromare.it

Strumenti	Boa DATAWELL Directional wavec MKI dal 01.06.1989 al 31.12.2001	
Posizione	37° 38' 43.19" N	12° 34' 57.0" E
Altezze di soglia	2.5 m	4.5 m

Figure 4.4: Mazara del Vallo DATAWELL position, source Idromare web site.

As told above, from the web site it is possible to find the data regarding the significant wave height, the wave period and the direction of the waves propagation. These data are shown is the next figures.

sec m	<=1.5	<=3	<=4.5	<=6	<=7.5	<=9	<=10.5	<=12	<=13.5	<=15	<=16.5	<=18	>18	TOT
>9.5														
<=9.5														0
<=9														0
<=8.5														0
<=8														0
<=7.5													1	1
<=7								3						3
<=6.5							1	3	1					5
<=6						1	8	16	7				1	33
<=5.5						8	34	40	8				1	91
<=5						12	128	68	5					213
<=4.5						27	176	78	9					290
<=4					3	133	349	118	7				1	611
<=3.5					94	562	586	79	4					1325
<=3				4	445	1294	721	109	8	1	3			2585
<=2.5				182	1884	2328	682	111	14	1			2	5204
<=2			10	1768	5468	2998	882	188	40	3			3	11360
<=1.5			1050	6255	8637	2781	1212	423	32	4			7	20401
<=1		428	8207	13988	8164	2915	1045	158	10		3	6	409	35333
<=0.5		3129	8298	8855	4784	2058	168	34	7			1	1019	28353
TOT	0	3557	17565	31052	29479	15117	5992	1428	152	9	6	7	1445	105808

Figure 4.5: Mazara del Vallo DATAWELL, Survey of the significant wave height in meter on the y-axis and the peak wave period in second on the x-axis. The survey is referred to the period from 01/07/1989 to 04/04/2008. The expected surveys are 61352 and the missed ones are 44457 (42%of the expected ones). 27% of the effectives are with a wave height under 0,5m; source Idromare web site.

'N m	<=15	<=30	<=45	<=60	<=75	<=90	<=105	<=120	<=135	<=150	<=165	<=180	<=195	<=210	<=225	<=240	<=255	<=270	<=285	<=300	<=315	<=330	<=345	<=360	TOT
>10																									
<=10																									0
<=9.5																									0
<=9																									0
<=8.5																									0
<=8	1																								1
<=7.5																			3						3
<=7												1							4						5
<=6.5									2	1	1	1	1						22	4				1	33
<=6		1							11				2	2	2	4	2	4	56	12		1	2		99
<=5.5			1						17	2	2	1	6	6	2	8	4	21	120	30	14	1	1	3	239
<=5	2	1	1	4			2	3	15	3	11	13	2	2	5	17	4	28	128	36	7	3	1	2	290
<=4.5	1	2	7	3	2	1	5	5	39	23	9	7	12	3	4	24	15	40	307	74	14	6	3	7	613
<=4	7	8	12	7	3	13	8	12	137	74	16	18	24	38	35	23	27	106	515	173	31	17	10	16	1330
<=3.5	27	18	16	22	16	21	21	35	266	166	31	32	39	50	55	44	60	194	1009	310	77	31	33	28	2601
<=3	31	42	52	28	27	42	54	86	451	441	105	81	71	81	80	95	111	373	1920	692	221	66	59	50	5259
<=2.5	78	74	79	64	73	85	117	169	1130	1099	402	272	248	197	161	181	239	767	3615	1611	428	117	84	65	11355
<=2	170	129	149	131	137	196	242	299	1857	2292	966	586	529	420	339	296	460	1325	5406	2792	939	341	200	185	20386
<=1.5	312	278	248	246	243	290	348	782	2330	3568	2616	1660	1164	957	757	814	1045	2270	6539	4412	2293	1309	425	405	35311
<=1	168	167	132	162	180	197	308	442	985	1401	1477	1332	1047	883	773	678	826	1366	2681	2274	1579	714	251	183	20206
<=0.5	105	93	85	80	90	113	123	154	242	356	507	540	543	628	685	585	671	784	774	666	374	152	97	84	8531
TOT	902	813	782	747	771	958	1228	1987	7482	9426	6143	4544	3688	3267	2898	2769	3464	7278	23100	13086	5977	2758	1166	1029	106262

Figure 4.6: Mazara del Vallo DATAWELL, Survey of the significant wave height in meter on the y-axis and the medium wave direction of the propagation in °N on the x-axis. The survey is referred to the period from 01/07/1989 to 04/04/2008. The expected surveys are 61352 and the missed ones are 44911 (42%of the expected ones). 8% of the effectives are with a wave height under 0,5m; source Idromare web site.

In the tables above the numbers indicate the number of events happened. Since the analysis has the target to focus the wave state of that location the data were utilized for operating limit state instead that ultimate limit state. The difference is that in the ultimate limit analysis the aim is the investigation of the maxim wave height to design the strength of different elements, whereas in the operating analysis the intent is to examine the probability of occurrence for the final study of the power take off.

Therefore in this document there is not the comparison between the observed values and the values predicted with a theoretical distribution as the Weibull or the Gumbel, instead there is an elaboration based on the real possible performances.

For any event dividing the number of times of the event itself occurred by the total number of the observations the probability of occurrence is given. At this point a table with for each division step of the wave height corresponding vary wave periods with diverse probability is made. To be able to assign a single wave period at a given wave height is to do an average weighted where the weight is the probability of occurrence. The two tables below show this procedure.

sec	0,75	2,25	3,75	5,25	6,75	8,25	9,75	11,25	12,75	14,25	15,75	17,25	19	
m														TOT
0-0,5		0,02957	0,07843	0,08369	0,04521	0,01945	0,00159	0,00032	0,00007			0,00001	0,00963	0,26797
0,6-1,0		0,00405	0,07757	0,13220	0,07716	0,02755	0,00988	0,00149	0,00009		0,00003	0,00006	0,00387	0,33394
1,1-1,5			0,00992	0,05912	0,08163	0,02628	0,01145	0,00400	0,00030	0,00004			0,00007	0,19281
1,6-2,0			0,00009	0,01671	0,05168	0,02833	0,00834	0,00178	0,00038	0,00003			0,00003	0,10736
2,1-2,5				0,00172	0,01781	0,02200	0,00645	0,00105	0,00013	0,00001			0,00002	0,04918
2,6-3,0				0,00004	0,00421	0,01223	0,00681	0,00103	0,00008	0,00001	0,00003			0,02443
3,1-3,5					0,00089	0,00531	0,00554	0,00075	0,00004					0,01252
3,6-4,0					0,00003	0,00126	0,00330	0,00112	0,00007				0,00001	0,00577
4,1-4,5						0,00026	0,00166	0,00074	0,00009					0,00274
4,6-5,0						0,00011	0,00121	0,00064	0,00005					0,00201
5,1-5,5						0,00008	0,00032	0,00038	0,00008				0,00001	0,00086
5,6-6,0						0,00001	0,00008	0,00015	0,00007				0,00001	0,00031
6,1-6,5							0,00001	0,00003	0,00001					0,00005
6,6-7,0								0,00003						0,00003
7,1-7,5													0,00001	0,00001

Table 4.1: Probabilistic analysis for the significant wave height and the peak wave period of Mazara del Vallo. The numbers in the table indicate the probability of occurrence of every event.

Wave State	H [m]	Hs [m]	Tp [sec]	Tz [sec]	Prob [%]	P onda [kW/m]
1	0,175	0,250	5,48	3,92	26,80	0,13
2	0,525	0,750	5,78	4,13	33,39	1,23
3	0,875	1,250	6,63	4,73	19,28	3,91
4	1,225	1,750	7,24	5,17	10,74	8,37
5	1,575	2,250	7,88	5,63	4,92	15,05
6	1,925	2,750	8,56	6,11	2,44	24,41

Table 4.2: Wave State for Mazara del Vallo.

4.1.2- Yearly average efficiency and yearly energy production

Firstly a comparison among the Danish wave states and the Italian wave states was made.

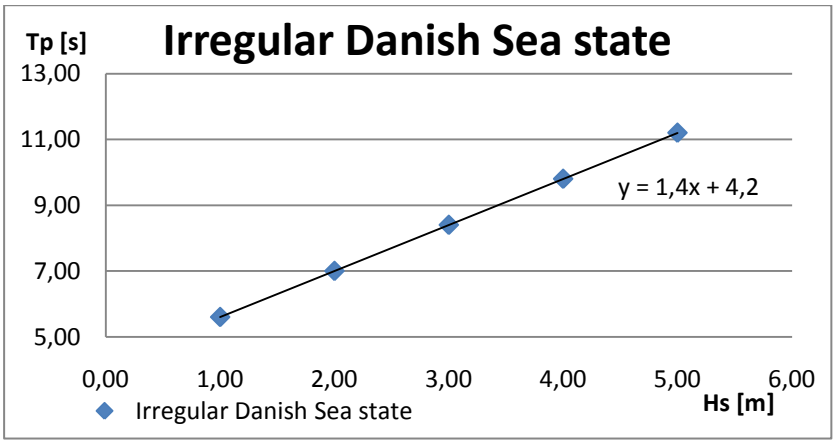

Figure 4.7: Trend of the irregular Danish Sea State, from "Danish approach to development and evaluation of wave energy devices" Kofoed & Frigaard (2009)

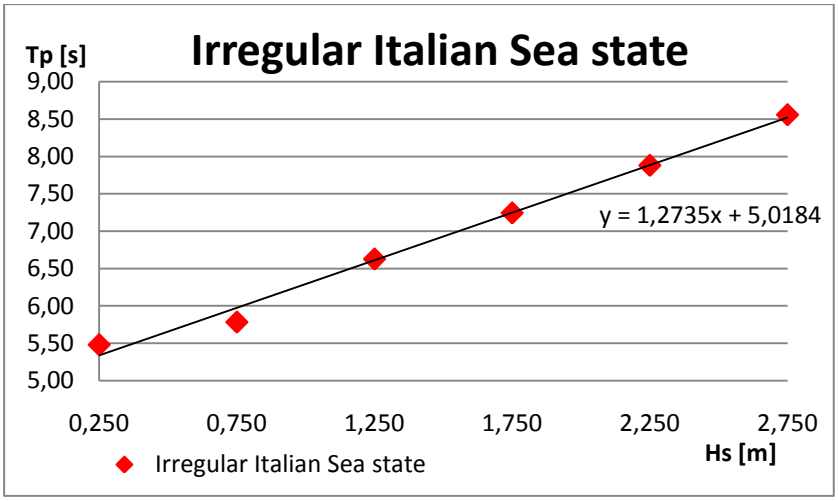

Figure 4.8: Trend of the irregular Italian Sea States

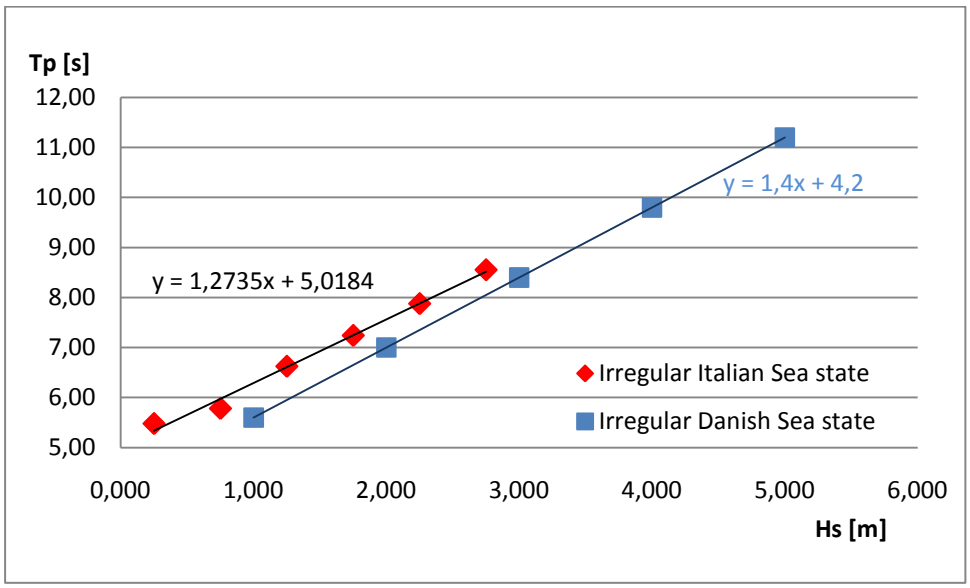

Figure 4.9: Comparison between the trend of the irregular Italian Sea States and the Danish one.

Due to the reason that in all the graphs above the trends are similar it was deemed appropriate to apply the Danish results to the Italian case.

Furthermore to calculate the yearly average efficiency and the yearly energy production for the Italian situation an hypothesis regarding the Danish efficiency trend was done. This hypothesis is concerning the efficiency values for the wave state characterized by small wave height and small wave period, and in particular it consists to declare that the trend efficiency is the same, there is no reason to presume a peak or a different behaviour.

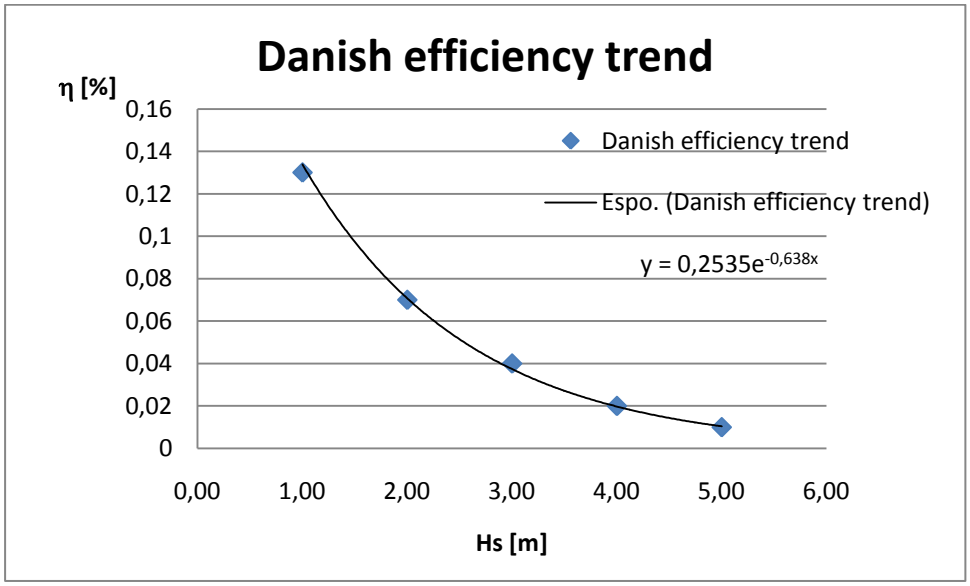

Figure 4.10: Danish efficiency trend for the WavePiston carries out by the laboratory result.

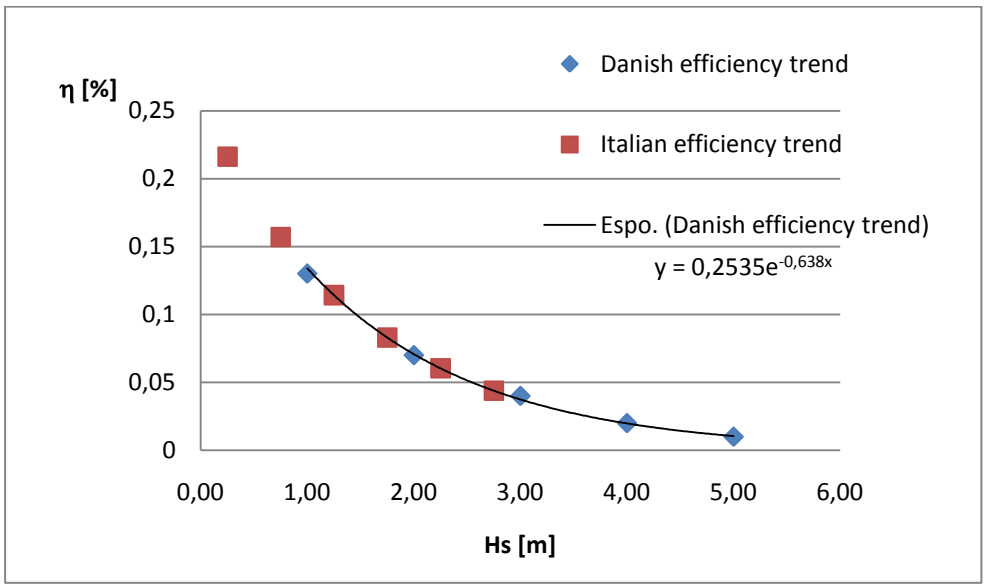

Figure 4.11: Extrapolation of the Italian efficiency trend for the WavePiston using the Danish efficiency trend.

Note the efficiency and the wave power, it is feasible estimate the yearly efficiency and the yearly energy production as just done in the previous chapter.

The tables below show the output energy of the WavePiston wave energy converter for an installation in the South Italian Sea, the yearly available average wave power is 3,43 kW/m compared to the Danish of 12,0 kW/m, and the yearly power generated is about 0,30 kW/m compared to 0,55 kW/m of the Danish Sea, corresponding to a yearly energy production per meter of 2,66 MWh/y/m compared to the Danish one of 4,24 MWh/y/m.

Wave state	Hs [m]	Tp [s]	wave Power [kW/m]	Probability [%]	Prob*Power wave [kW/m]	η	η* Probability	Power generated [kW/m]	Pgenerated*Prob [kW/m]
1	0,25	5,48	0,13	26,80	0,035	0,22	0,058	0,028	0,007
2	0,75	5,78	1,23	33,39	0,410	0,16	0,052	0,193	0,064
3	1,25	6,63	3,91	19,28	0,753	0,11	0,022	0,446	0,086
4	1,75	7,24	8,37	10,74	0,898	0,08	0,009	0,694	0,075
5	2,25	7,88	15,05	4,92	0,740	0,06	0,003	0,908	0,045
6	2,75	8,56	24,41	2,44	0,596	0,04	0,001	1,070	0,026

Table 4.3: Summary of the performance of the WavePiston wave energy converter in an Italian installation. The value of the power that can be converted from the waves into useful mechanical power by the WavePiston model is referred to one plate of 15m of width . The device is subjected to irregular wave.

In the next table, for a more immediate comprehension the same values are reported even referred to the width of the plate.

Wave state	Hs [m]	Tp [s]	wave Power [kW/plate]	Probability [%]	Prob*Power wave [kW/plate]	η	η* Probability	Power generated [kW/plate]	Pgenerated*Prob [kW/plate]
1	0,25	5,48	1,94	26,80	0,519	0,22	0,058	0,419	0,112
2	0,75	5,78	18,40	33,39	6,146	0,16	0,052	2,891	0,965
3	1,25	6,63	58,58	19,28	11,294	0,11	0,022	6,689	1,290
4	1,75	7,24	125,49	10,74	13,474	0,08	0,009	10,416	1,118
5	2,25	7,88	225,68	4,92	11,100	0,06	0,003	13,616	0,670
6	2,75	8,56	366,09	2,44	8,944	0,04	0,001	16,054	0,392

Table 4.4: Summary of the performance of the WavePiston wave energy converter in an Italian installation. The value of the power that can be converted from the waves into useful mechanical power by the WavePiston model is referred to one plate of 15m of width . The device is subjected to irregular wave.

yearly average wave power [kW/m]	3,43
yearly average wave power [kW/plate]	51,48
overall efficiency	0,15
yearly average power production [kW/m]	0,30
yearly average power production [kW/plate]	4,55
max power generated [kW/m]	1,07
max power generated [kW/plate]	16,05
yearly energy production [MWh/year/m]	2,66
yearly energy production [MWh/year/plate]	39,84
Load factor	0,28

Table 4.5: Summary of the performance and the estimated energy that can be converted from the waves into useful mechanical energy by the WavePiston device subjected to irregular wave in the Italian Sea.

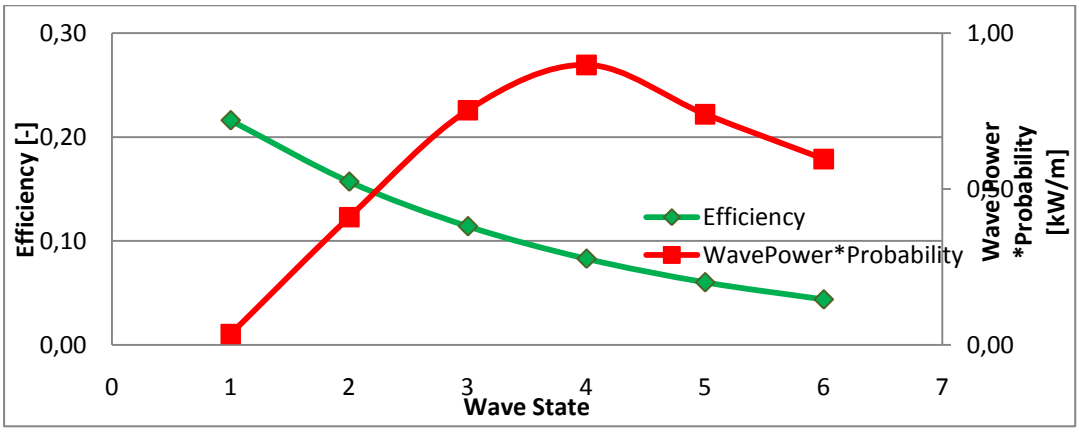

Figure 4.12: Representation of the average efficiency of a plate of 15m width of the WavePiston device in the green line, instead the red line is the product of the probability of occurrence and the available wave power.

4.2- Numerical Model

4.2.1- Theoretical Equations

The intention of this part is to find out a numerical model able to predict the behaviour of the WavePiston wave energy converter varying the wave parameters. This means that the purpose is to understand the power take off of the device regardless the laboratory tests. In the next pages, the procedure is exposed, starting with the theoretical equations. Each unit of the WavePiston, so each energy converter plate, is equivalent to a single degrees freedom body, where the spring stiffness considers the real spring that will stop the excessive movement of the plate and the damping is represented by the friction force and the external force is explainable with the Morison equation.

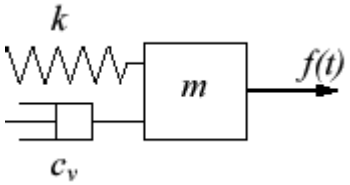

Figure 4.13: A single unit of the WavePiston device is seen as a single degrees freedom body.

The equation for a single degrees freedom body is:

$$m\ddot{x} + c\dot{x} + kx = f(t)$$

The external force is given by the Morison equation, as:

$$f(t) = F_I + F_D + F_{FK}$$

Where:

- F_I is the inertial force;
- F_D is the drag force;
- F_{FK} is the Froude-Krylov force.

Their formulations are:

$$F_I = \rho_w * c_M * Volume(\dot{u} - \ddot{x})$$

$$F_D = \frac{1}{2} c_D * \rho_w * Area(u - \dot{x})|(u - \dot{x})|$$

$$F_{FK} = \rho_w * Volume * \dot{u}$$

The problem to solve is represented by the following equation:

$$m\ddot{x} + c\dot{x} + kx = F_I + F_D + F_{FK}$$

$$m\ddot{x} + c\dot{x} + kx = \rho_w * c_M * Volume(\dot{u} - \ddot{x}) + \frac{1}{2} c_D * \rho_w * Area(u - \dot{x})|(u - \dot{x})| + \rho_w * Volume * \dot{u}$$

4.2.1.1- External forces' investigation

In fluid dynamics the Morison equation is a semi-empirical equation for the inline force on a body in oscillatory flow. This equation was introduced in the 1950 by Morison, O'Brien, Johnson and Schaaf. The Morison equation is used to estimate the wave loads in the design of generic offshore structures.

Mainly the Morison equation is the sum of two forces: an inertia force, in phase with the local flow acceleration, and a drag force proportional to the square of the instantaneous flow velocity. An empirical hydrodynamic coefficient is contained in each force.

The Morison equation has two forms, one in the case of fixed body in an oscillatory flow and another where the body is moving as well.

4.2.1.1.1- Fixed body in an oscillatory flow

In an oscillatory flow, with flow velocity *u(t)*, the Morison equation gives the inline force parallel to the flow direction as:

$$F(t) = F_I + F_D$$

Where:

- F(t) is the total inline force on the object;
- $F_I(t)$ is the inertia force $F_I = \rho_w(1 + c_M)Volume * \dot{u}$ in this case the inertia force includes the Froude-Krylov force, and c_M is the added-mass coefficient, Volume is the volume of the body;
- $F_D(t)$ is the drag force $F_D = \frac{1}{2}c_D * \rho_w * Area * u * |u|$ Area is the reference area, i.e. the cross-sectional area of the body perpendicular to the flow direction.

For example, for a circular cylinder of diameter *D* in oscillatory flow, the reference area per unit cylinder length is *D* and the cylinder volume per unit cylinder length is $Volume = \frac{1}{4}\pi * D^2$. While for the device in exam, the reference area is the product of the width and the depth of the plate.

Besides the inline force, there are also oscillatory lift forces perpendicular to the flow direction, due to vortex shedding. These are not covered by the Morison equation, which is only for the inline forces.

4.2.1.1.2- Moving body in an oscillatory flow

In the case that, even the body is moving, with a velocity $\dot{x}(t) = v(t)$, the Morison equation becomes:

$$F_I + F_D + F_{FK} = \rho_w * c_M * Volume(\dot{u} - \ddot{x}) + \frac{1}{2}c_D * \rho_w * Area(u - \dot{x})|(u - \dot{x})| + \rho_w * Volume * \dot{u}$$

The Froude-Krylov is the force introduced by the unsteady pressure field generated by undisturbed waves. It can be calculated as:

$$F_{FK} = -\iint_{S_w} p \cdot \vec{n}\, ds$$

Where:

- S_w is the wetted surface of the floating body
- p is the pressure in the undisturbed waves
- $\vec{n}$ is the body's normal vector pointing into the water.

In the simplest case the formula may be expressed as:

$$F_{FK} = Area * p_{dyn} = Area * \rho_w * g * \frac{H}{2} = \rho_w * Volume * \dot{u}$$

Even if the Morison equation is useful to have an initial idea on the external loads, the Morison equation has some limitations, as:

1. The Morison equation is a heuristic formulation of the force fluctuations in an oscillatory flow. The first assumption is that the flow acceleration is more-or-less uniform at the location of the body. For instance, this requires that the main dimension of the body is much smaller than the wavelength. If the main dimension of the body (for example the diameter for a cylinder body) is not small compared to the wavelength, diffraction effects have to be taken into account.
2. Second, the Morison equation is able to illustrate the force history very well, although this depends on the two empirical coefficients, and they depend to the Keulegan-Carpenter number. However, from experiments it is found that in the intermediate regime of the Keulegan-Carpenter number, where both drag and inertia are giving significant contributions, the Morison equation is not capable to describe the force history very well.
3. Third, when extended to orbital flow which is a case of non unidirectional flow, for instance encountered by a horizontal cylinder under waves, the Morison equation does not give a good representation of the forces as a function of time.
4. The maximum force exerted by breakers or incipient breakers is impulsive in nature, reaching a value much greater than that produced by unbroken waves but enduring for only a short time interval. This impulsive force greatly exceeds the drag force computed from the particle velocities of the breaker.
5. It is not obvious the instant of maximum force, as it mainly depends on two forces having the same trend but not in phase. Hence the maximum load is not when the crest comes, that is the moment where the inertia force is max.

4.2.1.2- Simplifying assumptions

Even if the main target is the estimation of the WavePiston performance, regardless the laboratory results, a first step of study is done to carry out a model that giving in input the laboratory condition gives in output results comparable to the laboratory ones.

For that there were done some assumptions:

- the body is considered fixed in the Morison equation, this means that there is no Froude-Krylov force and that there is no dependent by the velocity of the body movement;
- the solution is not in a closed analytical form, so it is not continue but it is studying with the finite difference method, so the solution is known only in the particular time domain points.

$$\ddot{x} + \frac{c}{m}\dot{x} + \frac{k}{m}x = \frac{1}{m}\rho_w(1 + c_M) * Volume * \dot{u} + \frac{1}{2 * m}\rho_w c_D Area(u)|u|$$

With the finite difference method the equation becomes:

$$\frac{(x_{j+1} - x_j)}{\Delta t^2} + \frac{c}{m} * \frac{(x_{j+1} - x_j)}{\Delta t} + \frac{k}{m}\frac{(x_{j+1} + x_j)}{2} = \frac{1}{m}\rho_w(1 + c_M)Volume(\dot{u}) + \frac{1}{2 * m}c_D\rho_w Area(u)|u|$$

where u is the flow velocity, and it is expressed as:

$$u(t) = \omega\frac{H}{2}\frac{\cosh(\frac{2\pi}{L}(h+z))}{senh(\frac{2\pi}{L}h)}\cos(\omega t)$$

The solution of the general equation was studied by the utilization of Matlab software.

In the Matlab editor further assumptions were made, as:

- the stiffness of the device should be carried out by particular laboratory test, where it is possible to obtain the corresponding force after the imposition of a known displacement. The stiffness should be the ratio between the difference of two displacements and the equivalent difference of the forces. To time question it was not possible to realize this experiment, hence it is assumed a stiffness of 100 [N/m], this value means that to move the energy converter plate of 1cm there is the necessity of a force of 1N;
- the damping coefficient assumes vary value, so it is possible to represent the variation of the friction on the device, in order to find the best combination load-waves. Thus the damping coefficient has not an unique value.

Through the Matlab script is achievable the trends of the displacements and the velocity of the energy converters plates, and the power consequently to the variation of the damping value.

The results are reported below in a graph way.

In the figure below, with a red solid curve, there is the harmonic signal of the wave incident that represents the external force. Whereas, velocity of the plate movement is symbolized with the magenta points.

Obviously, the plate velocity has a more limited range than the external force one, however it still has an harmonious trend.

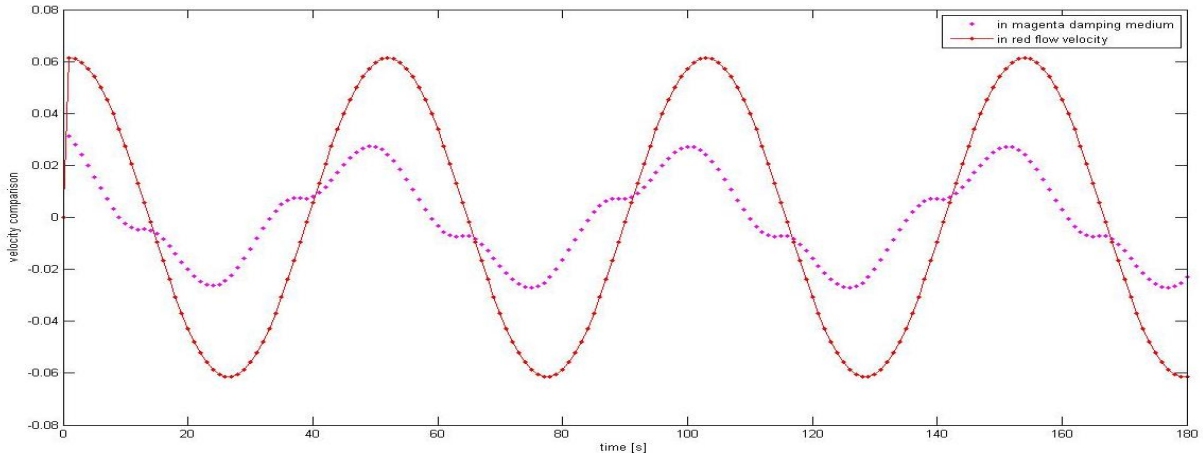

Figure 4.14: Lab_fixed_body model. Comparison between the flow velocity in the red solid line, and the velocity of the body movement for a damping mean value.

The figure below is related to the same wave conditions, the three curves refer to different displacements that the plate is subjected consequently to a variation of the damping value. The blue points represent the situation without damping, while the black ones are for the maximum damping value in exam.

Clearly, the range of the displacement decreases from the situation without damping, that represents the free movement, to the situation with the maximum damping, that correspond to the maximum movement resistance.

Furthermore, as well as for the velocity, even for the displacement is predictable the same trend of the external force, hence an harmonious one.

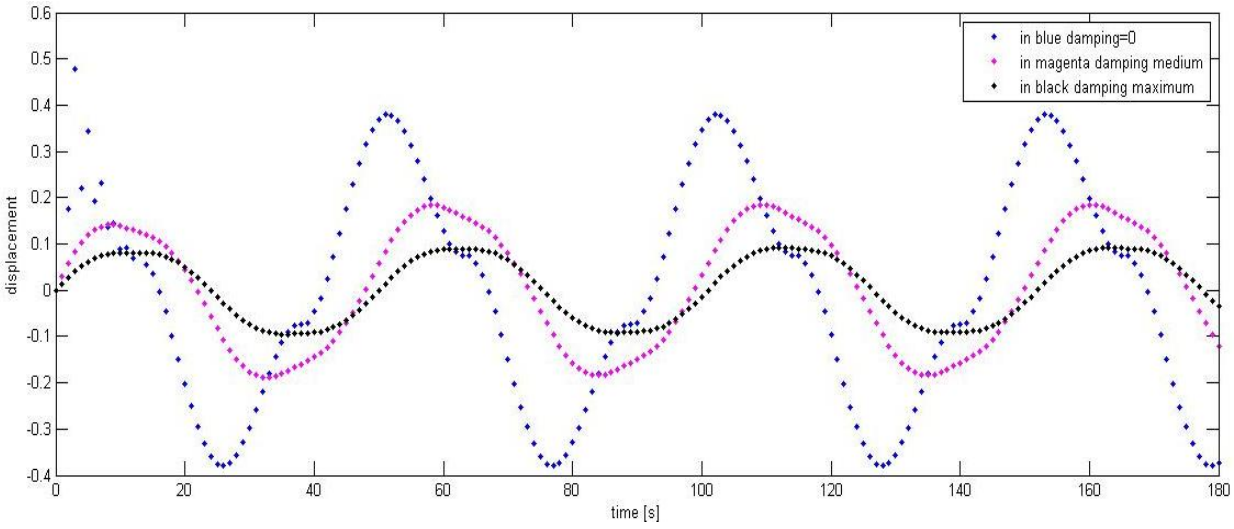

Figure 4.15: Lab_fixed_body model.
Different displacements due to the variation of the damping values from 0 to 100[Ns/m].

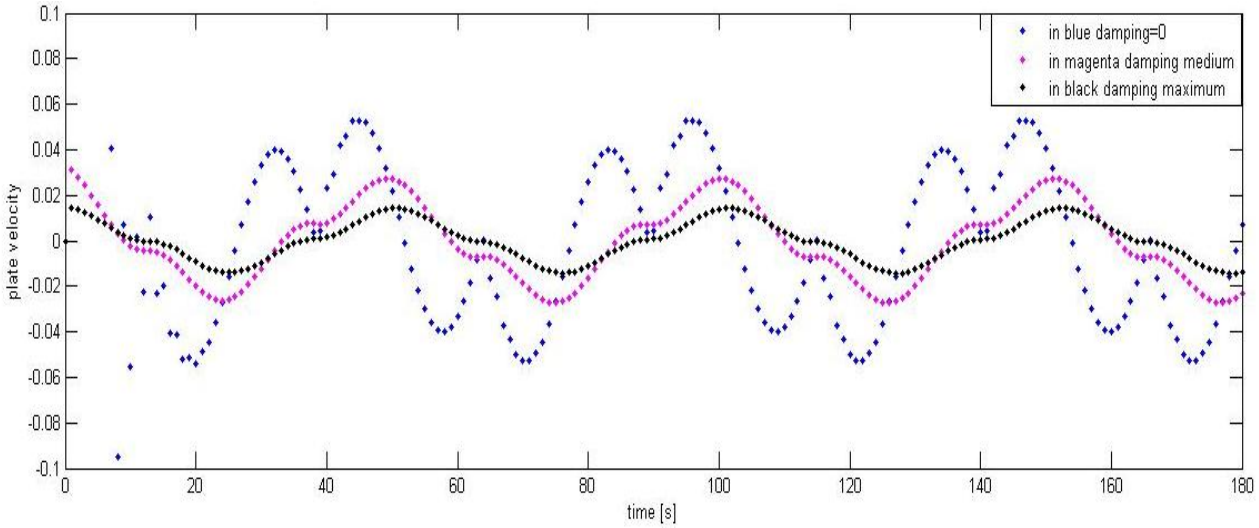

Figure 4.16: Lab_fixed_body model. Different curves, each represents the plate velocity during three different simulations. A simulations differs from others due to the variation of the damping values from 0 to 100[Ns/m].

As before, the figure above is related to the same wave conditions, the three curves refer to different plate velocity consequently to a variation of the damping value. The blue points represent the situation without damping, while the black ones are for the maximum damping value in exam.

Clearly, the range of the velocity decreases from the situation without damping (that represents the free movement where the plate should be integral with the water and its flow), to the situation with the maximum damping (that correspond to the maximum movement resistance, and the plate should be nearest to the fixed conditions).

The figures below summarize the effects of the variation of the damping value.

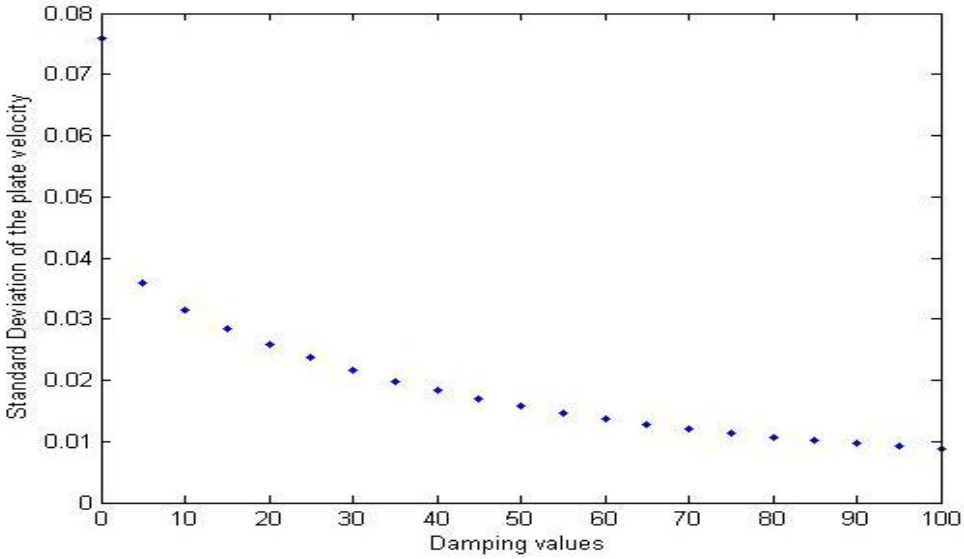

Figure 4.17: Lab_fixed_body model.
Different standard deviation of the plate velocities related to the variation of the damping values from 0 to 100[Ns/m].

As expected, the figure 4.17 summarizes a decrease in the standard deviation of the velocity from the situation “free movement and damping zero” to the situation to maximum damping.

Whereas, the figure 4.18 qualifies that the standard deviation of the force increases with an increase of the damping value, this is explainable because without damping, the plate is free to move as the water and so the plate does not make any resistance, instead with a maximum damping it seems like the plate is fixed and makes the maximum movement resistance.

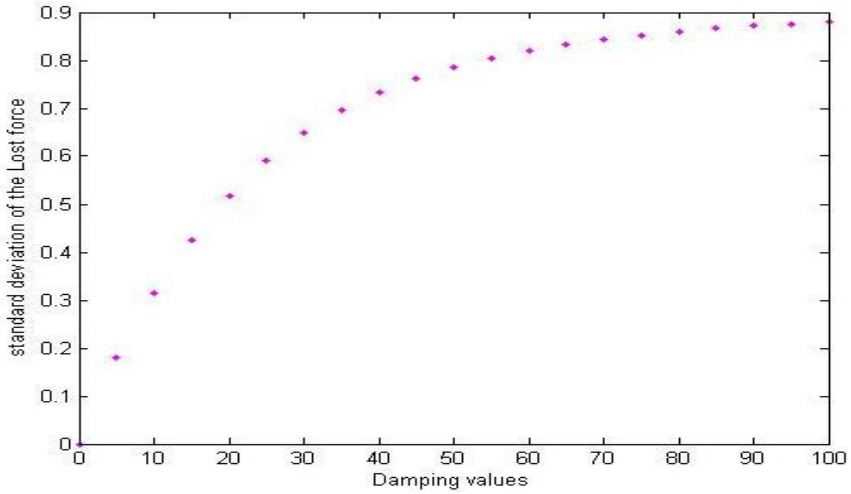

Figure 4.18: Lab_fixed_body model. Different standard deviation of the force impressed on the plate related to the variation of the damping values from 0 to 100[Ns/m].

In view of the fact that velocity and force have opposite trends, the best way to choose the best damping value is to consider even the power generated trend. In fact, the power generated from the device is obtained as a multiplication between the velocity and the force impressed.

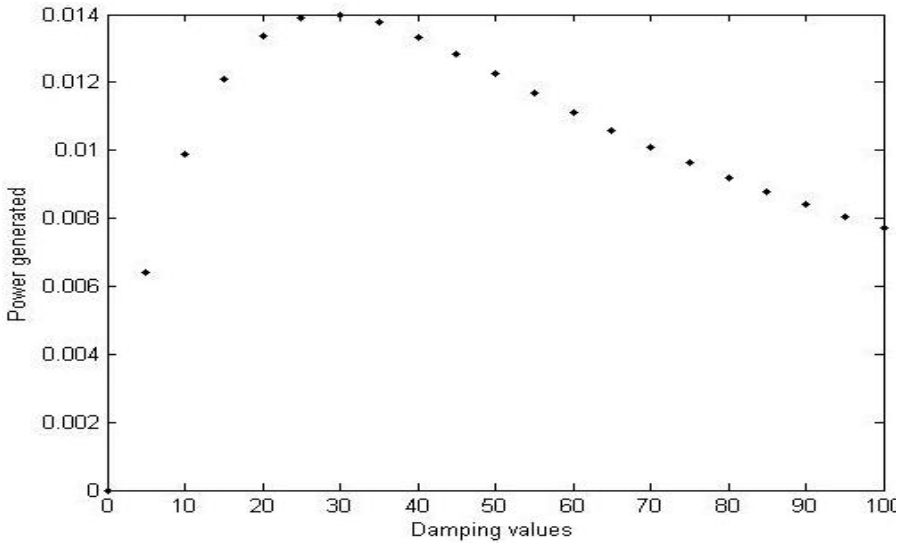

Figure 4.19: Lab_fixed_body model. Different power generated related to the variation of the damping values from 0 to 100[Ns/m].The power generated is calculate as the multiplication between the plate velocity and its force impressed.

As expected, the best damping values is not little, otherwise the velocity might be high but not the force, and at the same time it is not big, for the opposite reason. The results show that the best values is around a damping value c, of 30Ns/m.

For an easier view, the same result is reported related to the standard deviation force. In this graph the maximum power is for a standard deviation force of 0,65N, and from the figure 4.18 it is verifiable that correspond to a damping value of 30Ns/m.

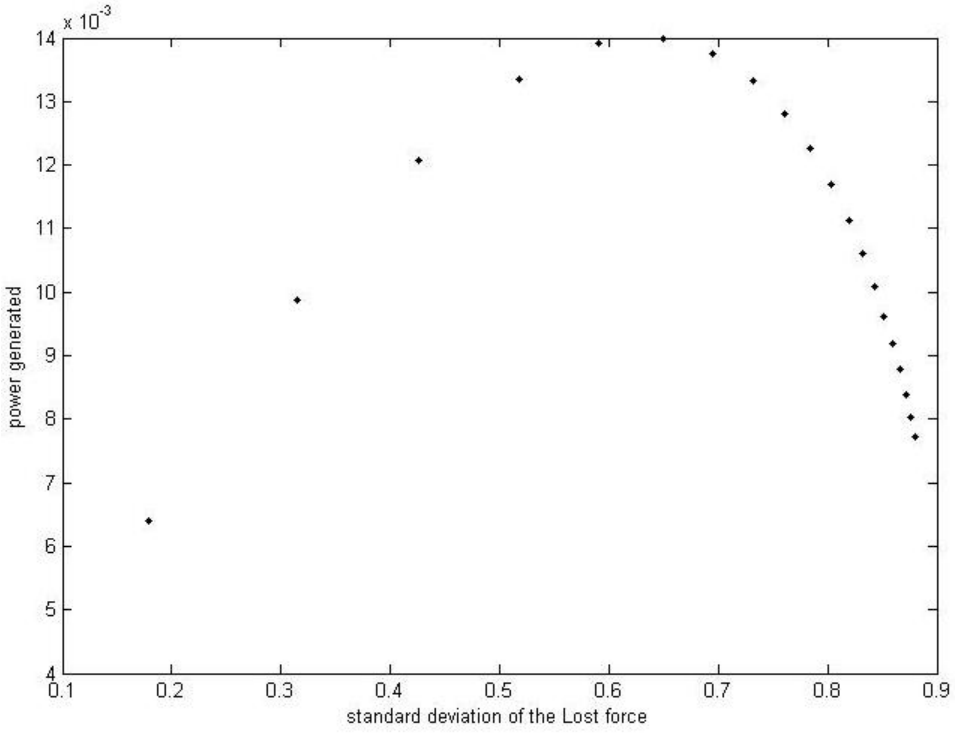

Figure 4.20: Lab_fixed_body model. Different power generated related to the variation of the damping values from 0 to 100[Ns/m].The power generated is calculate as the multiplication between the plate velocity and its force impressed.

To get closer to the main target of the numerical model, i.e. the estimation of the WavePiston performance, regardless the laboratory results; the Matlab script is modified in order to consider the prototype body in moving as well.

For this second model, some assumptions were done:

- as before, the solution is not in a closed analytical form, so it is not continue but it is studying with the finite difference method, so the solution is known only in the particular time domain points;
- the movement of the body implies in the Morison equation that the external force is decreased respect the fixed body case. The Froude-Krylov force is a third distinct contribution.

Other results related to this study are reported in the appendixes.

A last study might be the verification of the reflection analysis made by WaveLab3.33.

The reflection analysis consists in the comparison of the incident wave spectrum and the reflected wave spectrum, with the aim to find the k_R reflection coefficient. The reflection coefficient is defined as the ration between H_R, i.e. the reflected wave height and H_I, i.e. the incident wave height.

Usually the reflection analysis starts with the evaluation of the elevation values measured by the wave gauges, to separate the values of the incident waves to the ones referred to the reflected waves. Colleting all the values of the wave height, a spectrum is made, and it is even possible to make a study in the frequency domain. The frequency values could then been inserted in a Matlab script made on purpose, and called reflexng.m, that is based on the linear wave theory. This script needs in input some parameters, such as the wave height values measured through the wave gauges, the sampling frequency, the water depth, etc. Through the same script, the main output is the trend of the wave height during the sampling time, because thanks to it, the statistic distribution of the wave power can be built, and the system rapidity response can be known as well.

This last part is not a part of the analyzing done.

5- Conclusions

5.1- Observations and suggestions

Even if during the laboratory period, all the obtained records from the measuring instruments are stored in order to judge their overall performance and accuracy, unexpected and strange behaviours of the results sometimes complicate the task of data analysis.

For example, several times, any kind of displacement measure is not recorded because the plate's movement is not fluent but it is a jerky movement. This sometimes limits the data's validity of a part of the sampling file or requires to repeat more times the same test.

For the same reason, in numerous tests, several velocity values are null values, due to the non measurement of the displacement, hence the expected laboratory efficiency could plausibly be underestimated.

It is reasonable that the real device doesn't present some limitations that the laboratory prototype has, such as the out range reached for the high wave state with the consequence of a possible rupture of the model itself, obstacles represented by the fixed anchoring structure on the first front energy convertor plate and, problems to estimate the real incident and reflected wave power due to the absence of the wave gauges behind the device.

Most of the test were carried out with a scaling ratio of 1:30. The efficiency trend suggests that increasing the scale from 1:30 to 1:40 or 1:50 could improve the performance and moreover the ratio scale increasing could give more information about the hypothesis done on the continuous evolution of the efficiency regarding the sea state characterized by a small wave height and a small wave period.

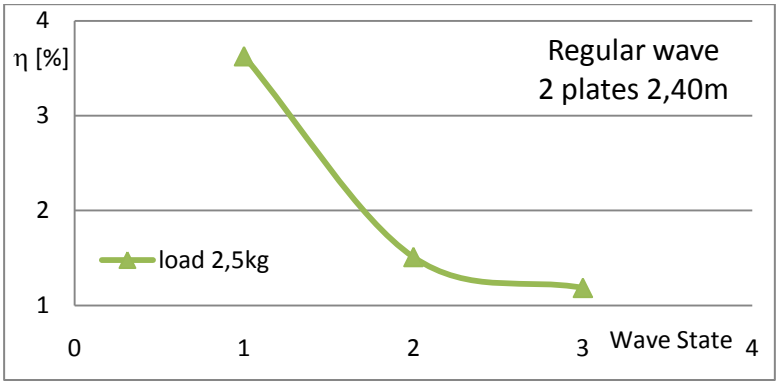

Figure 5.1: Typical efficiency trend of the WavePiston prototype

Therefore a higher scaling ratio would probably increase the average performance and power production of the device. However, from the mechanical and structural point of view, the ratio scale increasing would enhance stresses and loads.

The mechanical and structural limitations should be investigated thoroughly in order to identify the right size.

Furthermore, due to the frequent movement of the prototype in and out of the wave tank during the course of the testing, the exact setup was not perfectly constant. This is another source of likely small error whose real affect is unknown.

5.2- Summarizing

To extrapolate the overall efficiency of the WavePiston device, a laboratory prototype was done and then studied in the Aalborg University, in Denmark. The evaluation of the wave energy converter is achieved following the "*Assessment of Wave Energy Devices. Best Practice as used in Denmark*", Kofoed and Frigaard et al.,2008.

The main key for the model performance is the shape of the energy collector plates. To obtain the efficiency it is necessary to identify the mechanical power that the device can generated, this is the multiplication between the velocity of the plate displacement and the force that is impressed on the plate itself.

To model the friction effect, the device was tested with varying "PTO loads" on the plates, since to represent different resistance conditions to the motion of the wings. The ideal PTO loading, which corresponds to the highest amount of energy that it is extractable from the device, is equivalent at 1,5kg, or analogously at 6,5N as average standard deviation of the impressed force, that it is reported to 1:30, while for the full-scale this value is analogue to 27kN.

As numerous experiments on other OWCs and OWSCs asserted, the efficiency of the WavePiston decreases in a non-linear way from the lower to the higher wave states. This means that a change of the ratio scale could increase the efficiency. This trend represents the real behaviour of the device and it is not dependent to the choice of the loads.

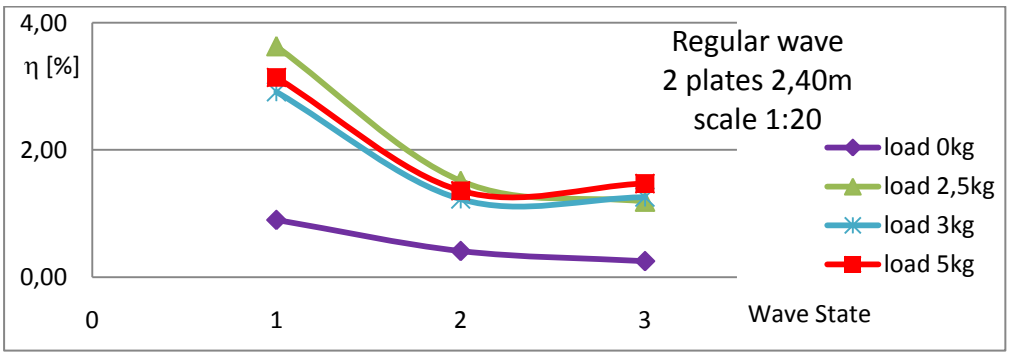

Figure 5.2: In this graph it is illustrated the non-linear trend of the overall efficiency of the device for the first three regular wave states in the scale 1:20. It is possible to note that for each load the efficiency has the same trend.

The reference configuration, corresponding to the greatest power conversion from wave power to mechanical power, is with only two wings at a distance of 2,40m, each wings of the shape of 0,5m x 0,1m in width and depth. In scale 1:30 the real dimensions of the plate of the device becomes 15m for the width and 3m for the depth.

In order to understand the mainly device behaviours, hence to find the best configuration, several tests were done about the dependence to the wave height, wave period, wave direction propagation, etc. as show in the table below.

REGULAR WAVE and/or IRREGULAR WAVE	Configuration 2 wings	Configuration 4 wings
Choice of the best load	X	X
Different incident angle wave	-	X
Variation of wave period or wave height	X	X
Relative distance between plates	X	X
Different shape plates	X	-

Table 5.1: Quick overview about the test program done

It is declarable that the variation of the wave period implies a range for the performance from 15,5% to 2,4%, while the variation of the wave height means a range for the performance from 6% to 2,5%, whereas the variation of the incident wave direction doesn't have a significant effect on the efficiency of the device, indeed the greatest loss of efficiency is approximately the 30% and this is found for incoming waves with an angle of attack of 30 °. In conclusion for the distance of the plates it is possible to assert that the closest configuration doesn't cause an efficiency decrease noticeable. Furthermore from the variation of the dimensions the results affirm that an increase in the depth might raise the efficiency since tree times more.

In the following pages are reported the result's graphs of the laboratory tests.

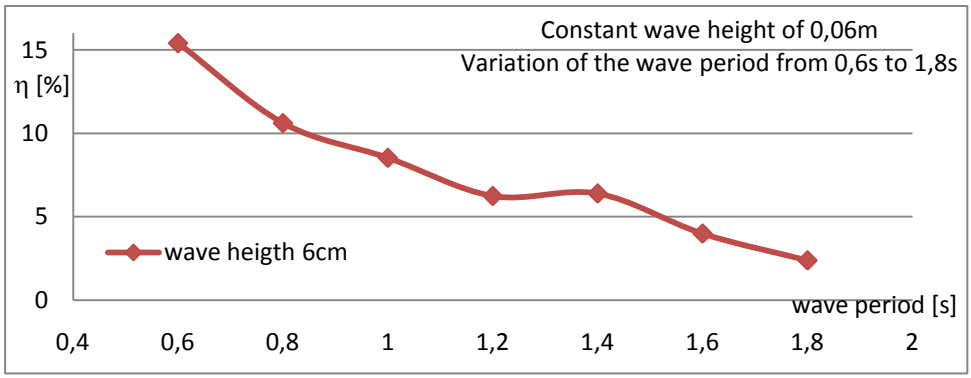

Figure 5.3: The performance values are included in a range from 15,5% to 2,4%.

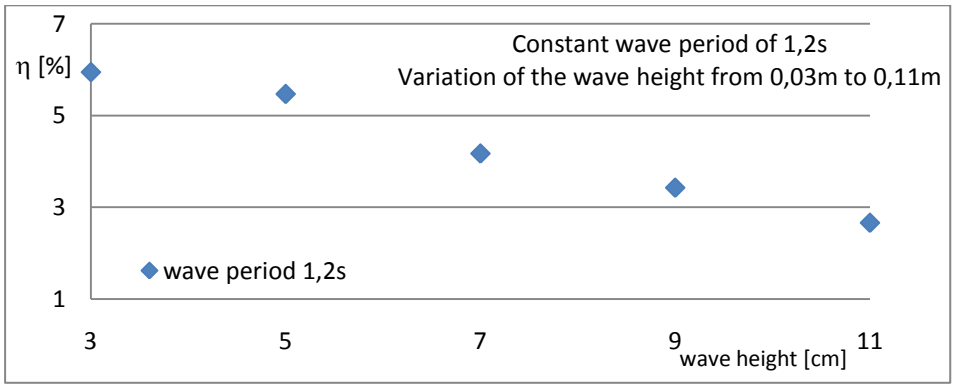

Figure 5.4: The performance values are included in a range from 6% to 2,5%.

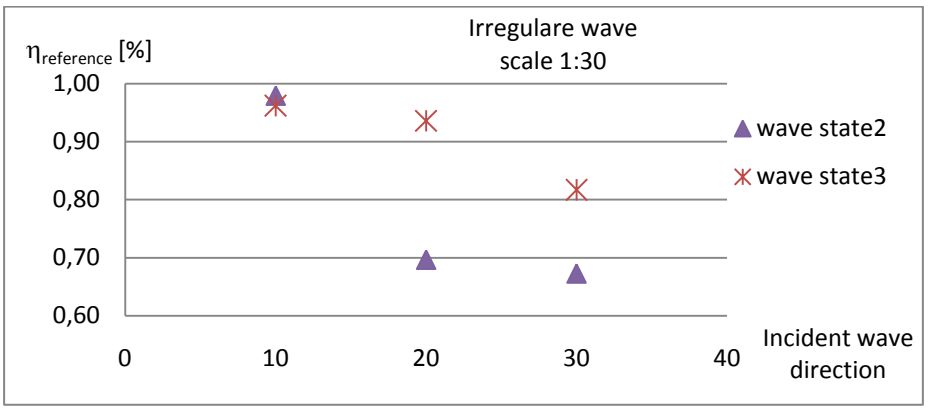

Figure 5.5: Ratio between the efficiency of the device and the incident wave angle. The performance values are referenced to the configuration where the device is in line with the wave propagation.

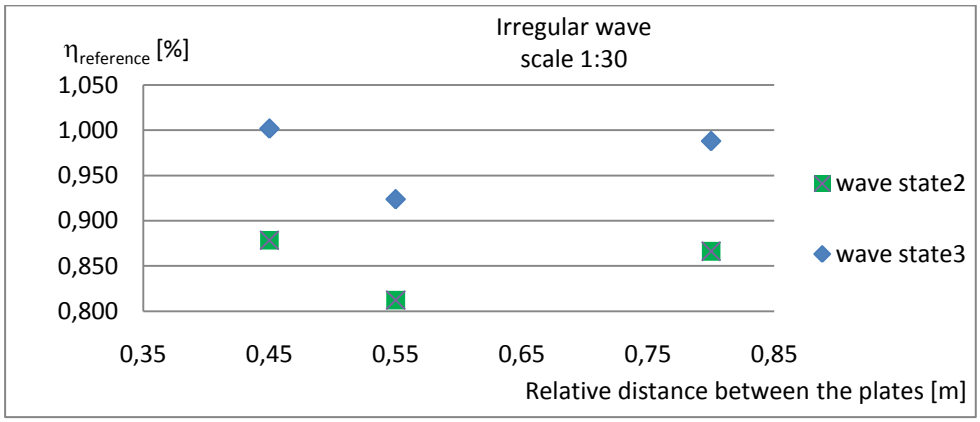

Figure 5.6: The performance values are referenced to the configuration where the device has two wings at a distance of 2,40m, from the graph it is possible to observe that the main loss in efficiency is in the wave state number 2.

Wave State	Distance 2,40m	Distance 0,80m	Distance 0,55m	Distance 0,45m
2	6,41	5,55	5,21	5,63
3	3,41	3,37	3,15	3,42

Table 5.2: The values are the average of the efficiency between the values of the front and the back plate. It can be noticed that the damping plates don't reduce significantly the efficiency of the device.

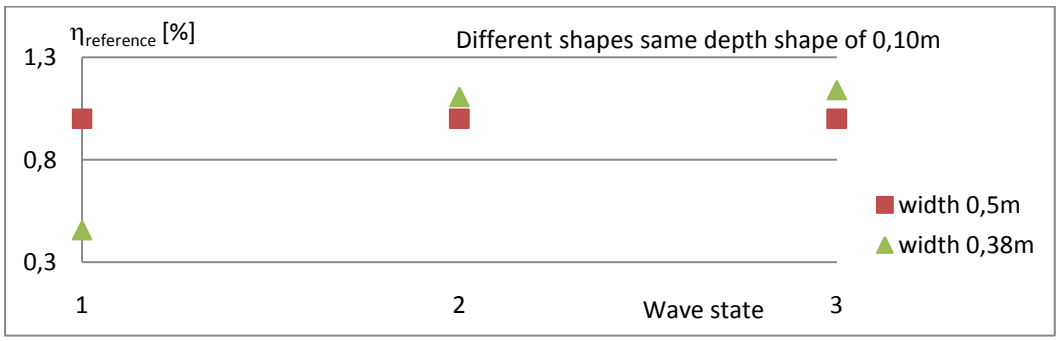

Figure 5.7: The efficiency increases, with max value of 20%, with a decrease of the width of the plates.

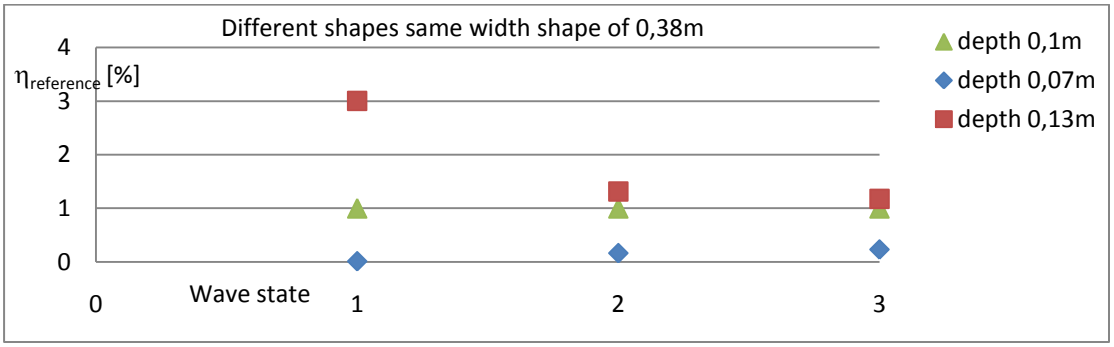

Figure 5.8: The efficiency increases with an increase of the depth of the plates for all the wave states. The greatest increase of the efficiency is about the 300% reported to the shape of 0,38m x 0,10m that it is more than the reference one of 0,50m x 0,10m. The depth of the plate can be considered a key parameter.

To fill the next summarizing table it is necessary to remember what the parameters represent.

The "efficiency" is the ratio between the power generated and the available power from the waves relatively to the same width crest. The "overall efficiency" is the efficiency corresponding to the device in the whole year.

The installed capacity of the PTO system is the maximum among the "generating power", i.e. the efficiency of the device multiplied by the average available power in the waves in a particular wave state.

The "power production" represents the average generated power of a wave state set on a year bases. This corresponds to multiplying the average product power in a wave state by the probability of occurrence of that wave state.

$$Power_{product} = Power_{generated_{WS}} * Probability\ of\ occurance_{WS} \qquad [kW]$$

$$Power_{product} = Power_{wave_{WS}} * Efficiency_{WS} * Probability\ of\ occurance_{WS} \qquad [kW]$$

The sum of the power production of every wave state gives the yearly average available mechanical power to the PTO system. From this yearly average power production, the yearly total energy production can be calculated. The "factor load" represents the average usage of the installed capacity.

Wave state	Tp [s]	Hs [m]	Power wave [W/m]	Prob [%]	Prob*Power wave [W/m]	Power generated [W/0,5m]	Efficiency	η*Probability	Prob*Power generated [W/m]
1	1,02	0,033	0,22	47	0,101	0,014	0,13	0,0590	0,013
2	1,28	0,067	2,20	23	0,498	0,076	0,07	0,0155	0,034
3	1,53	0,100	6,31	11	0,682	0,115	0,04	0,0039	0,025
4	1,79	0,133	16,32	5,1	0,832	0,163	0,02	0,0010	0,017
5	2,04	0,167	35,75	2,4	0,858	0,214	0,01	0,0003	0,010

Table 5.3: Summary of the performance of the WavePiston model. The reference configuration of the device is with two energy converter plates at the distance of 2,4m and with a load of 1,5kg. The device is subjected to irregular wave.

The yearly energy production is 0,86 kWh/year/m.

This value is a paltry value, indeed a 100W light bulb on for one hour in a day for one year consumes 36,5kWh/year, this means that the WavePiston model with an energy plate converter of 1m of width is capable to feed the same light bulb only for 2 minutes for day.

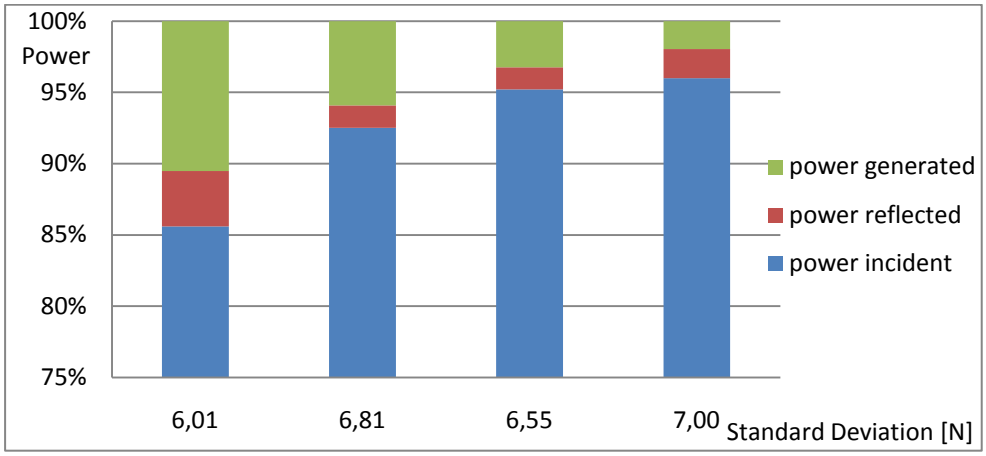

Figure 5.9: The graph shows the relation among the standard deviation of the force, impressed on the plate in the reference cases with irregular wave, and the wave incident power, the wave reflected power and the power generated by the device itself.

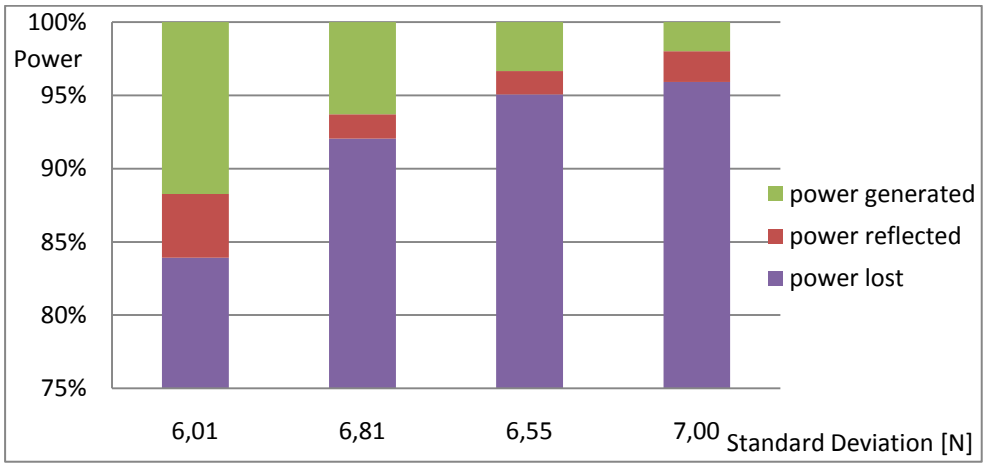

Figure 5.10: The graph shows the relation among the standard deviation of the force, impressed on the plate in the reference cases with irregular wave, and the wave reflected power, the power generated by the device itself and the power lost that it is calculated as the difference between the incident wave power and the power product by the device.

In the graphs above the x-axis is the average standard deviation of the force feels by the plates in the reference configuration of two energy plates converter at the distance of 2,4m with a load of 1,5kg in the cases of the first four irregular wave states.

Through both the graphs it is declarable that the power generated by the plates decreases from the first to the last wave state, and consequently, at the same time, the power lost increases from the first to the last wave state. Hence, one more time it means that the best performance is for the lower wave states.

5.3- Conclusions

As explained in the "*Danish approach to development and evaluation of wave energy devices*" the analysis realized can be considered as a proof of concept.

In according to what that document declares, in the phase 1 all the main instruments used to assess the wave energy devices are small scale testing in a hydraulic laboratory. These tests are performed in order to gain knowledge on the devices before a company actually builds and deploys a wave energy device in the sea. The laboratory tests will give information on:

1. Loads on the device
2. Movements of the device
3. Run-up / overtopping of the device
4. Energy production

The estimation of energy production in the first phase is rough. Typical small indicative laboratory tests cost 10000€ and they are followed by a 10 page report.

The examined prototype was design in reason to be fit to the laboratory conditions, though not exactly corresponding to the future real realizations.

In the laboratory the closest situation was with the wings 0,45m distant, whilst in full scale additional investigations should be made on the right inter-plate distance and on the amount of plates. In the full scale should be less space limitations and this gives the possibility to do some investigations not possible in the laboratory configurations.

Furthermore as the full-scale WavePiston wave energy converter design is intended to have a floating structure with a flexible mooring instead of a fixed structure, several the tests should be repeated with a flexible mooring instead of the fixed while measuring the mooring forces and the performance. The observations might be different, as the flexible moored structure may move differently for different wavelengths and/or wave states, and therefore perform as well. Moreover in case of floating structure it is advisable to carry out some new tests about the distance between two device to know the best configuration of them in the plan of a future farm.

Additionally the lab PTO system was a fixed load (weights), while the full-scale PTO system might consist of an adaptable load depending on the wave state and some other components such as springs, in order to keep the plates in place and/or reduce end-stop forces. This change in setup might give a different performance curve.

Through the WavePiston investigation is reasonable to declare that the WavePiston WEC is able to convert energy in the waves into useful mechanical energy, which then, through further mechanical and electrical systems, can be converted into electricity. The average power production capabilities of the WavePiston WEC have been estimated for a reference offshore location.

Wave state	Hs [m]	Tp [s]	Power wave [W/plate]	Probability [%]	Efficiency	Power generated [W/plate]
1	1,00	5,60	31,68	46,8	0,13	4,12
2	2,00	7,00	158,40	22,6	0,07	11,09
3	3,00	8,40	427,68	10,8	0,04	17,11
4	4,00	9,80	887,04	5,1	0,02	17,74
5	5,00	11,20	1584,00	2,4	0,01	15,84

Table 5.4: Summary of the performance of the WavePiston wave energy converter. The value of the power that can be converted from the waves into useful mechanical power by the WavePiston model is referred to one plate of 15m of width . The device is subjected to irregular wave, in 30m water depth.

yearly average wave power [kW/m]	12,00
yearly average wave power [kW/plate]	180,07
overall efficiency	0,080
yearly average power production [kW/m]	0,504
yearly average power production [kW/plate]	7,570
max power generated [kW/m]	1,183
max power generated [kW/plate]	17,74
yearly energy production [MWh/year/m]	4,42
yearly energy production [MWh/year/plate]	66,3
Load factor	0,39

Table 5.5: Summary of the performance and the estimated energy that can be converted from the waves into useful mechanical energy by the WavePiston device subjected to irregular wave.

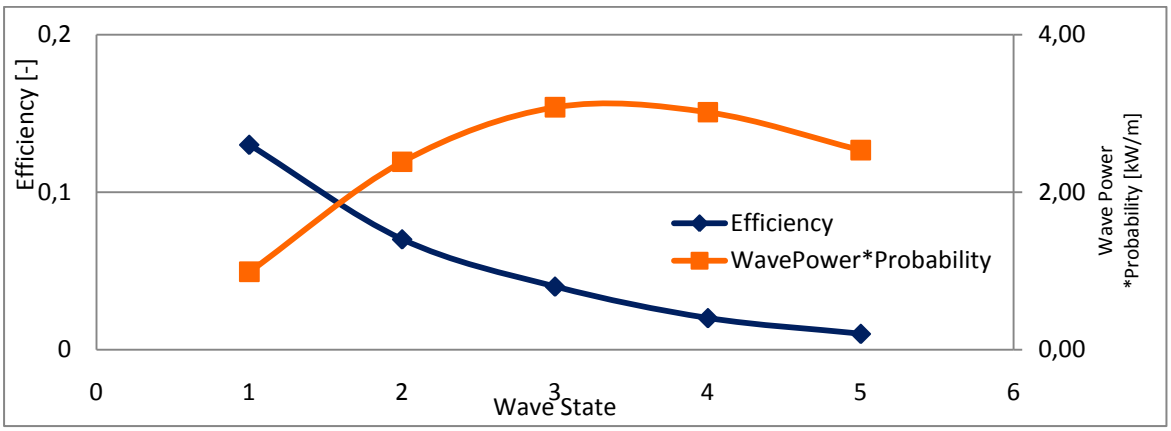

Figure 5.11: Representation of the average efficiency of a plate of 15m width of the WavePiston device in the blue line, instead the orange line is the product of the probability of occurrence and the available wave power.

In according to the Danish best practice, it is declarable that the risk of using unnecessary resources for the WavePiston device is minimized.

For this reason, combined with the high performance for the ordinary wave states with a small wave height and a small wave period it is rational an installation even in the moderate seas as the Italian sea.

Wave state	Hs [m]	Tp [s]	wave Power [kW/plate]	Probability [%]	Efficiency	Power generated [kW/plate]
1	0,25	5,48	1,94	26,80	0,22	0,419
2	0,75	5,78	18,40	33,39	0,16	2,891
3	1,25	6,63	58,58	19,28	0,11	6,689
4	1,75	7,24	125,49	10,74	0,08	10,416
5	2,25	7,88	225,68	4,92	0,06	13,616
6	2,75	8,56	366,09	2,44	0,04	16,054

Table 5.6: Summary of the performance of the WavePiston wave energy converter in an Italian installation. The value of the power that can be converted from the waves into useful mechanical power by the WavePiston model is referred to one plate of 15m of width . The device is subjected to irregular wave, in 30m water depth.

yearly average wave power [kW/m]	3,43
yearly average wave power [kW/plate]	51,48
overall efficiency	0,15
yearly average power production [kW/m]	0,30
yearly average power production [kW/plate]	4,55
max power generated [kW/m]	1,07
max power generated [kW/plate]	16,05
yearly energy production [MWh/year/m]	2,66
yearly energy production [MWh/year/plate]	39,84
Load factor	0,28

Table 5.7: Summary of the performance and the estimated energy that can be converted from the waves into useful mechanical energy by the WavePiston device subjected to irregular wave in the Italian Sea.

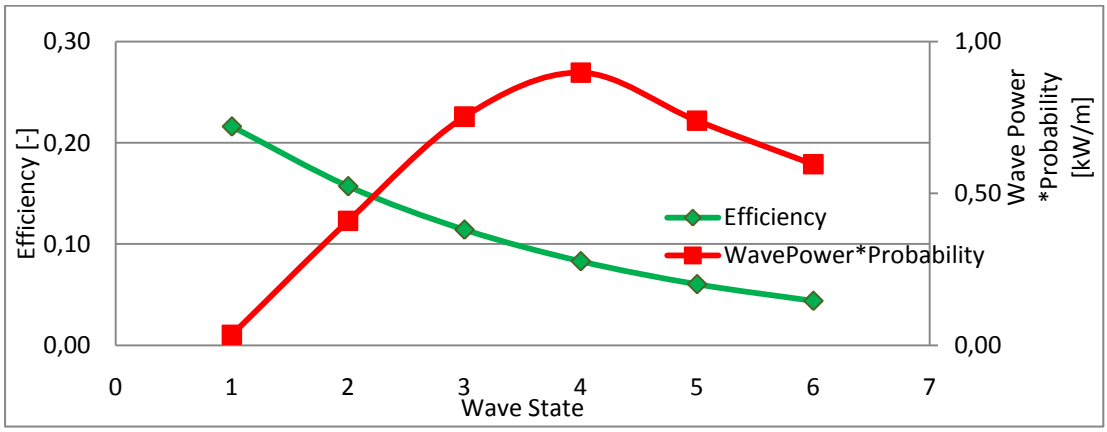

Figure 5.12: Representation of the average efficiency of a plate of 15m width of the WavePiston device in the green line, instead the red line is the product of the probability of occurrence and the available wave power.

The WavePiston wave Energy converter is not affected by the background currents, but it could be influenced by the surface currents as the return current called even rip current. This aspect is not investigated in the analysis made.

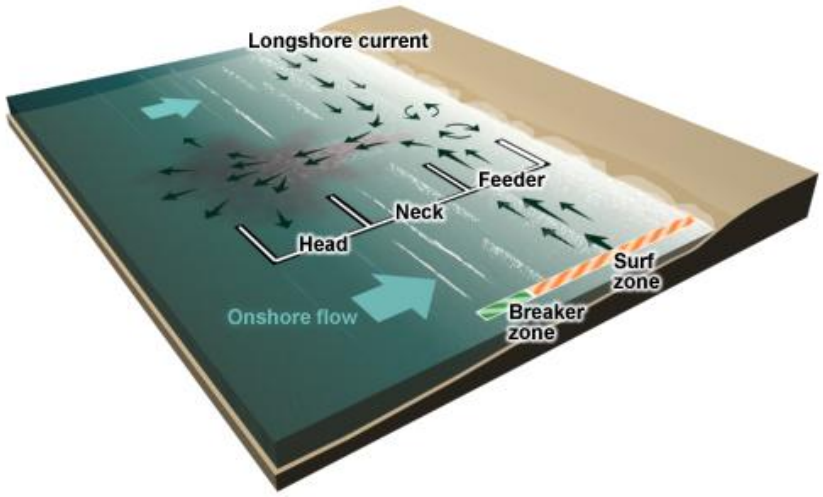

Figure 5.13: Rip current structure.

In general, every wave energy converter is intended to be placed in an aggressive situation, hence the corrosion resistance is one of the most important aspect to consider in the design and achievement of a wave energy converter and of its material, because the maintenance cost could be higher than the implementation cost.

Due to the movement of the prototype in and out the tank, it was possible to observe a beginning of the corrosion effect, even if these observations concern more the mooring part, that it is absent in the real future realization.

Figure 5.14: Beginning of corrosion effects in the mooring system of the WavePiston prototype.

There is good reason to be cautiously optimistic about the prospects of marine energy technologies supplying significant amounts of clean electricity.

This optimism is supported by the number of devices that are progressing through a development programme to begin sea trails at, or close to, full-size prototype scale.

5.4- Possible inconveniences in real installation

One of the most difficult aspect to considerate is not only the possibility of achieving a wave energy converter, i.e. the performance and cost study; but it is the correct use of the sea space from all the demands.

For example large-scale wave energy farms could be planned in areas that are in this moment intensely used for navigation purposes. In busy navigation routes, any obstacle increases the potential hazard of ship collisions and, ocean energy converters would be considered a danger within a rather large perimeter around shipping routes, even outside the main routes and in the vicinity of more industrial major ports, this may become the most important constraint for ocean energy converters development.

At the same time, advances in control and navigational warning systems can significantly improve the safety ship situation, once the navigational sector gets accustomed to the additional infrastructures at sea. From this point of view, even positive effects may arise regarding navigational safety and even maritime control issues: the marker systems of wave farms could incorporate modern communication systems, and assume the function of navigational guidance.

Further, farms distributed relatively widely over the open ocean could play an important role in a better control of the common practice of illegal discharges of cargo ships, or even in ad-hoc actions in oil spills, preventing major damages to the environment.

Another source of problem can be the fishing sector. Fishing is by far the most widespread and well-established usage of ocean space and due to the strong traditions of the sector and the constantly increasing need for seafood, it is considered a vital activity, hence it is logical that wave energy farms have to struggle with the opposition of fishermen communities.

A possibility for the wave energy farms might be in the coexistence with floating wind farms. The floating wind farms are typically moored in 50-200m deep water, and their distance would generally allow wave farms to be installed in-between (in an advanced stage, once mooring systems of different floating devices might be combined). This integration has more possibilities with the Oscillating Water Columns (OWCs) or the Oscillating Wave Surge Converters (OWSCs).

At last there is the need to consider that a shoreline or near-shore device has the benefits to be accessible directly from the shore, and so the operating and maintenance costs should be minimised, but at the same time there are two significant problems. Firstly the research of a suitable site with a suitable wave climate. Second problem is that a shore-side could be easily accessed by the public, with a consequentially high safety risk.

APPENDIX

A- File .dat WaveLab

B- File .txt WavePiston.vi

C- List of experiments

D- Matlab Editor to analyze the data

E- Matlab Editor for
the numerical models

FILE .dat WAVELAB

The file .dat is the output file from the wave gauges sampling. Usually it is composed by a first short description about which is the configuration used, and then by four columns, where there are the elevation values recorded by the four wave gauges.

Through the software WaveLab3.33 the data come from the wave gauges can be analyzed, and among the results, the most important are: the wave height and the wave period observed, the measured wave power for meter of wave crest. All this results are given for the waves incident and even for the reflected waves.

All the figures below are related to the reference configuration of the prototype, i.e. two energy converter plates at a distance of 2,40m of the shape of 0,5m of width and 0,1m of depth without hole. The device is subject to an external load of 1,5kg, corresponding to 6,5N as average of the deviation standard of the impressed force.

The exact data files are:

- RW_047_128_240_15_01 for the regular wave;
- IW_067_128_240_15_01 for the irregular wave.

Both files report the second Danish wave state.

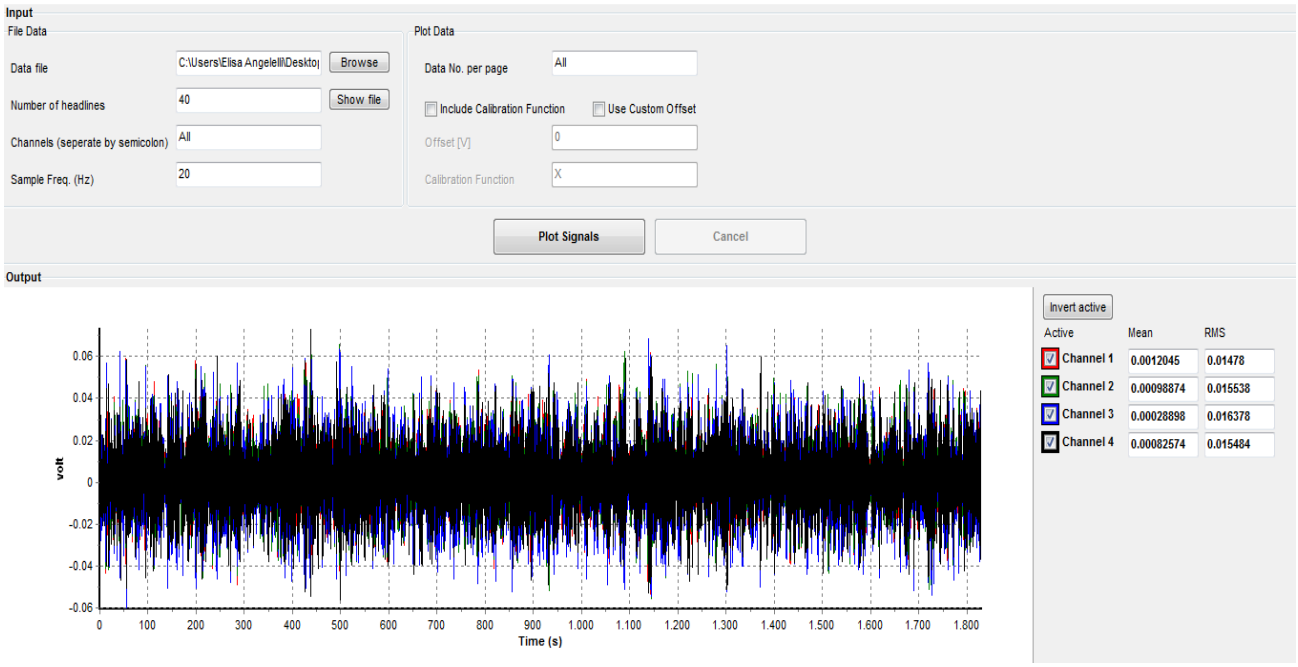

Figure A.1: Screen of the "Show Sampled Signal" for the Irregular test, in the picture is represented all the data from all the four channel, it is possible to show only one signal coming from a particular wave gauge choosing on the rigth the corresponding channel. To obtain this signal WaveLab3.33 needs in input only the file name.

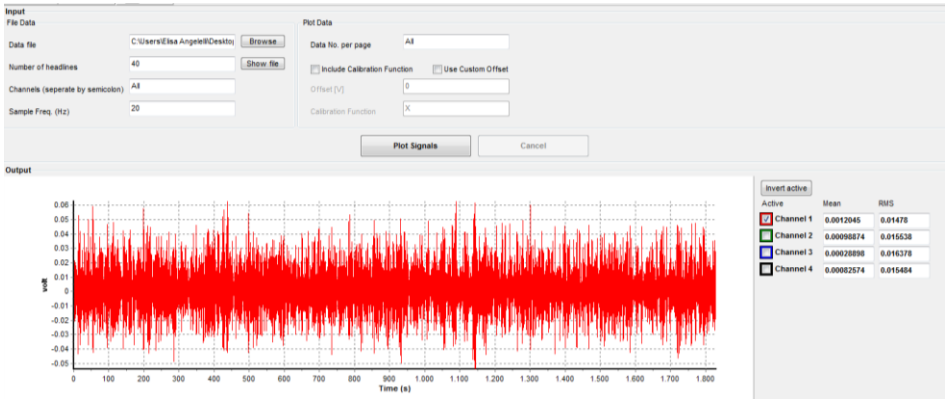

Figure A.2: Screen of the "Show Sampled Signal" for the Irregular test for the particular wave gauge of the channel1 that corresponds to the wave gauge nearest to the paddle system as a snake-front piston.

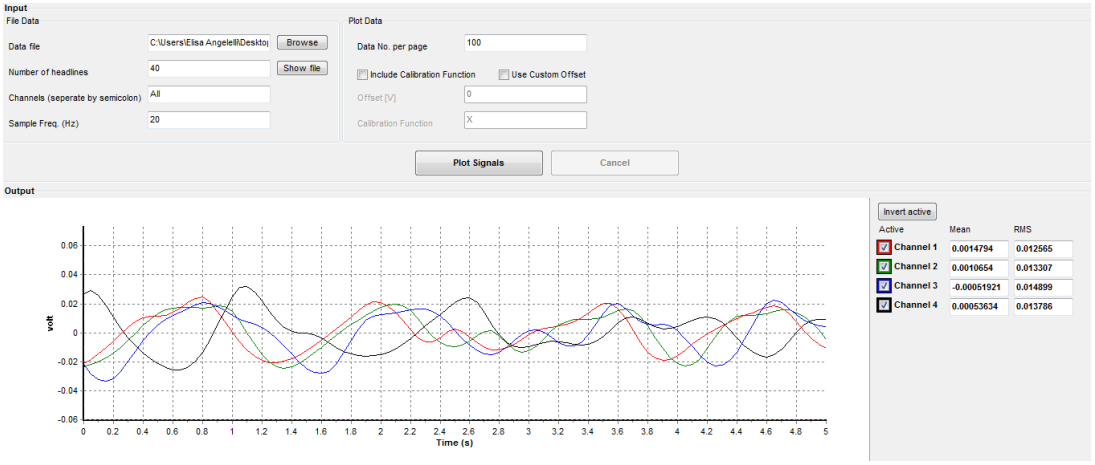

Figure A.3: Zoom of the "Show Sampled Signal" for the Irregular test.
The picture illustrates the signal with the data from all the four channel for a part of all the sampling time.

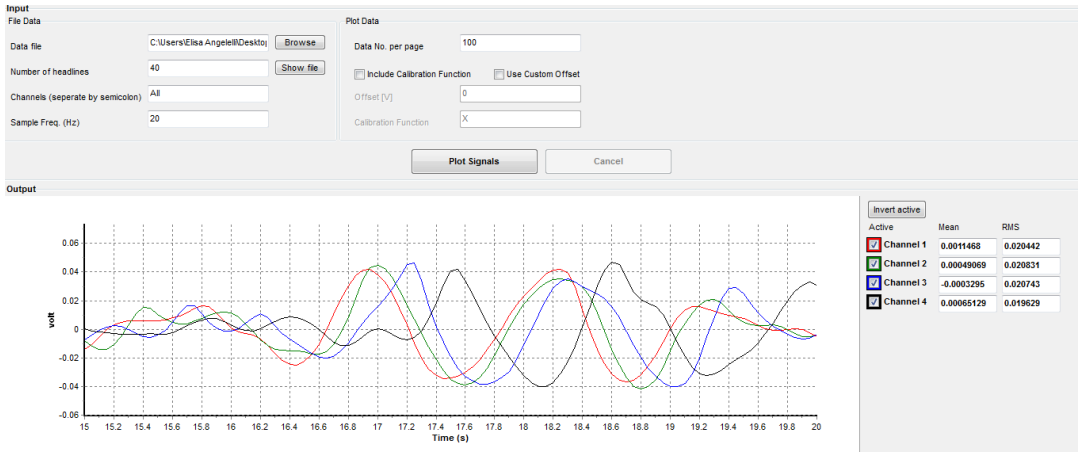

Figure A.4: Zoom of the "Show Sampled Signal" for the Irregular test.
The picture illustrates the signal with the data from all the four channel for a part of all the sampling time.

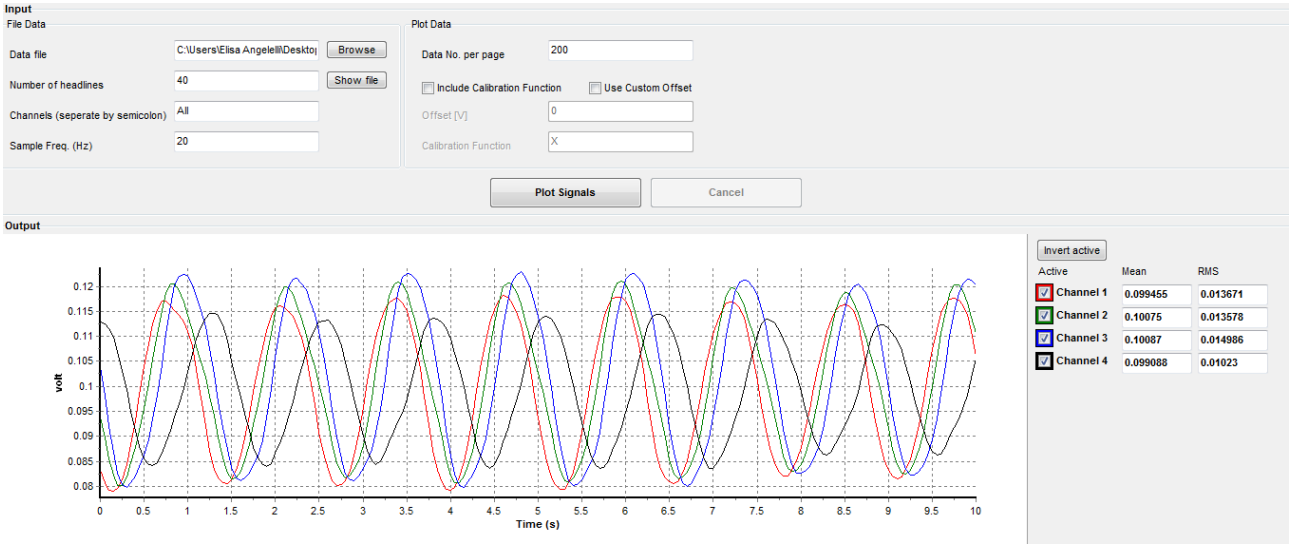

Figure A.5: Zoom of the "Show Sampled Signal" for the Regular test.
The picture illustrates the signal with the data from all the four channel for a part of all the sampling time. It is possible to note that in this case the data from the different wave gauges are more similar, and their trend is almost regular, and this is due to the aspect that all the waves have almost the same wave height.

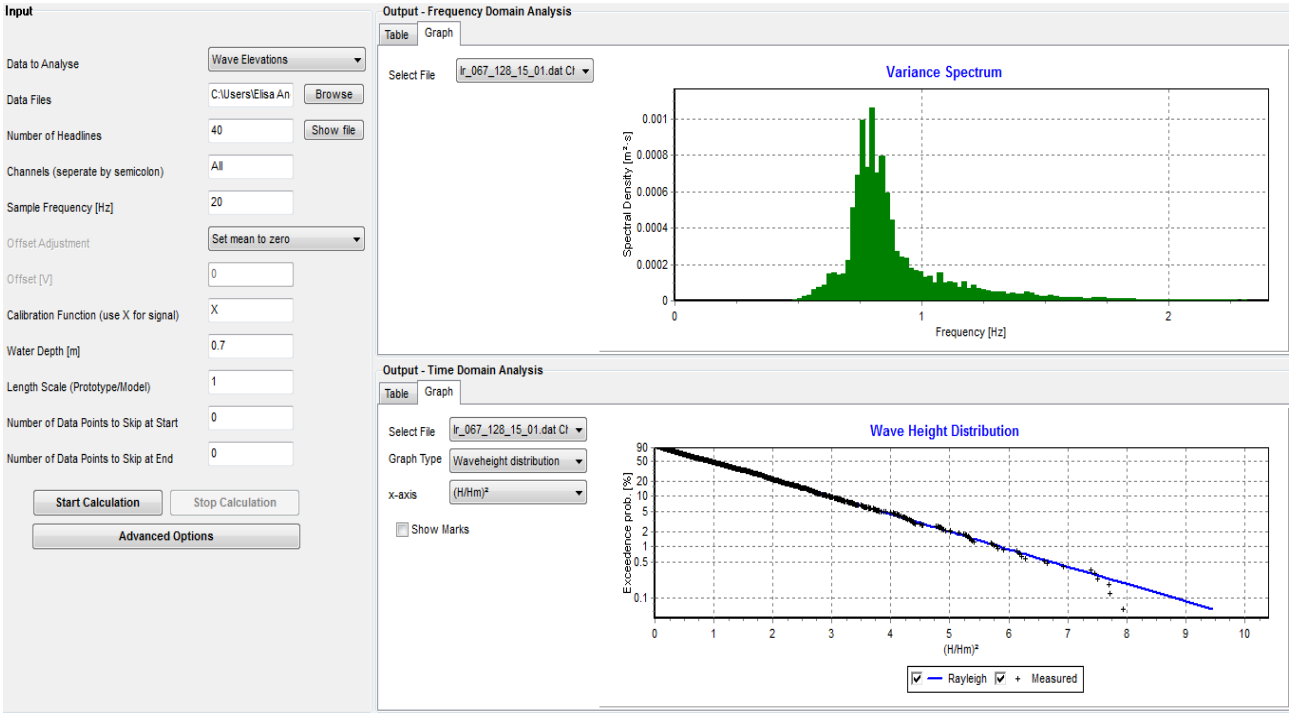

Figure A.6: Screen of the "Time Series Analysis" for the Irregular test.
In the top, the picture illustrates the variance spectrumof the signal in the frequency domain analysis, while in the bottom there is the time domain analysis that demonstrates the accuracy of the Rayleigh Distribution for the irregular waves, in fact the measured values represent with a black point overlap to the blue Rayleigh Distribution.

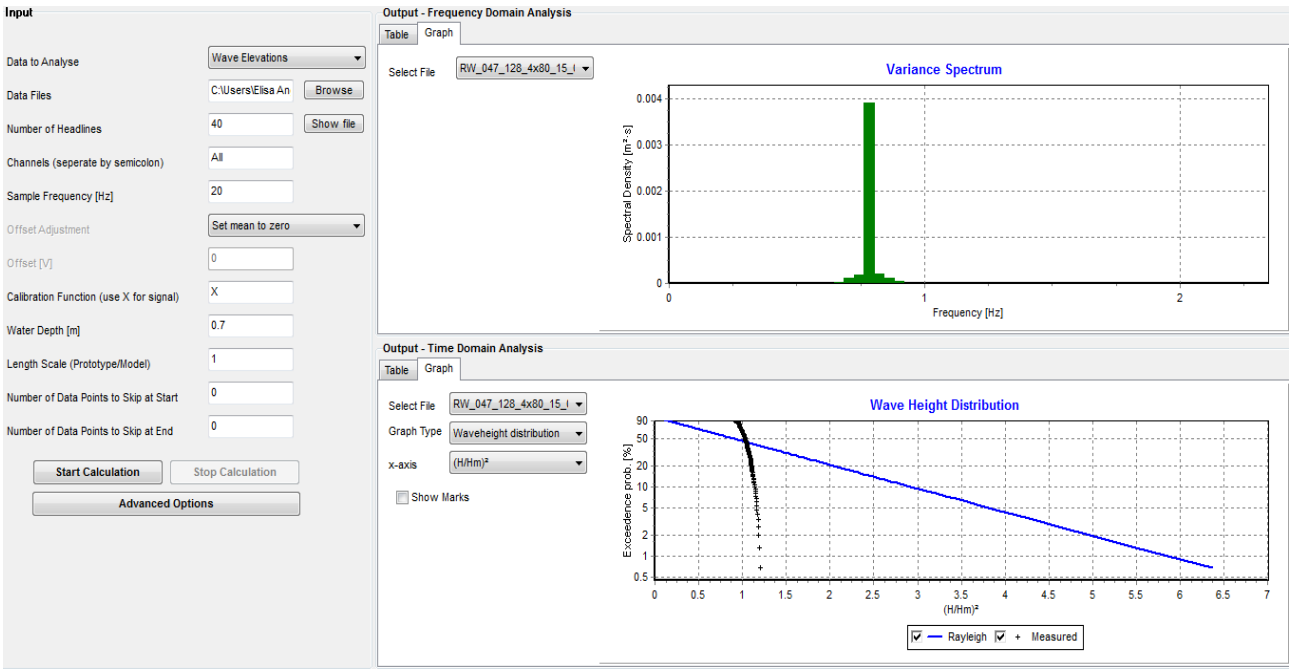

Figure A.7: Screen of the "Time Series Analysis" for the Regular test. As before, in the top, the picture illustrates the variance spectrumof the signal in the frequency domain analysis, and it is notable that the signal has an only main frequence, because every wave is characterized by the same wave height and wave period. In the bottom there is the time domain analysis that demonstrates that in this case the Rayleigh Distribution in not suittable for the regular waves, the measured values represent with a black point don't overlap to the blue Rayleigh Distribution, in fact the mesured points present almost the same values and they are arranged on a nearly vertical line.

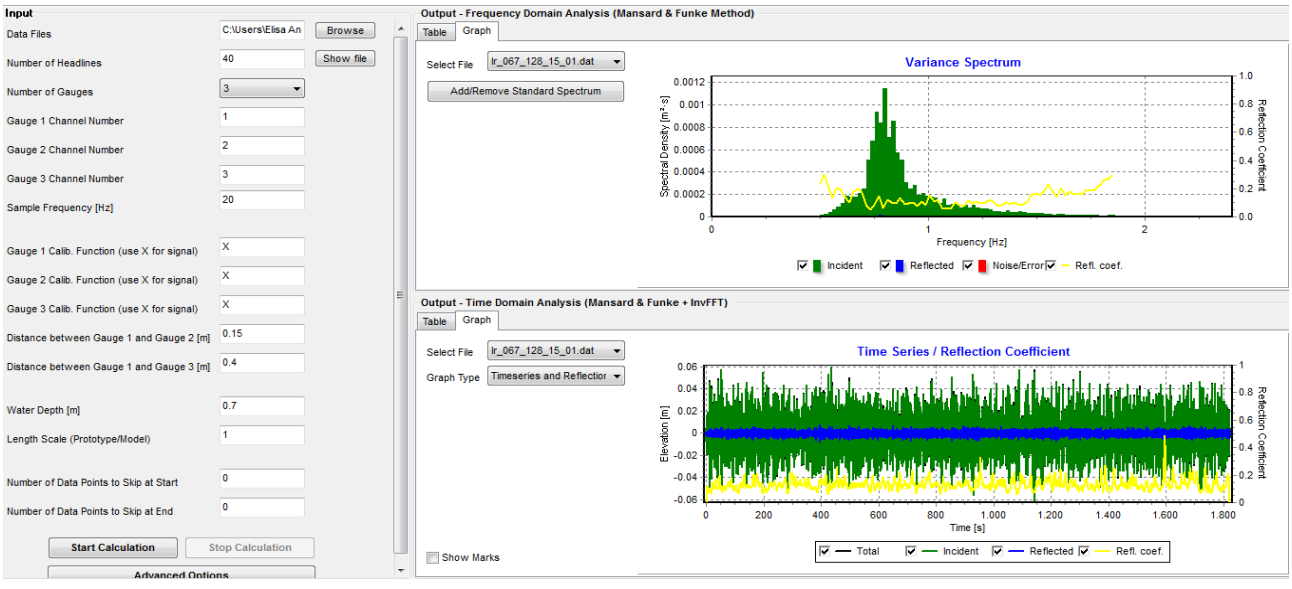

Figure A.8: Screen of the "Reflection Analysis" for the Irregular test.
In the top, the picture illustrates the variance spectrumof the signal in the frequency domain analysis, while in the bottom there is the time domain analysis.

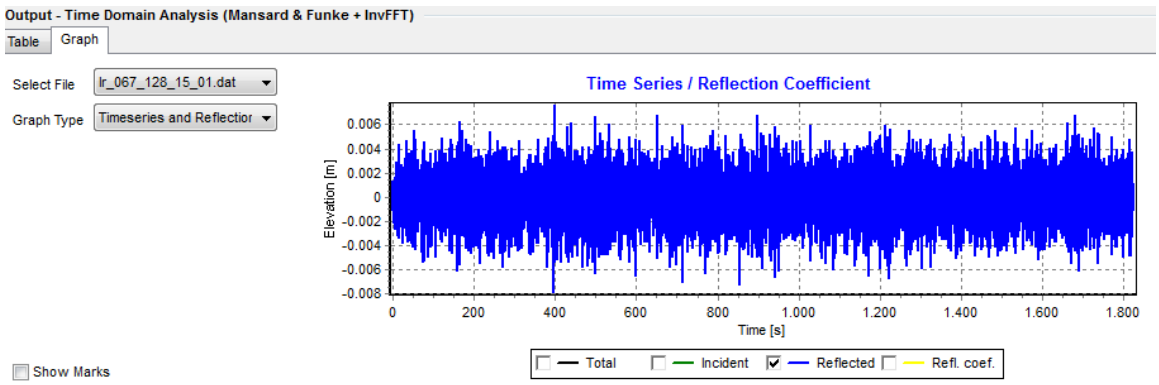

Figure A.9: Zoom of the "Reflection Analysis" for the Irregular test,in the time domain analysis only for reflected waves.

Figure A.10: Zoom of the "Reflection Analysis" for the Irregular test, in the time domain analysis for incident and reflected waves.

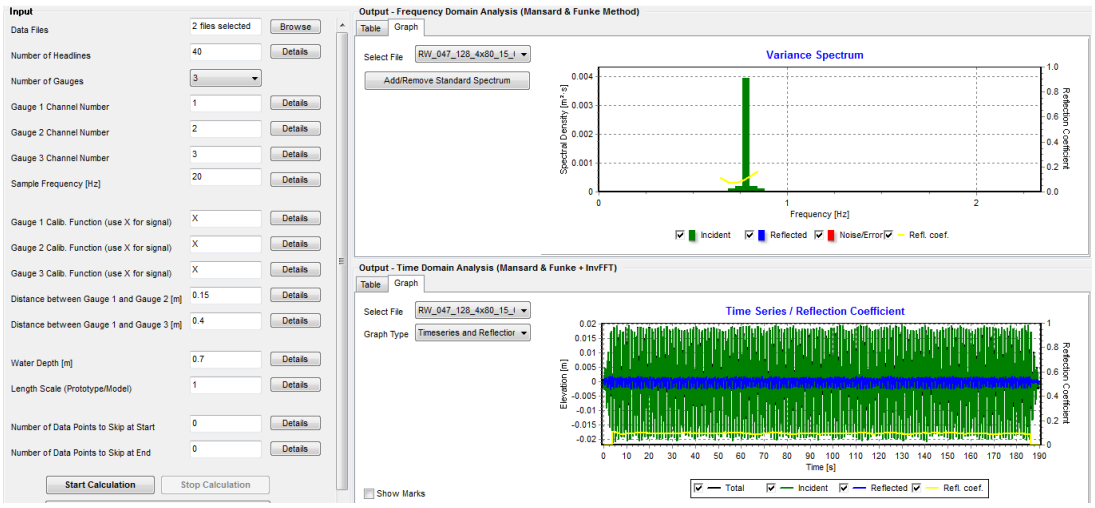

Figure A.11: Screen of the "Reflection Analysis" for the Regular test.
In the top, the picture illustrates the variance spectrumof the signal in the frequency domain analysis, while in the bottom there is the time domain analysis. In both cases there are the incident and the reflected waves.

WaveLab 3.34
The data is sampled on Tuesday the 2/23/2010 at 3:35:00 PM
Measures includes calibration coefficient and offset
Test description: Enter Description Here...
Sample frequency: 20 Hz
Sample duration: 1830 s

COLUMN 1:
Channel Description: Channel 01
Calibration Function: 0.05538*X
Offset: 1.828 V
Position (X-Coord.): 0 m
Position (Y-Coord.): 0 m

COLUMN 2:
Channel Description: Channel 02
Calibration Function: 0.04817*X
Offset: 2.094 V
Position (X-Coord.): 0 m
Position (Y-Coord.): 0 m

COLUMN 3:
Channel Description: Channel 03
Calibration Function: 0.05402*X
Offset: 1.861 V
Position (X-Coord.): 0 m
Position (Y-Coord.): 0 m

COLUMN 4:
Channel Description: Channel 04
Calibration Function: 0.04867*X
Offset: 2.072 V
Position (X-Coord.): 0 m
Position (Y-Coord.): 0 m

-0.01318	-0.00911	0.01014	0.00719
-0.01433	-0.01220	0.00335	0.01178
-0.01398	-0.01416	-0.00348	0.01494
-0.01215	-0.01495	-0.00917	0.01773

There are four columns one for each wave gauges, the sampling is with 20 Hz, i.e. 20 records every second.

FILE .txt WavePiston.vi

The file .txt is the output file from the displacement sensors (LVDT) and the force transducers, those present on the plate near the sliding rail with the weights, i.e. the plate representing the PTO system. Usually it is composed by a first short description about which is the sampling time and the calibration values, and then by five columns, where the first whose corresponds to the instant of the sampling, while the second and the third are the displacement values related respectively to the front and back plate; whereas the last two columns contain the impressed force filled by the plates related, again, respectively to the front and the back plate. From the first column it is understandable that the sampling frequency is 10Hz.

Through a Matlab script made on purpose, the data come from the PTO system can be analyzed, and the most important result is the average value of the power potentially generable from the device, because if it is compared with the wave power available, it might give the efficiency of the model.

All the data below are related to the reference configuration of the prototype, i.e. two energy converter plates at a distance of 2,40m of the shape of 0,5m of width and 0,1m of depth without hole. The device is subject to an external load of 1,5kg, corresponding to 6,5N as average of the deviation standard of the impressed force. The exact data file is IW_067_128_240_15_01, it is an irregular wave test, and it is reported to the second Danish wave state.

Author,Administrator
TimeStamp,23-02-2010 15:03
Sample Clock Rate,1000,00
Cal data
0,01
- 0,05
0,01
- 0,05
9,30
- 20,60
7,42
- 21,00

Sec after start	LVDT 1 [m]	LVDT 2 [m]	Load 1 [N]	Load 2 [N]
74,58	0,018	0,013	-0,909	6,759
74,68	0,018	0,012	7,467	6,587
74,78	0,017	0,011	8,351	6,322
74,88	0,016	0,010	7,936	5,073
74,98	0,015	0,010	7,970	1,521
75,08	0,015	0,010	8,473	-2,277
75,18	0,014	0,010	6,377	-1,819
75,28	0,014	0,010	-2,012	-1,389
75,38	0,016	0,010	-8,835	-5,150
75,48	0,019	0,011	-7,926	-8,958
75,58	0,022	0,012	-7,151	-8,588
75,68	0,023	0,013	-5,450	-8,023
75,78	0,023	0,014	3,079	-5,294

	File name	WS	scale	Hs [m]	real Hs [m]	Tp [s]	Distance [m]	Load	Wave power incident [W/m]	Wave power reflected [W/m]	Power generated front [W/0,5m]	back [W/0,5m]	**average [W/m]**	efficiency front	efficiency back	**efficiency [%]**
22/02/2010	RW_035_125_240_00_01	1	20	0,035	0,040	1,25	2,40	0	1,95	0,02	0,012	0,017	**0,015**	0,638	0,889	**0,764**
	RW_070_157_240_00_01	2	20	0,070	0,068	1,57	2,40	0	7,95	0,02	0,026	0,029	**0,055**	0,323	0,361	**0,342**
	RW_070_157_240_00_02	2	20	0,070	0,067	1,57	2,40	0	7,72	0,02	0,030	0,033	**0,063**	0,782	0,866	**0,824**
	RW_110_188_240_00_01	3	20	0,110	0,113	1,88	2,40	0	24,83	0,65	0,091	0,086	**0,177**	0,735	0,690	**0,713**
	RW_070_157_240_00_03	2	20	0,070	0,067	1,57	2,40	0	7,56	0,04	0,033	0,035	**0,068**	0,871	0,925	**0,898**
	RW_110_188_240_00_02	3	20	0,110	0,108	1,88	2,40	0	21,89	0,65	0,044	0,045	**0,089**	0,404	0,415	**0,410**
	RW_140_220_240_00_01	4	20	0,140	0,158	2,2	2,40	0	52,73	1,01	0,067	0,065	**0,132**	0,254	0,247	**0,251**
	RW_070_157_240_20_01	2	20	0,070	0,065	1,57	2,40	2	7,01	0,02	0,091	0,127	**0,218**	2,596	3,618	**3,107**
	RW_110_188_240_20_01	3	20	0,110	0,112	1,88	2,40	2	25	0,84	0,122	0,153	**0,275**	0,979	1,221	**1,100**
	RW_140_220_240_20_01	4	20	0,140	0,161	2,2	2,40	2	54,31	1,55	0,206	0,250	**0,456**	0,757	0,919	**0,838**
	RW_070_157_240_50_01	2	20	0,070	0,063	1,57	2,40	5	6,33	0,11	0,090	0,109	**0,199**	2,841	3,439	**3,140**
	RW_110_188_240_50_01	3	20	0,110	0,119	1,88	2,40	5	28,59	1,15	0,202	0,186	**0,388**	1,411	1,302	**1,357**
	RW_140_220_240_50_01	4	20	0,140	0,163	2,2	2,40	5	53,51	1,33	0,391	0,396	**0,787**	1,462	1,480	**1,471**
23/02/2010	RW_070_157_240_30_01	2	20	0,070	0,068	1,57	2,40	3	8,26	0,04	0,124	0,117	**0,241**	2,992	2,830	**2,911**
	RW_110_188_240_30_01	3	20	0,110	0,116	1,88	2,40	3	28,23	0,73	0,175	0,171	**0,346**	1,241	1,214	**1,228**
	RW_140_220_240_30_01	4	20	0,140	0,164	2,2	2,40	3	57,14	1,67	0,365	0,353	**0,718**	1,279	1,237	**1,258**
	RW_070_157_240_25_01	2	20	0,070	0,069	1,57	2,40	2,5	8,17	0,04	0,153	0,144	**0,297**	3,745	3,513	**3,629**
	RW_110_189_240_25_01	3	20	0,110	0,122	1,89	2,40	2,5	28,17	1,2	0,226	0,200	**0,426**	1,604	1,420	**1,512**
	RW_140_291_240_25_01	4	20	0,140	0,165	2,91	2,40	2,5	57,32	1,67	0,333	0,347	**0,680**	1,162	1,211	**1,187**
	RW_035_125_240_25_01	1	20	0,035	0,038	1,25	2,40	2,5	1,83	0,01	0,056	0,062	**0,118**	6,111	6,814	**6,463**
	IR_067_128_240_25_01	2	30	0,067	0,064	1,28	2,40	2,5	2,59	0,05	0,073	0,075	**0,148**	5,631	5,761	**5,696**
	IR_033_102_240_25_01	1	30	0,033	0,023	1,02	2,40	2,5	0,27	0,01	0,008	0,011	**0,019**	5,784	7,951	**6,868**
	IR_100_153_240_25_01	3	30	0,100	0,096	1,53	2,40	2,5	7,26	0,19	0,134	0,134	**0,268**	3,691	3,681	**3,686**
	IR_133_179_240_25_01	4	30	0,133	0,139	1,79	2,40	2,5	17,71	0,6	0,198	0,193	**0,391**	2,239	2,182	**2,211**
	IR_167_204_240_25_01	5	30	0,167	0,185	2,04	2,40	2,5	35,75	1,76	0,270	0,215	**0,485**	1,512	1,202	**1,357**

	File name	WS	scale	Hs [m]	real Hs [m]	Tp [s]	Distance [m]	Load	Wave power i. [W/m]	Power w refl [W/m]	Power generated [W/0,5m]	back [W/0,5m]	**average [W/m]**	efficiency front	efficiency back	**efficiency [%]**
23/02/2010	IR_100_153_240_15_01	3	30	0,100	0,093	1,53	2,40	1,5	6,74	0,11	0,116	0,113	**0,229**	3,454	3,363	**3,409**
	IR_067_128_240_15_01	2	30	0,067	0,062	1,28	2,40	1,5	2,36	0,04	0,073	0,078	**0,151**	6,191	6,625	**6,408**
	IR_033_102_240_15_01	1	30	0,033	0,021	1,02	2,40	1,5	0,22	0,01	0,012	0,015	**0,027**	10,861	13,884	**12,373**
	IR_133_179_240_15_01	4	30	0,133	0,132	1,79	2,40	1,5	15,94	0,34	0,164	0,161	**0,325**	2,058	2,022	**2,040**
	IR_067_128_4x80_15_01	2	30	0,067	0,063	1,28	0,80	1,5	2,52	0,04	0,073	0,067	**0,140**	5,756	5,346	**5,551**
	IR_100_153_4x80_15_01	3	30	0,100	0,094	1,53	0,80	1,5	6,96	0,12	0,121	0,114	**0,235**	3,462	3,274	**3,368**
24/02/2010	RW_071_153_4x80_15_01	3	30	0,071	0,067	1,53	0,80	1,5	7,48	0,11	0,151	0,126	**0,277**	4,041	3,378	**3,710**
	RW_024_102_4x80_15_a10_01	1	30	0,024	0,019	1,02	0,80	1,5	0,38	0,01	0,020	0,000	**0,020**	10,561	0,000	**5,281**
	RW_047_128_4x80_15_a10_01	2	30	0,047	0,046	1,28	0,80	1,5	2,89	0,07	0,052	0,076	**0,128**	3,628	5,246	**4,437**
	RW_071_153_4x80_15_a10_01	3	30	0,071	0,066	1,53	0,80	1,5	7,58	0,16	0,156	0,114	**0,270**	4,103	3,013	**3,558**
	IR_067_128_4x80_15_a10_01	2	30	0,067	0,062	1,28	0,80	1,5	2,42	0,03	0,069	0,062	**0,131**	5,698	5,172	**5,435**
	IR_100_153_4x80_15_a10_01	3	30	0,100	0,096	1,53	0,80	1,5	7,13	0,14	0,119	0,112	**0,231**	3,330	3,151	**3,241**
	RW_071_153_4x80_15_a30_01	3	30	0,071	0,067	1,53	0,80	1,5	7,6	0,17	0,124	0,113	**0,237**	3,265	2,971	**3,118**
	IR_067_128_4x80_15_a30_01	2	30	0,067	0,060	1,28	0,80	1,5	2,26	0,04	0,043	0,041	**0,084**	3,834	3,638	**3,736**
	IR_100_153_4x80_15_a20_01	3	30	0,100	0,095	1,53	0,80	1,5	7,08	0,14	0,116	0,108	**0,224**	3,267	3,037	**3,152**
	RW_060_180_4x80_15_1	-	-	0,060	0,059	1,8	0,80	1,5	6,99	0,15	0,099	0,068	**0,167**	2,827	1,938	**2,383**
	RW_060_160_4x80_15_1	-	-	0,060	0,052	1,6	0,80	1,5	4,76	0,09	0,097	0,093	**0,190**	4,072	3,913	**3,993**
	RW_060_140_4x80_15_1	-	-	0,060	0,047	1,4	0,80	1,5	3,21	0,03	0,106	0,099	**0,205**	6,621	6,167	**6,394**
	RW_060_120_4x80_15_1	-	-	0,060	0,059	1,2	0,80	1,5	4,07	0,1	0,114	0,140	**0,254**	5,619	6,868	**6,244**
	RW_060_100_4x80_15_1	-	-	0,060	0,055	1	0,80	1,5	2,97	0,06	0,142	0,112	**0,254**	9,543	7,521	**8,532**
	RW_060_080_4x80_15_1	-	-	0,060	0,060	0,8	0,80	1,5	2,67	0,05	0,163	0,121	**0,284**	12,199	9,031	**10,615**
	RW_060_060_4x80_15_1	-	-	0,060	0,058	0,6	0,80	1,5	1,5	0,03	0,129	0,102	**0,231**	17,258	13,562	**15,410**
	RW_110_120_4x80_15_01	-	-	0,110	0,112	1,2	0,80	1,5	16,39	0,05	0,248	0,188	**0,436**	3,020	2,295	**2,658**
	RW_090_120_4x80_15_01	-	-	0,090	0,093	1,2	0,80	1,5	10,38	0,06	0,197	0,158	**0,355**	3,796	3,051	**3,424**
	RW_070_120_4x80_15_01	-	-	0,070	0,072	1,2	0,80	1,5	6,17	0,06	0,144	0,113	**0,257**	4,668	3,671	**4,170**
	RW_050_120_4x80_15_01	-	-	0,050	0,049	1,2	0,80	1,5	2,97	0,05	0,088	0,074	**0,162**	5,945	4,992	**5,469**
	RW_030_120_4x80_15_01	-	-	0,030	0,027	1,2	0,80	1,5	0,81	0,02	0,014	0,034	**0,048**	3,546	8,346	**5,946**

	File name	WS	scale	Hs [m]	real Hs [m]	Tp [s]	Distance [m]	Load	Wave power i. [W/m]	Power w refl [W/m]	Power generated [W/0,5m]	back [W/0,5m]	average [W/m]	**efficiency front**	efficiency back	**efficiency [%]**
24/02/2010	IR_100_53_4x55_15_01	3	30	0,100	0,094	1,53	0,55	1,5	6,99	0,12	0,117	0,103	0,220	**3,360**	2,938	**3,149**
	IR_100_53_4x45_15_01	3	30	0,100	0,061	1,53	0,45	1,5	6,78	0,12	0,121	0,111	0,232	**3,562**	3,268	**3,415**
	IR_067_128_4x55_15_01	2	30	0,067	0,093	1,28	0,55	1,5	2,35	0,03	0,070	0,053	0,123	**5,939**	4,471	**5,205**
	IR_067_128_4x45_15_01	2	30	0,067	0,061	1,28	0,45	1,5	2,3	0,04	0,070	0,060	0,130	**6,084**	5,173	**5,629**
11/03/2010	only 2Hz results not reliable															
12/03/2010	RW_060_180_4x80_15_05	-	-	0,060	0,053	1,8	0,80	1,5	5,63	0,01	0,091	0,073	0,164	**3,245**	2,585	**2,915**
	RW_060_160_4x80_15_05	-	-	0,060	0,050	1,6	0,80	1,5	4,25	0,04	0,106	0,106	0,212	**4,994**	4,985	**4,990**
	RW_060_140_4x80_15_05	-	-	0,060	0,044	1,4	0,80	1,5	2,84	0,06	0,114	0,137	0,251	**8,000**	9,649	**8,825**
	RW_060_120_4x80_15_05	-	-	0,060	0,058	1,2	0,80	1,5	3,92	0,01	0,121	0,164	0,285	**6,162**	8,364	**7,263**
	RW_060_100_4x80_15_05	-	-	0,060	0,052	1	0,80	1,5	2,42	0,02	0,137	0,137	0,274	**11,319**	11,339	**11,329**
	RW_060_080_4x80_15_05	-	-	0,060	0,057	0,8	0,80	1,5	2,34	0,02	0,178	0,142	0,320	**15,170**	12,119	**13,645**
	RW_060_060_4x80_15_05	-	-	0,060	0,055	0,6	0,80	1,5	1,53	0,06	0,109	0,098	0,207	**14,240**	12,777	**13,509**
	RW_024_102_4x80_15_01	1	30	0,024	0,015	1,02	0,80	1,5	0,2	0,01	0,001	0,000	0,001	**0,633**	0,000	**0,317**
	RW_047_128_4x80_15_01	2	30	0,047	0,039	1,28	0,80	1,5	2,03	0,02	0,074	0,090	0,164	**7,323**	8,886	**8,105**
	RW_071_153_4x80_15_02	3	30	0,071	0,060	1,53	0,80	1,5	5,94	0,02	0,138	0,150	0,288	**4,631**	5,053	**4,842**
	IW_100_153_4x80_15_05	3	30	0,100	0,085	1,53	0,80	1,5	5,62	0,05	0,109	0,133	0,242	**3,865**	4,739	**4,302**
	RW_024_102_4x80_17_01	1	30	0,024	0,015	1,02	0,80	1,7	0,19	0,01	0,000	0,000	0,000	**0,000**	0,000	**0,000**
	RW_047_128_4x80_17_01	2	30	0,047	0,040	1,28	0,80	1,7	2,05	0,02	0,074	0,089	0,163	**7,238**	0,089	**3,664**
	RW_071_153_4x80_17_01	3	30	0,071	0,060	1,53	0,80	1,7	5,96	0,02	0,159	0,149	0,308	**5,338**	5,002	**5,170**
	IW_100_153_4x80_17_03	3	30	0,100	0,085	1,53	0,80	1,7	5,66	0,05	0,133	0,137	0,270	**4,692**	4,838	**4,765**
	IW_033_102_4x80_17_S_01	1	30	0,033	0,020	1,02	0,80	1,7	0,2	0,01	0,013	0,006	0,025	**16,806**	8,229	**12,518**
	IW_067_128_4x80_17_S_01	2	30	0,067	0,056	1,28	0,80	1,7	1,94	0,03	0,075	0,072	0,191	**10,014**	9,667	**9,841**
	IW_100_153_4x80_17_S_01	3	30	0,100	0,085	1,53	0,80	1,7	5,69	0,05	0,134	0,136	0,351	**6,099**	6,184	**6,142**
10/04/2010	IW_033_102_240_15_S_50x10_01	1	30	0,033	0,022	1,02	2,40	1,5	0,24	0,01	0,018	0,014	0,032	**14,650**	11,611	**13,131**
	IW_067_128_240_15_S_50x10_01	2	30	0,067	0,058	1,28	2,40	1,5	2,12	0,05	0,066	0,077	0,143	**6,252**	7,242	**6,747**
	IW_100_153_240_15_S_50x10_01	3	30	0,100	0,084	1,53	2,40	1,5	5,45	0,08	0,120	0,132	0,252	**4,412**	4,848	**4,630**

	File name	WS	scale	Hs [m]	real Hs	Tp [s]	Distance [m]	Load	Wave power	Power w refl	Power generated	back [W/0,5m]	**average [W/m]**	efficiency front	efficiency back	**efficiency [%]**
10/04/2010	IW_033_102_240_15_S_38x13_01	1	30	0,033	0,019	1,02	2,40	1,5	0,18	0,01	0,013	0,012	**0,032**	19,088	16,873	**17,981**
	IW_067_128_240_15_S_38x13_01	2	30	0,067	0,055	1,28	2,40	1,5	1,87	0,04	0,063	0,077	**0,182**	8,789	10,815	**9,802**
	IW_100_153_240_15_S_38x13_01	3	30	0,100	0,083	1,53	2,40	1,5	5,46	0,09	0,117	0,141	**0,335**	5,633	6,798	**6,216**
	IW_033_102_240_15_S_38x10_01	1	30	0,033	0,019	1,02	2,40	1,5	0,18	0,01	0,005	0,003	**0,010**	7,821	4,160	**5,991**
	IW_067_128_240_15_S_38x10_01	2	30	0,067	0,054	1,28	2,40	1,5	1,85	0,04	0,049	0,056	**0,136**	7,016	7,906	**7,461**
	IW_100_153_240_15_S_38x10_01	3	30	0,100	0,083	1,53	2,40	1,5	5,44	0,09	0,101	0,117	**0,283**	4,894	5,665	**5,280**
	IW_033_102_240_15_S_38x07_01	1	30	0,033	0,018	1,02	2,40	1,5	0,16	0,01	0,000	0,000	**0,000**	0,123	0,000	**0,062**
	IW_067_128_240_15_S_38x07_01	2	30	0,067	0,054	1,28	2,40	1,5	1,88	0,05	0,008	0,009	**0,022**	1,104	1,321	**1,213**
	IW_100_153_240_15_S_38x07_01	3	30	0,100	0,084	1,53	2,40	1,5	5,53	0,09	0,026	0,025	**0,066**	1,237	1,190	**1,214**
11/04/2010	RW_060_060_240_20_01	-	-	0,060	0,060	0,6	2,40	2	1,85	0,03	0,104	0,137	**0,241**	11,223	14,779	**13,001**
	RW_060_080_240_20_01	-	-	0,060	0,057	0,8	2,40	2	2,31	0,02	0,213	0,168	**0,381**	18,399	14,505	**16,452**
	RW_060_100_240_20_01	-	-	0,060	0,058	1	2,40	2	3,03	0,04	0,167	0,170	**0,337**	11,034	11,236	**11,135**
	RW_060_120_240_20_01	-	-	0,060	0,062	1,2	2,40	2	4,78	0,04	0,121	0,147	**0,268**	5,044	6,169	**5,607**
	RW_060_140_240_20_01	-	-	0,060	0,052	1,4	2,40	2	4,04	0,02	0,130	0,131	**0,261**	6,456	6,468	**6,462**
	RW_060_160_240_20_01	-	-	0,060	0,052	1,6	2,40	2	4,56	0,02	0,118	0,089	**0,207**	5,159	3,894	**4,527**
	RW_060_180_240_20_01	-	-	0,060	0,055	1,8	2,40	2	5,92	0,11	0,086	0,100	**0,186**	2,895	3,384	**3,140**
	RW_024_102_240_20_02	1	30	0,024	0,012	1,02	2,40	2	0,13	0,005	0,000	0,000	**0,000**	0,000	0,000	**0,000**
	RW_047_128_240_20_02	2	30	0,047	0,046	1,28	2,40	2	2,68	0,03	0,069	0,111	**0,180**	5,173	8,278	**6,726**
	RW_071_153_240_20_02	3	30	0,071	0,065	1,53	2,40	2	6,35	0,1	0,134	0,185	**0,319**	4,207	5,825	**5,016**
	RW_035_125_240_20_02	1	20	0,035	0,031	1,25	2,40	2	1,14	0,05	0,000	0,046	**0,046**	0,000	8,097	**4,049**
	IW_033_102_240_20_02	1	30	0,033	0,021	1,02	2,40	2	0,21	0,01	0,008	0,001	**0,009**	7,508	0,805	**4,157**
	RW_024_102_240_00_02	1	30	0,024	0,012	1,02	2,40	0	0,12	0,003	0,007	0,000	**0,007**	12,387	0,165	**6,276**
	RW_047_128_240_00_02	2	30	0,047	0,043	1,28	2,40	0	2,43	0,03	0,036	0,037	**0,073**	2,925	3,014	**2,970**
	RW_071_153_240_00_02	3	30	0,071	0,064	1,53	2,40	0	6,22	0,09	0,056	0,055	**0,111**	1,787	1,780	**1,784**
	RW_035_125_240_00_02	1	20	0,035	0,030	1,25	2,40	0	1,13	0,04	0,024	0,022	**0,046**	4,198	3,914	**4,056**
	IW_033_102_240_00_02	1	30	0,033	0,021	1,02	2,40	0	0,22	0,01	0,011	0,001	**0,012**	10,073	1,277	**5,675**
	IW_033_102_240_15_S_50x10HOLE_01	1	30	0,033	0,021	1,02	2,40	1,5	0,21	0,01	0,000	0,000	**0,000**	0,006	0,024	**0,015**
	IW_067_128_240_15_S_50x10HOLE_01	2	30	0,067	0,060	1,28	2,40	1,5	2,2	0,05	0,001	0,012	**0,013**	0,888	1,100	**0,994**
	IW_100_153_240_15_S_50x10HOLE_01	3	30	0,100	0,090	1,53	2,40	1,5	6,44	0,09	0,047	0,052	**0,099**	1,472	1,608	**1,540**

In the previous pages, each table contains the main information concerning the laboratory results.

For example, the first test reported is RW_035_125_240_00_01. Hence, the data file name has a structure as AA_BB_CC_DD_EE_FF, where:

- AA indicates if the wave is regular (RW) or irregular (IR);
- BB indicates the wave height;
- CC indicates the wave period;
- DD indicates the distance between the energy converter plates;
- EE indicates the load;
- FF indicates the number of the test.

The information contained in the file name are reported in the subsequent columns of the table, such as: the wave state, the wave period, the wave height. Furthermore, in the table, the column subsequent to the wave height corresponds to the measured wave height, whereas for the wave period this difference is negligible.

The incident and the reflected wave power are referred to the values measured from the wave gauges, and then analyzed through the software WaveLab3.33.

Regard the wave power, there are differences among the theoretical values and the measured ones, and moreover among measured values in different tests, but referring to the same wave state. However, it is declarable that these differences are insignificant for the work done.

The power generated values are calculated as the ratio between the total energy product by the device and the total sampling duration, or analogously as the average among the power generated at each sampling instant.

$$Power\ generated = \frac{Average\ total\ energy}{Total\ duration}$$

$$Average\ total\ energy = P_j * \Delta t_j$$

$$Power\ generated = \frac{\sum Power\ generated\ for\ each\ record\ instant}{Total\ number\ of\ records}$$

$$Power\ generated\ for\ each\ record\ instant = P_j = F_j * \frac{x_{j+1} - x_j}{\Delta t_j}$$

The value between the front plate and the back one, concerning the power generated, is determined refer to a width of the plate of 1m, hence it is more understandable.

Whereas to obtain the efficiency values a comparison, between the power generated and the wave power available, is done for each test.

MATLAB ANALISYS' FILE

The wave is usually described through a harmonic signal, consequently the displacement and the force felt by the energy converter plate should be represented through harmonic signals.

Through the sampling plot of one signal of the force, it is evident that the trend is harmonic how it should be, but it has not a zero mean. This is a mistake, because it means that at t=0, when there should not be any force, in reality there is an "inconvenience force" measured, which value coincides with the average value of the signal. It is analogous to say that the graph is shifted, without modifying its trend.

Therefore it is necessary to subtract the offset value to each force measured value.

The offset problem is also present in the records of the displacements, and the meaning is obviously the same, i.e. at the start instant, t=0, when there should not be any displacement, in reality the plate is not to the original position. However, regard the displacements, the offset is not a problem, because the aim of the study is to have the difference Δx between two subsequent record instants, and not the real displacement x, for each record instant.

As it is predictable, immediately, the device doesn't achieve the steady state. This aspect is illustrated in the figure D.1, for this reason it is required to cut the first minute of the sampling for the regular tests, and the first two or three minutes for the irregular tests. However, to consider the first few minutes does not involve a serious mistake.

Moreover calculating the Δt, it is observable that several times the Δt is different to the one fixed with the frequency sampling. It is declarable that:

- the time of recording could be wrong due to problem between usb/router, etc.
- the time, which the machine takes results, is correct and it corresponds to the frequency chosen.

In the next pages, the Matlab script and its results are reported.

```
% The target of this script is to analyze the results coming from
% WavePiston.vi, to find:
% - the average generated power
% - the efficiency of the device for a particular wave state
% - the standard deviation of the impressed force on the energy converter plate

clear all
close all

addpath(genpath('LABORATOR'))
                        % specifies the path to search the file
fid = fopen('RW_060_180_4x80_15_T_04.txt','rt');
                        % indicates which file take in examination

for i=1:15;
    line = fgetl(fid);
end

deltat=0.1;             % sampling frequency 10Hz

count = 1;
while ~feof(fid),                   % while the file is not end
line = strrep(line,',','.');        % string replace
data(count,:) = sscanf(line,'%f %f %f %f %f')';
count = count+1;
line = fgetl(fid);
end
line = strrep(line,',','.');
            % when the while cycle is finished, there is one more line to read
data(count,:) = sscanf(line,'%f %f %f %f %f')';
            % the data matrix will contain all the numbers inside the input file
fclose(fid);
            % at the end of the while cycle, that the matrix data is finished,
              it is possible to create the displacement vector and force vector

% Creation of the displacement and force vector
displacement = data(:,[2 3]);
Force = data(:,[4 5]);
offset = mean(data(:,[4 5]));    % calculation of forces offset.
offset1= offset(1,1);            % It coincides with the mean, because the
offset2= offset(1,2);            % signal is harmonic

Force_ok(:,1) = Force(:,1)-offset1;
Force_ok(:,2) = Force(:,2)-offset2;

% To create the velocity vector the easiest way is to use another counter
velocity(1,:)=[0 0];            % initial condition for the velocity

for j= 1:(max(length(displacement))-1)
velocity(j+1,:)=(displacement(j+1,:)-displacement(j,:))/deltat;
end

power = velocity.*Force_ok;
average_power = 2*mean(power);
            % the multiplication for two is because the plate width is 0,5m,
```

```
            % while the wave incident power is for 1m of width crest
disp(['the front and the back average power,in W/m,are ',num2str(average_power)])

% Displacements
figure(1)
subplot(2,1,1), plot(data(:,2),'b')
legend('displacement of the front plate')
xlabel('time [s]');
ylabel('front plate');
subplot(2,1,2), plot(data(:,3),'r')
legend('displacement of the back plate')
xlabel('time [s]');
ylabel('back plate');

% Measured Forces
figure(2)
subplot(2,1,1), plot(data(:,4),'b')
legend('measured forces in the front')
ylabel('front plate');
xlabel('time [s]');
subplot(2,1,2), plot(data(:,5),'r')
legend('measured forces in the back')
ylabel('back plate');
xlabel('time [s]');

% Velocity calculated
figure(3)
subplot(2,1,1), plot(velocity(:,1),'b')
legend('velocity of the front plate')
xlabel('time [s]');
ylabel('front plate');
subplot(2,1,2), plot(velocity(:,2),'r')
legend('velocity of the back plate')
xlabel('time [s]');
ylabel('back plate');
```

```
the front and the back average power, in W/m, are  -0.63609    -0.45974
```

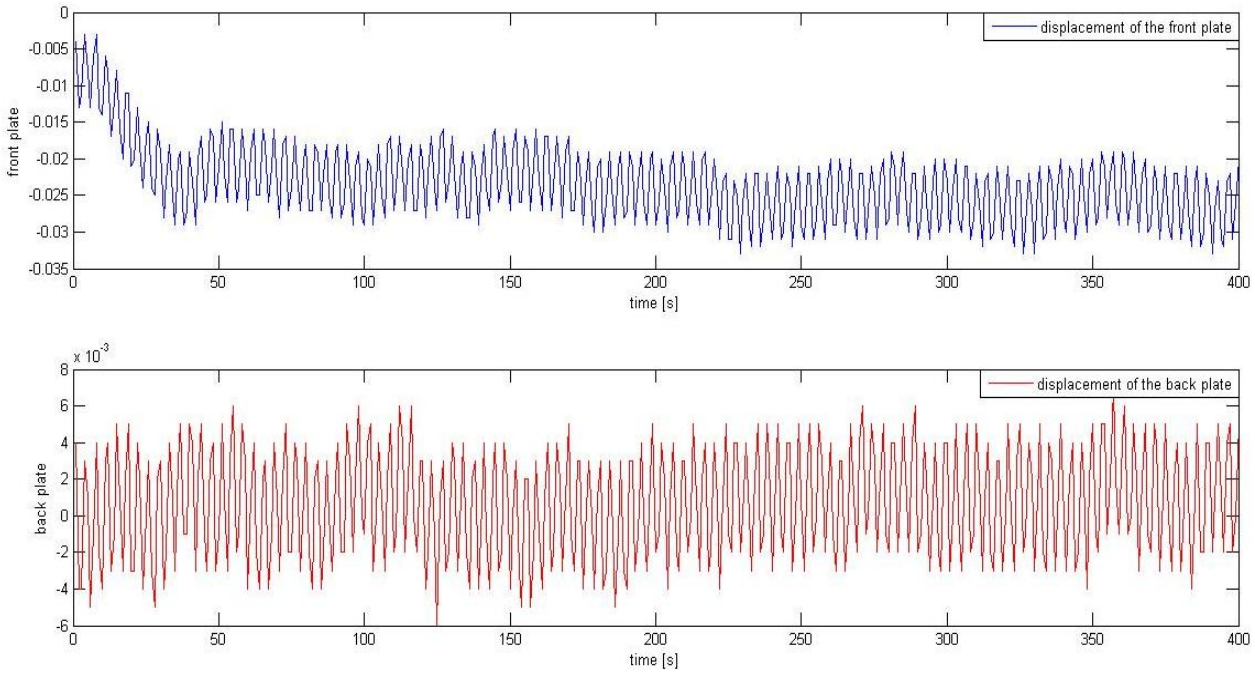

Figure D.1: Displacements of the front plate and the back plate during the sampling.
It is obviously that the device requires several instants to get the steady state.

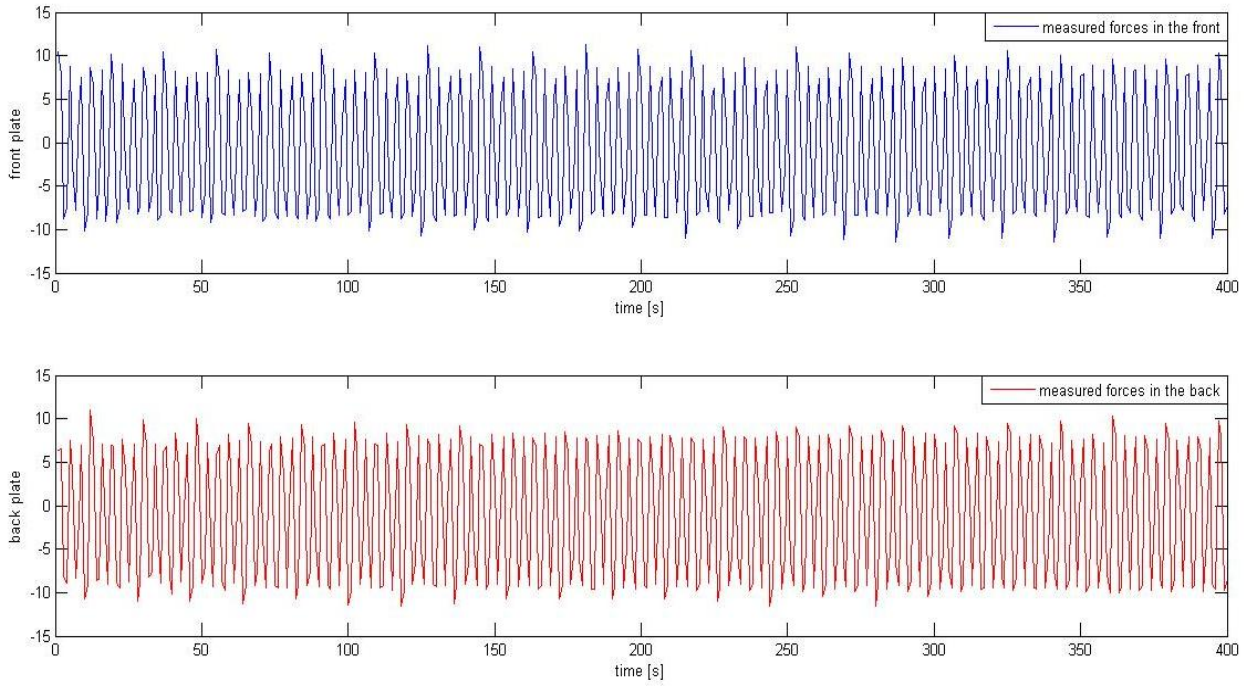

Figure D.2: Force impressed on the front plate and on the back plate during the sampling.
The regular trend of the displacement, it is due to the regular trend of the wave, and this is observable even in the impressed forces' trend.

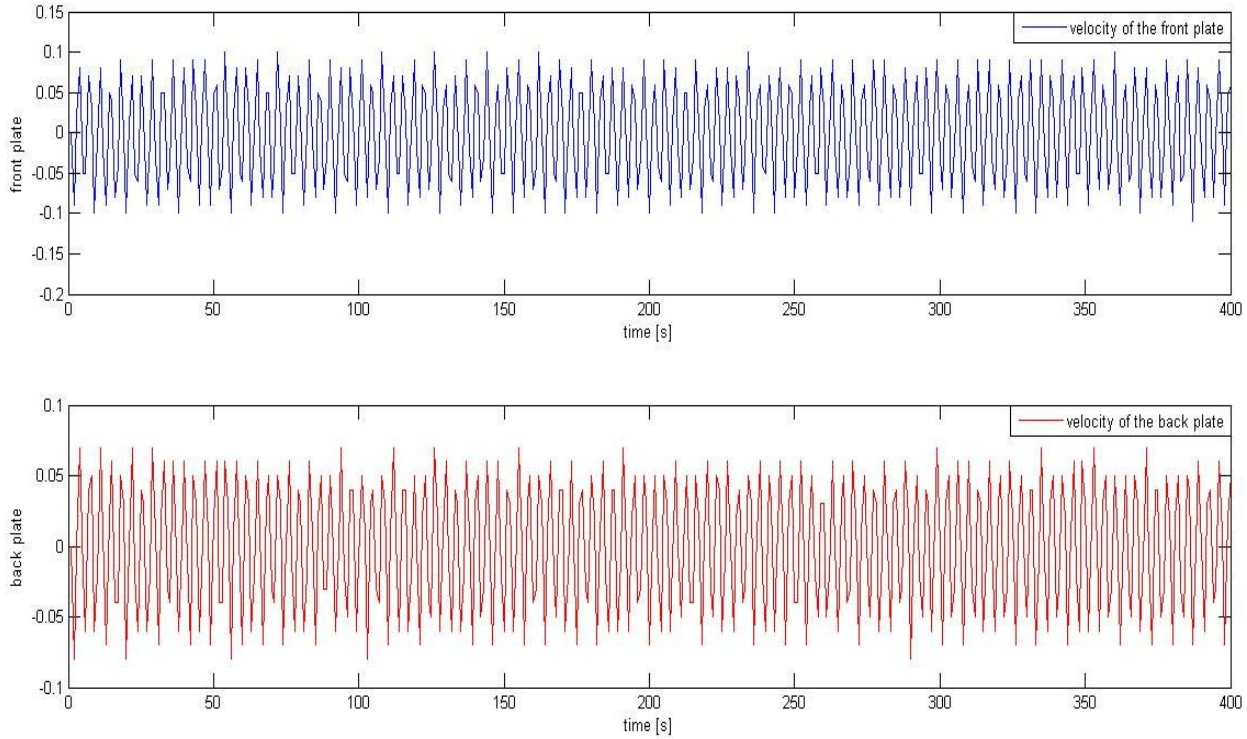

Figure D.3: Velocity on the front plate and on the back plate during the sampling.
The velocity trend depends on the displacement one, so it has the same regular trend.

SIMULATIONS WITH MATLAB

1- Introduction

As presented before, the WavePiston device can be represented as a single degrees freedom body.

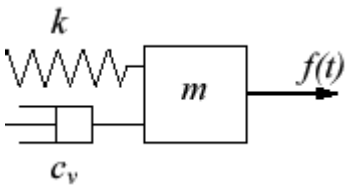

Figure E.0: A single unit of the WavePiston device is seen as a single degrees freedom body.

The main target of the numerical model is to predict the behaviour of the WavePiston device in different location, changing the wave parameters of regular waves, and regardless the laboratory results.

Nevertheless, to achieve that aim, the first stage is to build a numerical model able to estimate the efficiency in the laboratory case.

Furthermore, to begin the simulation analysis, some simplifying assumption are made; hence, below, it is presented for first the numerical model able to guess the performance of a fixed body in the laboratory condition, then there is the numerical model for the body in movement in the laboratory condition, and at last there is the numerical model for the body in movement in real condition.

The wave is usually described through a harmonic signal, consequently the displacement and the force felt by the energy converter plate should be represented through harmonic signals.

For all the numerical models concerning the laboratory conditions, a particular value for the stiffness is hypothesized, i.e. k_p= 100 N/m, it means that to move the plate of 1cm, it is necessary a force of 1N (1N=100g). This value should be changed, depending on the result of particular test, where by imposing a known displacement and reading the strength corresponding it is possible to find the stiffness as the ratio $\Delta F/\Delta x$.

Whereas, for the damping coefficient, the two models have not an unique value for it, but there are many values, and different results correspond to the variation of the damping values.

It is predictable that a small value of the damping implies a large range for the displacement, hence of the velocity, but at the same time a low value of the force impressed, because the plate does not make resistance to the flow motion.

Thus, to obtain the best performance, the damping value might have a mean value.

These comments are verified with the numerical models' graphs.

2- First model: Simulation of a fixed body in the laboratory condition

```
% NUMERICAL MODEL_1
% Target: Reproduce laboratory conditions

% Basic equation is the dynamic equation for a normal oscillating body
% m*acc+ c*vel+ k*x = External force
% where External force is the force given by Morison Equation with a fixed body
is F(u, upunto, xpunto, x2punti)= F inertia + F drag
% where u= is the flow velocity
%       x= is the plate displacement


clear all
close all

row = 1030;          % row= density salt water [kg/m3]
ro= 7740;            % ro= density of the steel plate [kg/m3]
roprimo= ro-row;     % roprimo=density of the steel plate inside the water [kg/m3]

w= 0.5;          % w= width of the plate [m]
d= 0.1;          % d= depth of the plate [m]
s= 0.001;        % s= thickness [m]

kp=100;      % kp= steel plate stiffness  [N/m]
             % for the first attempt it is introduced a casual value.
             % The hypothesis is 100N/m, it means that to move the plate of 1cm
                it is necessary a force of 1N (1N=100g).
             % This value should be changed,depending on the result of particular
              test, where by imposing a known displacement and reading the
              strength corresponding it is possible to find the stiffness as the
              ratio ΔF/Δx.

mass= roprimo*w*d*s;
volume=w*d*s;

% Values of the First Danish Regular Wave State, in scale 1:30
Hs= 0.024;    % Hs= significant wave height [m]
Tp= 1.02;     % T= Tp= wave period [s]
L= 1.61;      % L= wave length [m]
h= 0.7;       % h= water depth [m]

k= 2*pi/L;
omega=2*pi/Tp;

% Wave Power per meter of wave crest [kW/m]
Tz=Tp/1.4;
Te=1.2*Tz;
Wavepower=0.44*(Hs^2)*Te;


% External force
CD=2;      % CD= drag coefficient;
CM=1;      % CM= mass coefficient;
```

```
z=-(d/2); % presa di riferimento quota baricentro piatto
rap=(cosh(k*(h+z))/sinh(k*h));

q=1;
for vi=0:5:100            % C= damping [Ns/m]=[kg/s]
                          % step of 5, from a cycle to the subsequent

j=1;
vx(q,1)=0;           % initial conditions
vu(q,1)=0;           % u= flow velocity
vvel(q,1)=0;

for t=1:1:180         % computing time 3 minutes, with a step of 1 sec
    vt(1,j+1)=t;
    u=omega*(Hs/2)*rap*cos(omega*vt(1,j));
    vu(q,j+1)=u;

    upunto=-rap*(omega^2)*(Hs/2)*sin(omega*vt(1,j+1));
    deltat=vt(1,j+1)-vt(1,j);        % sampling frequency

    Fi=ro*(1+CM)*volume*upunto;       % Inertia force

    modulo=cos(omega*vt(1,j+1));
            % it is only depending on the trend of the velocity flow

if modulo>=0
        C1= CD*ro*omega^2*(Hs^2)*rap^2*(cos(omega*vt(1,j+1)))^2/(8*roprimo*s);
                                                    %C1= Fd/mass
        Fexternal=Fi+C1*mass;                       % Fexternal=Fi+Fd;
    else
        C1= -CD*ro*omega^2*(Hs^2)*rap^2*(cos(omega*vt(1,j+1)))^2/(8*roprimo*s);
                                                    %C1= Fd/mass
        Fexternal=Fi+C1*mass;                       % Fexternal=Fi+Fd;
    end

    B=(1/(deltat^2)+(vi/(mass*deltat))-(k/(2*mass)));
    C2=Fi/mass;

    A=(1/(deltat^2)+(vi/(mass*deltat))+(k/(2*mass)));

    x= (vx(q,j)*B+C1+C2)/A;          % x= plate displacement
    vx(q,j+1)=x;

    velocity=(vx(q,j+1)-vx(q,j))/deltat;
    vvel(q,j+1)=velocity;

    Flost=vi*velocity;
    vFlost(q,j+1)=Flost;
    vStdFlost(1,q)=std(vFlost(q,:));

    vFexternal(q,j+1)=Fexternal;

    Fimpressed=Fexternal-Flost;
    vFimpressed(q,j+1)=Fimpressed;
```

```
    stdFimpressed=std(vFimpressed(q,:));

    Power=abs(velocity*Flost)/w;
            % Calculation of the power generated per meter of plate's width, in
            a particular instant j
    vPower(q,j+1)=Power;
    averagePower=mean(vPower(q,:));

    j=j+1;
end

allvi(1,q)=vi;

stdvel=std(vvel(q,:));
vstdvel(1,q)=stdvel;

vStdFimpressed(1,q)=stdFimpressed;
allAveragePower(1,q)=averagePower;

efficiency= allAveragePower(1,q)*100/(Wavepower*1000);
      % To calculate the efficiency there is the need to compare the wave power
      with the average power generated for each damping value
veff(1,q)=efficiency;

q=q+1;
end

% Flow velocity
figure(1)
plot(vt,vu,'r.-')
xlabel('time [s]');
ylabel('flow velocity');

% Different displacement for different damping values
figure(2);
plot(vt,vx(1,:),'.b',vt,vx(10,:),'.m',vt,vx(21,:),'.k')
legend('in blue damping=0','in magenta damping medium', 'in black damping
maximum')
xlabel('time [s]');
ylabel('displacement');

% Different velocity for different damping values
figure(3)
plot(vt,vvel(1,:),'.b',vt,vvel(10,:),'.m',vt,vvel(21,:),'.k')
legend('in blue damping=0','in magenta damping medium', 'in black damping
maximum')
xlabel('time [s]');
ylabel('plate velocity');

% Velocity comparison between flow velocity and the one for the mean damping
values
figure(4);
plot(vt,vvel(10,:),'.m',vt,vu,'r.-')
legend('in magenta damping medium', 'in red flow velocity')
xlabel('time [s]');
```

```
ylabel('velocity comparison');

% Standard deviation of the velocity
figure(5)
plot(allvi,vstdvel,'.b')
xlabel('Damping values');
ylabel('Standard Deviation of the plate velocity');

% Average power product for each damping value
figure(6)
plot(allvi,allAveragePower,'.k')
xlabel('Damping values');
ylabel('Power generated');

% Standard deviation of the velocity
figure(7)
plot(allvi,vStdFlost,'.m')
xlabel('Damping values');
ylabel('standard deviation of the Lost force');

% Efficiency for each damping value
figure(8)
plot(allvi,veff,'.b')
xlabel('Damping values');
ylabel('efficiency');

figure(9)
plot(allvi,vstdvel,'.b',allvi,vStdFlost,'.m',allvi,allAveragePower,'.g')
legend('in blue standard deviation of the plate velocity','in magenta standard
deviation of the Lost force', 'in green power generated')
xlabel('Damping values');

figure(10)
plot(vStdFlost,vstdvel,'.r')
xlabel('standard deviation of the Lost force');
ylabel('standard deviation of the plate velocity');

figure(11)
plot(vStdFlost,allAveragePower,'.k')
xlabel('standard deviation of the Lost force');
ylabel('power generated');

figure(12)
subplot(2,2,1),plot(vt,vu,'r.-')
ylabel('flow velocity');
subplot(2,2,2),plot(vt,vx(1,:),'.b',vt,vx(10,:),'.m',vt,vx(21,:),'.k')
ylabel('displacement for different damping values');
subplot(2,2,3),plot(vt,vvel(1,:),'.b',vt,vvel(10,:),'.m',vt,vvel(21,:),'.k')
ylabel('plate velocity for different damping values');
subplot(2,2,4),plot(vt,vvel(1,:),'.b',vt,vvel(10,:),'.m',vt,vvel(21,:),'.k',vt,v
u,'r.-')
legend('plate velocity for different damping values compared to the flow
velocity');
```

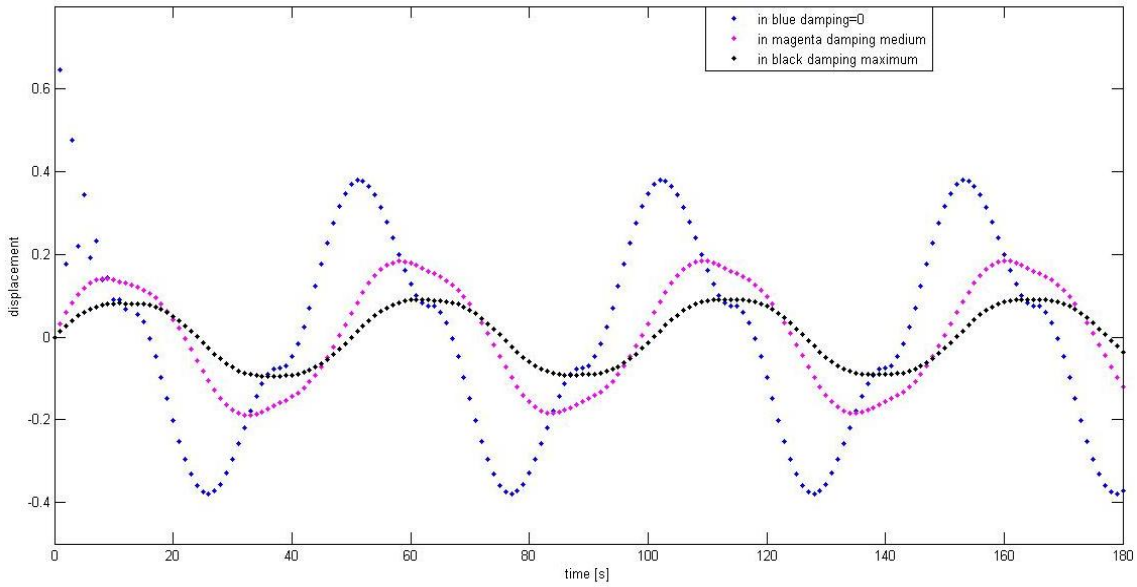

Figure E.1: Displacement for different damping values.
In blue, it is the displacement for a zero value of damping.
In magenta, it is the displacement for a mean value of damping.
In black, it is the displacement for a maximum value of damping.

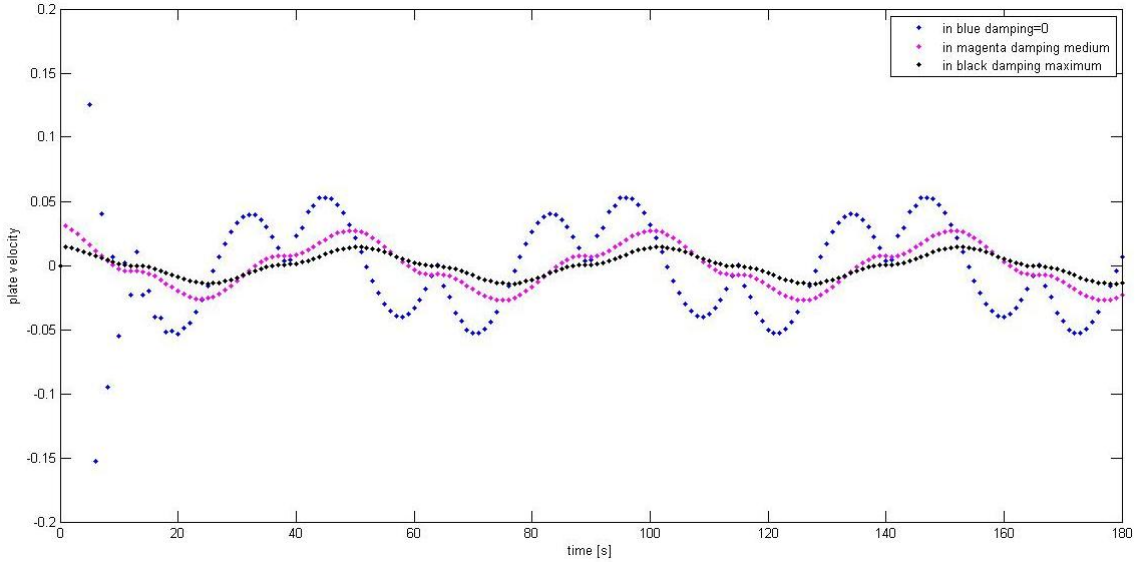

Figure E.2: Velocity of the movement of the plate for different damping values.
In blue, it is the velocity for a zero value of damping.
In magenta, it is the velocity for a mean value of damping.
In black, it is the velocity for a maximum value of damping.

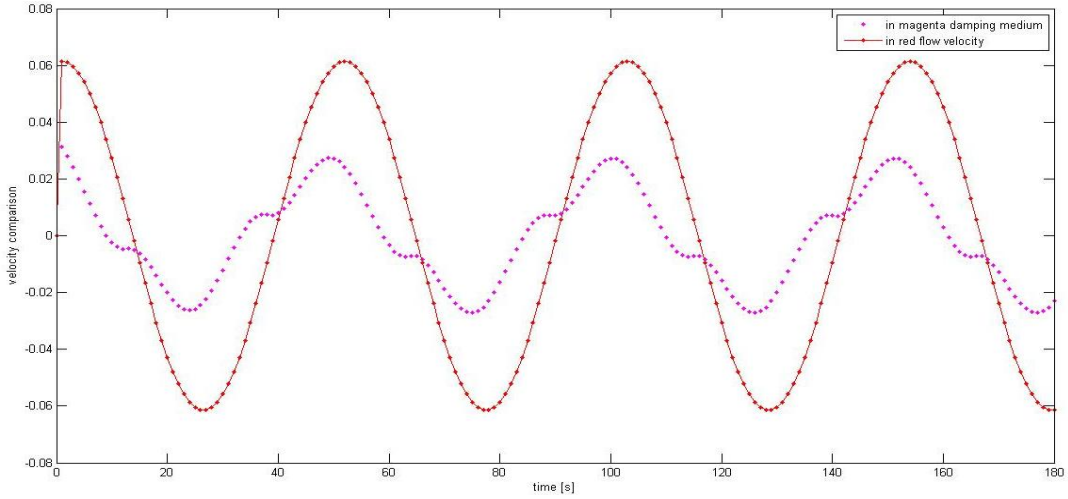

Figure E.3: Velocity comparison between the flow velocity and the velocity of the plate for the mean damping values.

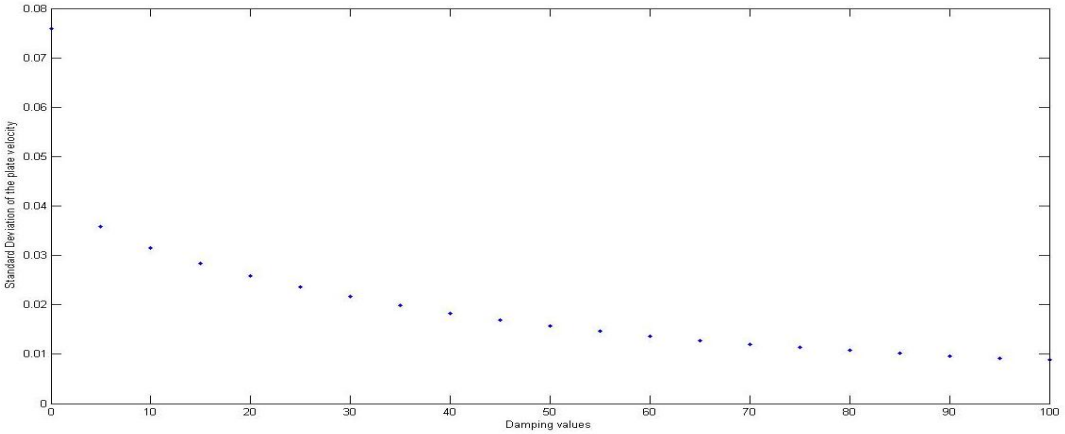

Figure E.4: Trend of the velocity due to the variation of the damping values.

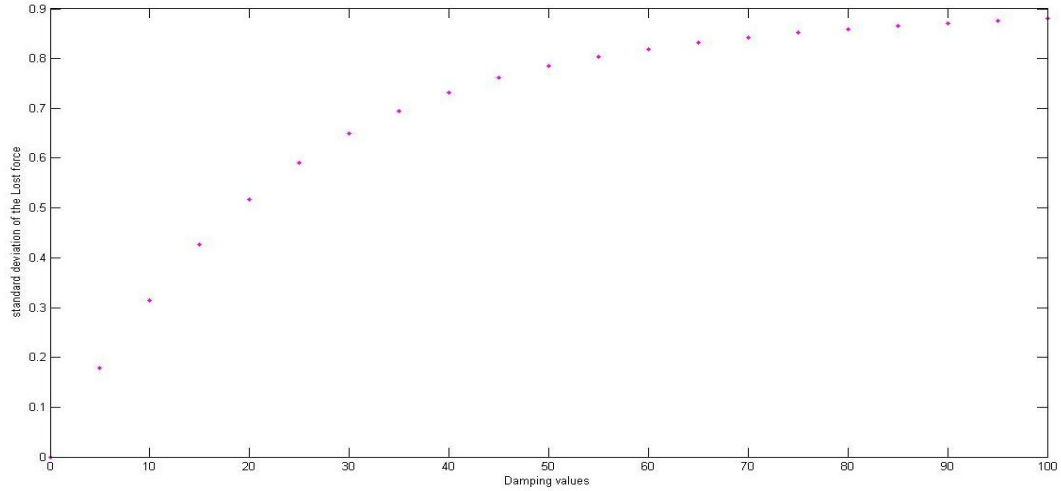

Figure E.5: Trend of the force impressed due to the variation of the damping values.

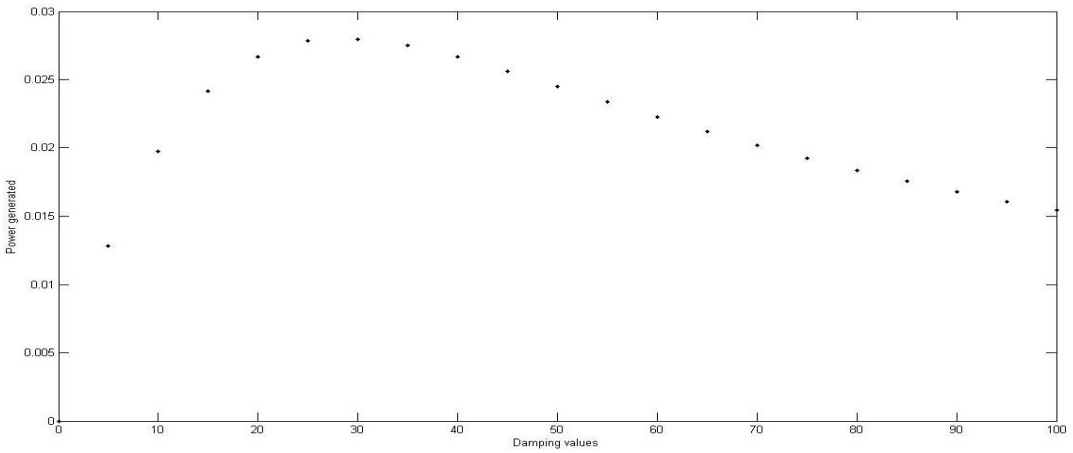

Figure E.6: Trend of the average power generated due to the variation of the damping values.

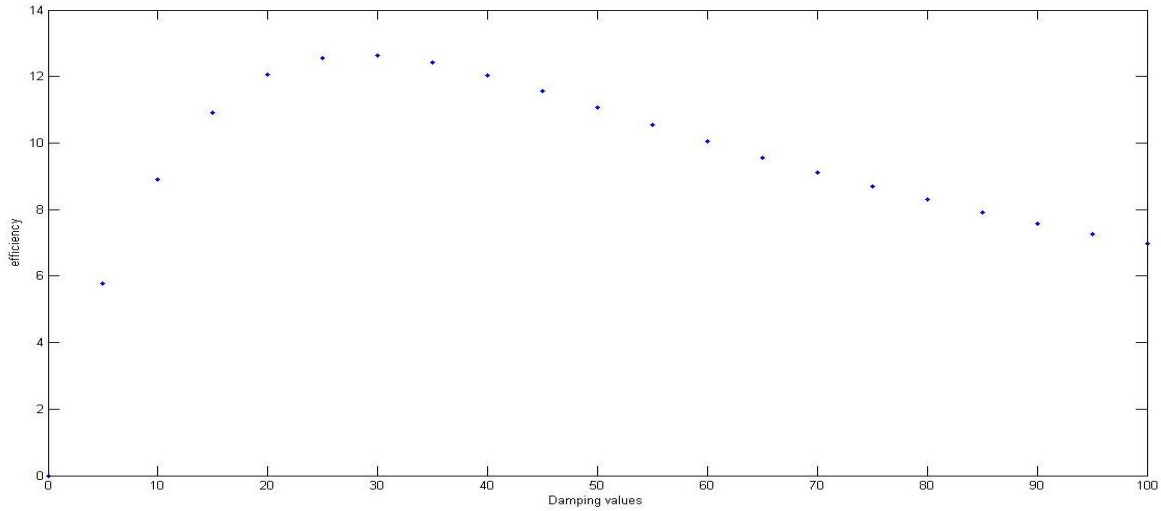

Figure E.7: Trend of the efficiency due to the variation of the damping values.

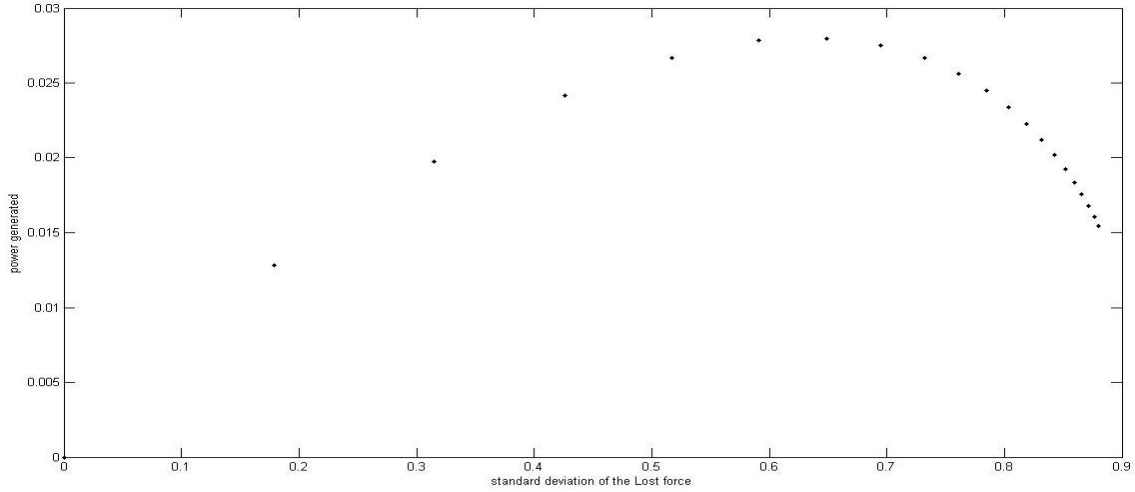

Figure E.8: Trend of the power generated in relation with the standard deviation of the force impressed.

3- Second model: Simulation of a body in movement in the laboratory condition

```
% NUMERICAL MODEL_2
% Target: Reproduce laboratory conditions

% Basic equation is the dynamic equation for a normal oscillating body
% m*acc+ c* vel+ k*x = External force
% where External force is the force given by Morison Equation with a body
% in movment F(u,upunto, xpunto, x2punti)= F inertia + F drag + F froude-Krylov
% where u= is the flow velocity
        x= is the plate displacement


clear all
close all

row = 1030;          % row= density salt water [kg/m3]
ro= 7740;            % ro= density of the steel plate = [kg/m3]
roprimo= ro-row;     % roprimo=density of the steel plate inside the water [kg/m3]

w= 0.5;          % w= width of the plate [m]
d= 0.1;          % d= depth of the plate [m]
s= 0.001;        % s= thickness [m]

kp=100;      % kp= steel plate stiffness  [N/m]
             % for the first attempt it is introduced a casual value.
             % The hypothesis is 100N/m, it means that to move the plate of 1cm
                it is necessary a force of 1N (1N=100g).
             % This value should be changed,depending on the result of particular
              test, where by imposing a known displacement and reading the
              strength corresponding it is possible to find the stiffness as the
              ratio ΔF/Δx.
mass= roprimo*w*d*s;
volume=w*d*s;
area=w*d;

% Values of the First Danish Regular Wave State, in scale 1:30
Hs= 0.024;    % Hs= significant wave height [m]
Tp= 1.02;     % Tp= wave period [s]
L= 1.61;      % L= wave length [m]
h= 0.7;       % h= water depth [m]

k= 2*pi/L;
omega=2*pi/Tp;

% Wave Power per meter of wave crest [kW/m]
Tz=Tp/1.4;
Te=1.2*Tz;
Wavepower=0.44*(Hs^2)*Te;


% external force
CD=2;      % CD= drag coefficient;
CM=1;      % CM= mass coefficient;
```

```
z=-(d/2); % presa di riferimento quota baricentro piatto
rap=(cosh(k*(h+z))/sinh(k*h));

q=1;
for vi=0:5:100           % C= damping [Ns/m]=[kg/s]
                         % step of 5, from a cycle to the subsequent
j=1;
vx(q,1)=0;       % initial conditions
vu(q,1)=0;       % u= flow velocity
vvel(q,1)=0;

for t=0.1:1:180     % computing time 3 minutes, with a step of 1 sec
vt(1,j+1)=t;
    u=omega*(Hs/2)*rap*cos(omega*vt(1,j));
    vu(q,j+1)=u;

    upunto=-rap*(omega^2)*(Hs/2)*sin(omega*vt(1,j+1));
    vupunto(q,j+1)=upunto;
    deltat=vt(1,j+1)-vt(1,j);       % sampling frequency

    partFi=ro*CM*volume*(vupunto(q,j+1));
           % partFi= it is the part of the inertia force that is not depending
           on the velocity of the plate
    Ffk=ro*volume*upunto;        % Ffk= body in movement


% Calculation of the displacement, assuming the abs positiv
    Ba=-((1/(deltat^2))+(vi/(mass*deltat))+(k/(2*mass)));
                % Ba= B part, not depending on abs sign
    Bmodulo=-(CD*ro*area/(2*mass))*((2*vu(q,j+1)/deltat)+(2*vx(q,j)/(deltat^2));
    B=Ba+Bmodulo;

    Ca=+vx(q,j)*((1/(deltat^2))+(vi/(mass*deltat))+
           -(k/(2*mass))+((CM*ro*volume)/((deltat^2)*mass)));
      % Ca= C1 part, not depending on abs sign
          Cmodulo=+vx(q,j)*((CD*ro*area)/(2*mass))*((vx(q,j)/(deltat^2))+
                  +(2*vu(q,j+1)/deltat))+((CD*ro*area)/(2*mass))*((vu(q,j+1))^2);
    C1=Ca+Cmodulo;

    C2=partFi/mass;
    C3=Ffk/mass;
    C=C1+C2+C3;

    A=((CD*ro*area)/(2*(deltat^2)*mass));

    g= polyeig(C,B,A);  % function to solve the equation: Ax^2+bx+C=0
                        % in input it needs the3 coefficients
                        % in output it gives a  vector g, including x1 e x2

    x=mean(g);          % x= plate displacment
    vx(q,j+1)=x;

    Fexternal=0.5*CD*ro*area*((vu(q,j+1)-((vx(q,j+1)-vx(q,j))/deltat)))^2+
      +ro*volume*CM*(vupunto(q,j+1)-(vx(q,j+1)-vx(q,j))/(deltat^2))+
      +C3*mass;
```

```
    vFexternal(q,j+1)=Fexternal;

    modulo= vupunto(q,j+1)-((vx(q,j+1)-vx(q,j))/deltat);

    if modulo>=0
        vx(q,j+1)=x;
    else
        A=-A;                % Re-calculation of the x value
        Bmodulo= -Bmodulo;
        B=Ba+Bmodulo;

        Cmodulo=-Cmodulo;
        C1=Ca+Cmodulo;
        C=C1+C2+C3;

        g= polyeig(C,B,A);
        x=mean(g);       % x= plate displacment
        vx(q,j+1)=x;

        Fexternal=0.5*CD*ro*area*((vu(q,j+1)-((vx(q,j+1)-vx(q,j))/deltat)))^2+
            +ro*volume*CM*(vupunto(q,j+1)-(vx(q,j+1)-vx(q,j))/(deltat^2))
            +C3*mass;
        vFexternal(q,j+1)=Fexternal;
    end

    velocity=(vx(q,j+1)-vx(q,j))/deltat;
    vvel(q,j+1)=velocity;

    Flost=vi*velocity;
    vFlost(q,j+1)=Flost;
    vStdFlost(1,q)=std(vFlost(q,:));

    Fimpressed=Fexternal-Flost;
    vFimpressed(q,j+1)=Fimpressed;
    stdFimpressed=std(vFimpressed(q,:));

    Power=abs(velocity*Flost)/w;
% Calculation of the power generated per meter of length crest, in a instant j
    vPower(q,j+1)=Power;
    averagePower=mean(vPower(q,:));

    j=j+1;

end

allvi(1,q)=vi;

stdvel=std(vvel(q,:));
vstdvel(1,q)=stdvel;

vStdFimpressed(1,q)=stdFimpressed;
allAveragePower(1,q)=averagePower;
```

```
% To calculate the efficiency there is the need to compare the wave power with
the average power generated for each damping value
efficiency= allAveragePower(1,q)*100/(Wavepower*1000);
veff(1,q)=efficiency;

q=q+1;
end

% Flow velocity
figure(1)
plot(vt,vu,'r.-')
xlabel('time [s]');
ylabel('flow velocity');

% Different displacement for different damping values
figure(2);
plot(vt,vx(1,:),'.b',vt,vx(10,:),'.m',vt,vx(21,:),'.k')
legend('in blue damping0','in magenta damping medium','in black damping maximum')
xlabel('time [s]');
ylabel('displacement');

% Different velocity for different damping values
figure(3)
plot(vt,vvel(1,:),'.b',vt,vvel(10,:),'.m',vt,vvel(21,:),'.k')
legend('in blue damping0','in magenta damping medium','in black damping maximum')
xlabel('time [s]');
ylabel('plate velocity');

% Velocity comparison between flow velocity and the one for the mean damping
values
figure(4);
plot(vt,vvel(10,:),'.m',vt,vu,'r.-')
legend('in magenta damping medium', 'in red flow velocity')
xlabel('time [s]');
ylabel('velocity comparison');

% Standard deviation of the velocity
figure(5)
plot(allvi,vstdvel,'.k')
xlabel('Damping values');
ylabel('Standard Deviation of the plate velocity');

% Average power product for each damping value
figure(6)
plot(allvi,allAveragePower,'.g')
xlabel('Damping values');
ylabel('Power generated');

% Standard deviation of the force
figure(7)
plot(allvi,vStdFlost,'.m')
xlabel('Damping values');
ylabel('standard deviation of the Lost force');

% Efficiency for each damping value
```

```
figure(8)
plot(allvi,veff,'.b')
xlabel('Damping values');
ylabel('efficiency');

figure(9)
plot(allvi,vstdvel,'.b',allvi,vStdFlost,'.m',allvi,allAveragePower,'.g')
legend('in blue standard deviation of the plate velocity', 'in magenta standard
deviation of the Lost force', 'in green power generated')
xlabel('Damping values');

figure(10)
plot(vStdFlost,vstdvel,'.r')
xlabel('standard deviation of the Lost force');
ylabel('standard deviation of the plate velocity');

figure(11)
plot(vt,vFexternal(1,:),'g.-',vt,vFexternal(10,:),'b.-',
                  vt,vFexternal(21,:),'r.-')
legend('Variation External force due to damping');

figure(12)
plot(vStdFlost,allAveragePower,'.k')
xlabel('standard deviation of the Lost force');
ylabel('power generated');
```

4- Third model: Simulation of a body in movement in the real condition

```
% NUMERICAL MODEL_3
% Target: Use the model to find the power take off (PTO) changing the sea state

% Basic equation is the dynamic equation for a normal oscillating body
% m*acc+ c* vel+ k*x = External force
% where External force is the force given by Morison Equation with a body
% in movement F(u,upunto, xpunto, x2punti)= F inertia + F drag + F froude-Krylov
% where u= is the flow velocity
% and x= is the plate displacement


clear all
close all

row = 1030;          % row= density salt water [kg/m3]
ro= input('Insert the density of the steel plate, in kg/m3, ' );
roprimo= ro-row;     % roprimo=density of the steel plate inside the water [kg/m3]

w= input('Insert the width of the plate, in m ' );
d= input('Insert the depth of the plate, in m ' );
s= input('Insert the thickness of the plate, in m ' );
kp= input('Insert the stiffness of the spring, in N/m ' );
vi= input('Insert the damping coefficient, in N*s/m ' );
mass= roprimo*w*d*s;
volume=w*d*s;
area=w*d;

Hs= input('Insert the significant wave height, in m ' );
Tp= input('Insert the peak wave period, in sec ' );
h= input('Insert water depth, in m ' );

g=9.81; % gravity acceleration [m/s2]
Lhypothesis= 1.61;
L=1.1;
diff= L-Lhypothesis;
while diff~=0
    L=(g*(Tp^2)/(2*pi)*tanh(2*pi*h/Lhypothesis));
    diff=L- Lhypothesis;
end
disp(['The wave length is ',L]);
k= 2*pi/L;
omega=2*pi/Tp;

% From off-shore to near-shore the wave period doesn't change
if (h/L)>(1/2)
    % Potenza dell'onda per metro di cresta d'onda [kW/m]
    Tz=Tp/1.4;
    Te=1.2*Tz;
    Wavepower=0.44*(Hs^2)*Te;
    disp('water depth condition');
else
    disp('shallow water condition');
end
```

```
% external force
CD=2;      % CD= drag coefficient;
CM=1;      % CM= mass coefficient;
z=-(d/2);
rap=(cosh(k*(h+z))/sinh(k*h));

j=1;
vx(1,1)=0;         % initial condition
vu(1,1)=0;         % u= flow velocity
vvel(1,1)=0;

for t=0.1:1:180      % computing time 3 minutes, with a step of 1 sec
vt(1,j+1)=t;
    u=omega*(Hs/2)*rap*cos(omega*vt(1,j));
    vu(1,j+1)=u;

    upunto=-rap*(omega^2)*(Hs/2)*sin(omega*vt(1,j+1));
    vupunto(1,j+1)=upunto;
    deltat=t(j)-t(j-1);      %sampling frequency

    partFi=ro*CM*volume*(vupunto(q,j+1));
      % partFi= inertia force part not depending on the movement of the plate
    Ffk=ro*volume*upunto;                          % Ffk= body in movement

    % Calculation with abs positiv
    Ba=-((1/(deltat^2))+(vi/(mass*deltat))+(k/(2*mass)));
           % B part not depending on abs sign
    Bmodulo=-(CD*ro*area)/(2*mass))*((2*vu(q,j+1)/deltat)+(2*vx(q,j)/(deltat^2));
    B=Ba+Bmodulo;

    Ca=+vx(q,j)*((1/(deltat^2))+(vi/(mass*deltat))-(k/(2*mass))+
           +((CM*ro*volume)/((deltat^2)*mass)));
           % C1 part not depending on abs sign
    Cmodulo=+vx(q,j)*((CD*ro*area)/(2*mass))*((vx(q,j)/(deltat^2))+
           +(2*vu(q,j+1)/deltat))+((CD*ro*area)/(2*mass))*((vu(q,j+1))^2);
    C1=Ca+Cmodulo;

    C2=partFi/mass;
    C3=Ffk/mass;
    C=C1+C2+C3;

    A=((CD*ro*area)/(2*(deltat^2)*mass));

    g= polyeig(C,B,A);  % function to solve the equation: Ax^2+bx+C=0
                        % in input it needs the3 coefficients
                        % in output it gives a  vector g, including x1 e x2

    x=mean(g);          % x= plate displacement
    vx(q,j+1)=x;

    Fexternal=0.5*CD*ro*area*((vu(q,j+1)-((vx(q,j+1)-vx(q,j))/deltat)))^2+
      +ro*volume*CM*(vupunto(q,j+1)-(vx(q,j+1)-vx(q,j))/(deltat^2))+C3*mass;
```

```
    vFexternal(q,j+1)=Fexternal;
    modulo= vupunto(q,j+1)-((vx(q,j+1)-vx(q,j))/deltat);

    if modulo>=0
        vx(q,j+1)=x;
    else
        A=-A;                % Re-calculation of x value
        Bmodulo= -Bmodulo;
        B=Ba+Bmodulo;

        Cmodulo=-Cmodulo;
        C1=Ca+Cmodulo;
        C=C1+C2+C3;

        g= polyeig(C,B,A);
        x=mean(g);
        vx(q,j+1)=x;

        Fexternal=0.5*CD*ro*area*((vu(q,j+1)-((vx(q,j+1)-vx(q,j))/deltat)))^2+
      +ro*volume*CM*(vupunto(q,j+1)-(vx(q,j+1)-vx(q,j))/(deltat^2))+C3*mass;
        vFexternal(q,j+1)=Fexternal;
    end

    velocity=(vx(1,j+1)-vx(1,j))/deltat;
    vvel(1,j+1)=velocity;

    % Force
    Flost=vi*velocity;
    vFlost(1,j+1)=Flost;
    StdFlost=std(vFlost(1,:));
    Fimpressed=Fexternal-Flost;
    vFimpressed(1,j+1)=Fimpressed;
    stdFimpressed=std(vFimpressed(1,:));
    %Calculation of power generated per meter of width plate, at the instant j
Power=abs(velocity*Flost)/w;
    vPower(1,j+1)=Power;
    averagePower=mean(vPower(1,:));

    j=j+1;
end
% To calculate the efficiency there is the need to compare the wave power with
the average power generated
efficiency= averagePower*100/(Wavepower*1000);
disp(['The efficiency is ',efficiency]);

%Displacement
figure(1);
plot(vt,vx,'.b')
xlabel('time [s]');
ylabel('spostamento');
%Velocity
figure(2)
plot(vt,vu,'.r')
xlabel('time [s]');
ylabel('velocità');
```

Chapter 1

- Williams, James. 2005. "*Oil Price History and Analysis*"
- Ocean Energy System, International Energy Agency (I.E.A.) (2009)*"Annual Report"*
- postnote January 2009 Number 324 Marine Renewable
- Gordon M. Barrow, "*Physical Chemistry"*, WCB, McGraw-Hill, 1979
- Berlanstein, Lenard R., (1992), "*The Industrial Revolution and work in nineteenth-century Europe"*
- Abbott Payson Usher (1920)*, "An Introduction to the Industrial History of England"*, http://books.google.com/books, retrieved 2009-07-26

Chapter 2

- *Coastal Engineering Manual* (CEM), US Army Corp of Engineers (2002)
- Wienke J., Sparboom U., Oumeraci H., "*Breaking Wave Impact on a Slender Cylinder*"
- Det Norske Veritas, 2005, "*Guidelines on design and operation of wave energy converters*", Carbon Trust.
- Ocean Energy System, International Energy Agency (I.E.A.) *"Ocean Energy Opportunity, present status and challenges"*
- Ocean Energy System, International Energy Agency (I.E.A.) (2006) *"Policy Report"*
- Ocean Energy System, International Energy Agency (I.E.A.) (2009) *"Annual Report"*
- Folley, M, Whittaker, T, Osterried, M (2004). "*The Oscillating Wave Surge Converter*," ISOPE Paper No. 2004-JSC-377
- J.R Joubert "*An investigation of the wave energy resource on the South African Coast, focusing on the spatial distribution of the South West Coast"*

Chapter 3

- Kofoed and Frigaard (2009) "*The Dragon of Nissum Bredning--Danish approach to development and evaluation of wave energy devices*" Journal of Ocean Technology 2009 Renewable Ocean Energy, Vol. 4, No. 4
- Arthur Pecher, J.P. Kofoed (2010) *"Experimental Study on the WavePiston Wave Energy Converter"*

Chapter 4

- Morison, J. R.; O'Brien, M. P.; Johnson, J. W.; Schaaf, S. A. (1950), "*The force exerted by surface waves on piles*"
- "Basic Coastal Engineering"

Chapter 5

- Kofoed and Frigaard (2009) "*The Dragon of Nissum Bredning--Danish approach to development and evaluation of wave energy devices*" Journal of Ocean Technology 2009 Renewable Ocean Energy, Vol. 4, No. 4
- Ocean Energy System, International Energy Agency (I.E.A.) (2009) *"Annual Report"*

http:// www.aau.dk

http:// www.wavepiston.dk

http: recession.org/history/1970s_oil_crisis

http:// earthguide.ucsd.edu/fuels/1970.html

http:// www.iea-oceans.org

http:// www.idromare.it

http:// www.telemisura.it

http:// www.geni.org

http:// www.parliament.uk

http://www.esru.strath.ac.uk

http://www.emec.org.uk

http://www.oceanor.no

http://edgar.jrc.ec.europa.eu/index.php

http://www.carbontrust.co.uk